ANALYSIS AND CONTROL OF GUN BARREL VIBRATIONS

A THESIS SUBMITTED TO
THE GRADUATE SCHOOL OF NATURAL AND APPLIED SCIENCES
OF
MIDDLE EAST TECHNICAL UNIVERSITY

BY

FIRAT BÜYÜKCİVELEK

IN PARTIAL FULFILLMENT OF THE REQUIREMENTS
FOR
THE DEGREE OF MASTER OF SCIENCE
IN
MECHANICAL ENGINEERING

DECEMBER 2011

Approval of the thesis:

ANALYSIS AND CONTROL OF GUN BARREL VIBRATIONS

submitted by **FIRAT BÜYÜKCİVELEK** in partial fulfillment of the requirements for the degree of **Master of Science in Mechanical Engineering Department, Middle East Technical University** by,

Prof. Dr. Canan ÖZGEN _____
Dean, Graduate School of **Natural and Applied Sciences**

Prof. Dr. Süha ORAL _____
Head of Department, **Mechanical Engineering**

Asst. Prof.Dr. Gökhan ÖZGEN _____
Supervisor, **Mechanical Engineering Dept., METU**

Dr. Tolga DURSUN _____
Co-Supervisor, **Project Director, ASELSAN**

Examining Committee Members:

Prof. Dr. Y. Samim ÜNLÜSOY _____
Mechanical Engineering Dept., METU

Asst. Prof. Dr. Gökhan ÖZGEN _____
Mechanical Engineering Dept., METU

Dr. Tolga DURSUN _____
Project Director, ASELSAN

Asst. Prof. Dr. Ender CİĞEROĞLU _____
Mechanical Engineering Dept., METU

Instructor Dr. S. Çağlar BAŞLAMIŞLI _____
Mechanical Engineering Dept., HU

Date: 30.12.2011

I hereby declare that all information in this document has been obtained and presented in accordance with academic rules and ethical conduct. I also declare that, as required by these rules and conduct, I have fully cited and referenced all material and results that are not original to this work.

Name, Last name: Fırat BÜYÜKCİVELEK

Signature:

ABSTRACT

ANALYSIS AND CONTROL OF GUN BARREL VIBRATIONS

BÜYÜKCİVELEK, Fırat

M.Sc. Department of Mechanical Engineering
Supervisor: Assist. Prof. O. Gökhan ÖZGEN
Co-Supervisor: Dr. Tolga DURSUN

December 2011, 159 pages

Modern battle tanks are equipped with gun stabilization systems using gyro and encoder data to stabilize the gun barrel, although these systems are very sensitive and reliable, these systems assume the gun barrel as a rigid beam, and do not use information from the barrel's free end, instead they use data from the turret and trunnion axis. As a result; the gun barrel deflection cannot be controlled with available gun stabilization systems.

Meanwhile use of longer gun barrels is newly being adopted in design of modern battle tanks (MBT) or in the modernization of already existing main battle tanks. Longer gun barrel is used to take the advantage of increased shooting range and increased kinetic energy during impact over shorter barrels which are currently being used. When field tests are done with two versions of the same tank with one having a shorter and the other one having a longer gun barrel i.e. there is random excitation from the ground when the tanks are on move, a dramatic decrease in the shooting accuracy of the long gun barrel is observed. The reason behind the decrease in accuracy lies in the dynamic characteristics of the long gun barrel; mainly due to increased receptance levels to induced vibration input while the tank is on move. This increase in receptance levels results in higher barrel flexure which also decreases the first shot hit probability. Another important effect of increased

receptance level is on the penetrator performance of the bullet since it increases the yaw state of the bullet.

Yaw is the angle at which the bullet hits its target. A possible solution to minimize the effect of increased barrel flexure of the longer gun barrel is the use of tuned vibration absorbers (TVA). In this thesis study, A TVA based solution is investigated to integrate a longer gun barrel to an already existing tank while keeping the dynamic response of the new gun barrel to the base excitation coming from the ground as the tank moves same as the original short gun barrel. For this purpose first the finite element model of the short gun barrel is developed and verified with the experimental study so that same modeling approach can be utilized to analyze the long barrel which physically does not exist at the moment. Utilizing the finite element model of the long gun barrel; dynamic behavior of two models is compared and a tuned vibration absorber is designed to improve the characteristics of the long gun barrel.

Keywords: Gun barrel vibrations, Tank firing systems, Vibration absorbers, Gun barrel model.

ÖZ

SİLAH NAMLUSU TİTREŞİMLERİNİN ANALİZİ VE KONTROLÜ

BÜYÜKCİVELEK, Fırat

Yüksek lisans, Makina Mühendisliği Bölümü
Tez Yöneticisi: Yrd. Doç. Dr. Gökhan ÖZGEN
Ortak Tez Yöneticisi: Dr. Tolga DURSUN

Aralık 2011, 159 sayfa

Modern savaş tankları cayro ve enkoder verilerini kullanan silah stabilizasyon sistemleri kullanmaktadırlar. Bu sistemler her ne kadar çok hassas ve güvenilir de olsalar silah namlusunu rijit bir kiriş elemanı olarak kabul ederler ve namlunun serbest ucundan gelen bir veri kullanmazlar. Bu sistemler namlunun dönüş ekseninden gelen veriyi stabilizasyonu sağlamada kullanırlar. Sonuç olarak mevcut silah stabilizasyon sistemleriyle namlu ucu deplasmanları kontrol edilememektedir.

Günümüzde üretilmekte olan modern savaş tanklarında ve mevcut tankların modernizasyonunda daha uzun silah namluları kullanılmaya başlanmıştır. Uzun namlular kısa namlulara göre daha uzak bir atış menzili ve vuruş anında daha fazla kinetik enerji avantajı sunar. Ancak uzun namlulu ve kısa namlulu iki tank ile yapılmış olan saha testlerinde iki tank da sahada hareket ettirilmiş ve yerden rastgele titreşime maruz kaldıklarında uzun namlulu tankın atış başarısında büyük ölçüde düşüş gözlemlenmiştir. Atış hassasiyetindeki bu düşüşün sebebi olarak uzun namlunun uzatılmış boyundan dolayı değişen dinamik karakteristiği görülmektedir. Boyu uzatılarak dinamik karakteristiği değiştirilmiş uzun namlulu silah titreşim altında daha fazla titremekte ve deplase olmaktadır bu da ilk atımda vuruş ihtimalini düşürmektedir. Namlu ucunda artan deplasmanın bir diğer etkisi de merminin sapma açısını arttırmak olarak görülmüştür.

Sapma açısı merminin hedefi vurma anında hedefle yaptığı açıdır. Sapma açısının artması merminin etkinliğini azaltmaktadır. Namlu ucunda meydana gelen eğilmenin kontrol altına alınması için kullanılabilecek olası çözümlerden biri ayarlı titreşim emici kullanımıdır.

Bu tez çalışmasında üretilecek bir uzun tank namlusu üzerine uygun ayarlı titreşim emici uygulaması üzerine çalışılmıştır. Çalışmada kısa namlulu tanka yerden gelen titreşim tipi ve seviyeleri uzun namlulu tanka uygulanmıştır. Bu amaçla ilk olarak kısa silah namlusu sonlu elemanlar kullanılarak modellenmiştir, bu model deneysel modal analiz ile doğrulanmıştır. Bu sayede sonlu elemanlar modelinde izlenen metod doğrulanmış ve henüz üretilmemiş olan uzun namlunun sonlu elemanlar ile doğru olarak modellenebilmesine olanak sağlanmıştır. İki namlunun da sonlu eleman modelleri elde edildikten sonra bu modellerin dinamik karakteristikleri incelenmiş, karşılaştırılmış ve uzun namlunun dinamik karakteristiğini iyileştirecek ayarlı titreşim emici tasarımı yapılmıştır.

Anahtar Kelimeler: Silah namlusu titreşimleri, Tank atış kontrol sistemleri, Titreşim emiciler, Tank top modeli

To My Father and My Uncle...

ACKNOWLEDGMENTS

The author wishes to express his deepest gratitude to his supervisor Asst. Prof. Dr. Gökhan ÖZGEN and co-supervisor Dr. Tolga DURSUN for their guidance, advice, criticism, encouragements and insight throughout the research.

The author would also like to thank his managers and colleagues, Enis Naci ÖZKAN, Sarper GÜRBÜZ, Ahmet Levent AVŞAR, Hakan ZALOĞLU, Murat VARLIK, Emre ŞENGÜL for their support, suggestions and comments.

The author wishes to thank Banu ULUÇAY, Türkan BÜYÜKCİVELEK, Ahmet Burak BÜYÜKCİVELEK, Sekinet ÖZÜAYDIN for their support and encouragement over many years.

TABLE OF CONTENTS

NOMENCLATURE

MBT	Main battle tank
TVA	Tuned vibration absorber
PSD	Power spectral density
LRF	Laser range finder
MRS	Muzzle reference system
Hz.	Hertz
GPa	Giga Pascal
VEM	Visco-elastic material
m_1	Mass of the main system
m_2	Mass of the vibration absorber
x_1	Response of main system
x_2	Response of tuned vibration absorber
k_1	Stiffness of main system
k_2	Stiffness of TVA
ω_1	Natural frequency of main system
ω_2	Natural frequency of TVA
a_1	Response amplitude of main system.
a_2	Response amplitude of TVA.
F	Forcing amplitude

ω	Forcing frequency
x_{st}	Static deflection
C	Damping of TVA
F	Frequency ratio
V	Forcing frequency ratio
μ	Mass ratio
C	Damping of the main system
M	Mass of elevation actuator

LIST OF FIGURES

FIGURES

LIST OF TABLES

TABLES

CHAPTER 1

INTRODUCTION

In modern battle tanks longer gun barrels are being adopted in order to achieve a increased range and increased kinetic energy during impact. Use of longer gun barrels results in subsequent increase in dynamic transverse response of the barrel (due to increased length) while the tank is moving. Available gun control systems do not use the displacement information from the tip of the barrel hence; the transverse displacement at the tip of the barrel cannot be compensated by the stabilization systems and this may adversely affect the overall system performance which is the first round hit probability of the battle tank.

It is seen from the field tests performed on two versions of a tank – one with a standard (short) barrel and the other one with a longer barrel - that increased barrel flexural response observed the longer gun barrel decreases the first shot hit probability thus the accuracy of the system compared to the short barreled tank [1]. During these tests it is also revealed that when tanks are stationary longer gun barrel performance is better than the shorter one as expected. The problem arises when both tanks start moving at constant speeds. It is seen that a drastic decrease occurs at the performance of long gun barrel.

Long gun barrel is manufactured independent from the short gun barrel. The length of short gun barrel is not extended with an additional part. It is seen that a drastic decrease occurs at the barrel performance, for main battle tanks which are modified with long barrel. For newly designed main battle tanks that occupy long barrel the

problem may arise also. For already assembled long gun barrels, negative effect of length extension can be minimized using tuned vibration absorbers. A tuned vibration absorbers if tuned and designed properly they can be effective alternative solution to control forced and free vibrations of mechanical structures. The main objective of this thesis study is to design a tuned vibrations absorber so that the road induced dynamic tip displacements of the longer gun barrel is kept the same as the tip displacement levels of shorter gun barrel. In order to achieve this objective proper structural dynamics modeling of the gun barrels and the tuned vibration absorbers is necessary. It is also necessary to clearly identify the type and characteristics of the vibration control problem in hand, i.e. find the modes that dominate the dynamic response of the barrel, find out if there are any dominant forcing frequencies present in the base displacement input caused by the road as the tank moves.

The aim of this thesis is to decrease the vibration response level of longer gun barrel to the vibration response level of shorter gun barrel by using tuned vibration absorbers. By achieving that objective, it is assumed that the first round hit probability (accuracy) of the gun systems with longer barrels will be increased.

In the first part of the thesis a detailed literature survey is done in order to define the problem clearly and possible solutions and approaches to solve the problem are found. In the following parts, problem models are constructed and verified with experimental tests. After all a tuned vibration absorber design alternative is given to solve the problem.

The thesis study starts with the literature survey which presented in the second chapter. Literature survey is utilized to understand and define the problem clearly. Literature survey is divided in to four main sections; the first section presents the aim of the study; in this section problem is reviewed and the aim of this thesis work is given. The second section gives a deeper understand of the problem definition.

Several concepts and definitions are given. Accuracy calculations and factors affecting accuracy of main battle tank are also revealed in the second section. Third section is about modeling of the gun barrel and analysis. Modeling techniques and computer software used in literature are given. At the end of the literature survey the final section deals with tuned vibration absorbers. A brief introduction is given about other possible solutions, and then information about tuned vibrations is given.

In the third part of the study, theoretical background of vibration absorbers are investigated, mathematical models are studied, some optimization plots are given for determining the TVA parameters.

In the fourth part, the finite element barrel model is constructed using ANSYS commercial software, this model is verified with experimental modal analysis. Since the objective of this thesis is to decrease the vibration activity level of longer gun barrel to the vibration activity level of shorter gun barrel by using tuned vibration absorbers, short and long gun barrel behaviors are investigated and compared under different conditions. Commercial ANSYS software has the capability to run several analyses using same finite element model.

Firstly static structural analysis is done for both gun barrels. It is seen that both barrels behave like fixed-free beams and longer gun barrel deflects more than the shorter one as expected. Secondly modal analysis is done for both gun barrels. This analysis is also used to verify the modeling of the shorter gun barrel. In modal analysis, dynamic characteristics of two barrels are obtained. Mode frequencies and corresponding mode shapes are obtained. Finally modal analysis data is used to do spectrum analysis. In that analysis ANSYS software allows user to apply PSD data from any location and read the response PSD of the location of interest. In this analysis the deflections of barrel ends' are also found and compared.

In the final part parameters of TVA is determined, optimization of TVA mass, stiffness and damping is done. Longer gun barrel model is modified and results are compared with the successive shorter gun barrel. At the end of the final part detailed design of tuned vibration absorber to be mounted on the muzzle end of the barrel is given. Two alternative conceptual design solutions are studied.First one is resonant beam type TVA and the second one is the spring-damper type TVA. Both alternative designs are analyzed in terms of required tuning and strength properties.

CHAPTER 2

LITERATURE SURVEY

The literature survey is divided into four main sections. In the first section the aim of the study is given. In the second section some main concepts related to gun systems, accuracy calculations etc. are given, this category is helpful to give some basic idea about the gun system technologies also. The third section is about modeling the whole problem. Not only the finite element gun barrel modeling but also vibration analysis models are investigated. In the final section of chapter 2 tuned vibration absorbers; their types and basic principles are given.

2.1 FIRE CONTROL PHENOMENA

The main objective of all gun systems is launching a projectile from a weapon station to a selected target successfully [2]. The weapon station can be a tank, helicopter, an air craft or any stationary cannon, the target can be a single soldier, a large building or combinations of them.

During fire, offsetting the weapon fire of direction to line of sight is the basic principle. The angle between the horizontal barrel position and the elevated barrel position is the prediction angle. For non guided missiles it must be calculated and applied prior to instant of firing. How much offset is necessary to hit the target is the main consideration of the gun control systems. Several variables, from wind velocity to air temperature affects as input to the control of system.

The control systems found in main battle tanks (MBT) process these variables as inputs and provide a successful shot. For MBTs with long gun barrel, barrel deflection must be included to these variables since it is seen from the tests that it affects the accuracy. Available control systems consider the barrel as it is rigid so that they do not take into account barrel deflection effect while predicting the offset angle.

2.1.1 FIRE CONTROL SYSTEMS IN MBT

Fire control systems in MBTs are designed to achieve a successful launch by overcoming four important objectives [2]:

1- Visual estimation of range.
2- Correction of such secondary (but still significant) effects as wind, range, muzzle velocity change etc.
3- Accommodation of only one range-elevation relationship on the ballistic reticle.
4- Night acquisition and target tracking.

First three of these parameters directly affect the true prediction angle calculation and the success of the launch. Laser range finder (LRF) to supply accurate target range is adopted as one of the primary gun firing control systems. Laser range finder directs a pulse of laser light at the target, receiving target-reflected light from this pulse, and converting the elapsed time between transmittal and reception to give data results in range between the MBT and the target.

Ballistic computer system working together with sensitive sensors provides a full fire control solution for secondary effects. Ballistic computer computes the fire control corrections to compensate the possible effects of gravity, drift, crosswind, horizontal target motion, ammunition temperature, altitude, air temperature, gun wear, trunnion cant, gunner's and commander's sight parallax, and gun jump. More

importantly all those effects are taken in to account computed and results in a single range-elevation relationship in ballistic reticle of the gunner's or commander's screen.

The last objective of a MBT to overcome is capability of operating at night. MBT visual sight line systems provide performing night viewing. In order to implement this optical/electro-optical approach, the developer provides the gunner a stabilized, periscope-type optical sight with integrated electro-optical sensors. Some of the MBT consists of second, independent thermal viewer for commander as well. This system also provides target tracking.

2.1.2 STABILIZATION SENSITIVITY

During world war 2, the need for a stabilized tank gun to fire accurately from a tank moving over rough terrain is emerged [2]. The goal was a stable platform to stabilize tank weapons completely during travel over rough terrain. Since it was hard to find azimuth and elevation servo controls to drive the turret and barrel accurately at high rates early applications are limited to low and medium weighted tanks. The technology improved during and after the war and now main battle tanks are equipped with such stabilization systems that enables the gun and sighting system can be stabilized and isolated from disturbances when they are on move.

In the case of our problem it is important to mention that these stabilization control systems that drives the servos do not use any information from the tip of the barrel. Data is only taken from gyros on the vehicle hull, turret, and sighting system.

2.1.3 ACCURACY OF THE FIRE CONTROL SYSTEM

The accuracy of the fire control systems is calculated as a measure of hit probability. The accuracies are improving continuously throughout the years. During the literature survey no military standard or a general common value for probability to achieve a successful shot is found. It is obvious that 100% probability

is theoretically a success but in practice it is not possible and indeed the accuracy and success of the gun system is basically depends on a deal between the supplier and customer.

Most commonly the customer announces the system requirements and suppliers/companies introduce their available solutions throughout a tendering process. The system accuracy tests are done in the field after integration of the system and, hit probabilities are examined. Two kinds of hit probabilities are in use commonly: First is the single-shot probability of hit which is defined as the probability of a single shot to intersect the target volume and the second is engagement hit probability which is defined as the probability of achieving a specified number of hits in the firing of a specified number of shots are used.

2.1.4 FACTORS AFFECTING THE ACCURACY

The accuracy of the system depends on many factors and can change drastically from one situation to other. Basically motion of the target and weapon station (scenario), the type of the target, type of the ammunition, distance and environmental factors affect the accuracy of the gun system.

The accuracy of the system mostly depends on the shot scenario. With improved and well-learnt ballistic applications the accuracy is very high for stationary targets. However a drastic drop occurs when the target and the weapon station start moving. The type of target also has an important role on accuracy; the target may be a single or an area target. If the target consists of a single soldier, vehicle or building it is single target. If the target consists of group of soldiers or vehicles it is called area target.

Other inputs affecting the accuracy are: range, elevation, azimuth, motion of the target. These are measured from the weapon station and depends on the target it self. Projectile weight, increase or decrease in muzzle velocity ballistic head winds

and tailwinds, air density and temperature, shell surface friction effects, crosswind and drift are some other factors that affect the accuracy of the shot.

2.1.5 ACCURACY CALCULATIONS

Accuracy calculations can be done by mathematical models, or directly from the field data. Since the accuracy depends on many factors it is hard to measure it with simple mathematical models or just equations. For an analytic solution accuracy calculations can be done via complex mathematical models of sub-components and adding the effect of environmental conditions in software that is specially designed.

For the accuracy calculations using filed data, targets are not treated as simple points in space. They are considered to extend over a finite area or volume; hence in field tests rectangular 2-D targets are used. In field-test evaluations, not only are hits on the target recorded, but also the miss distance, i.e., distance of closest approach is calculated, so that complete probability density distribution can be obtained.

In actual practice the determination of accuracy requirements for a successful shot, like the design process itself, is an iterative process. Below is the list of parameters affecting the accuracy of M1 tank gun. Probability calculations can be done using such a list as given in ***Table 2-1*** [2].

Table 2-1. *Compensations in direct fire engagements. [2]*

FACTOR	Compensation, mil			
	1200 m.		3000 m.	
	Vert.	Hor.	Vert.	Hor.
Super elevation	2.8	Na	7.6	Na
Traverse Rate	Na	14	Na	15
Elevation Rate	0.8	Na	0.9	Na
Range Rate	0.05	Na	0.16	Na
Trunnion Cant	0.01	0.25	0.03	0.68
Sight / Weapon Parallax	0	0	0.26	0.35
Tube Bend	2	Na	2	Na
Bore sight Alignment	0.15	0.15	0.15	0.15

Overall system error is calculated about 0.8 i.e. single shot hit probability is about 0.69. In the above tables artillery mil is used as the angle unit. Artillery mil corresponds to the arc which is 1/6400 of circle. 1 mil = 0.05635 degrees. Roughly speaking, 1 mil corresponds to 1 meter long arc at a distance of 1000 meters. Since the system of long barrels cannot be defined with all its in detail, accuracy of longer gun barrel is compared to accuracy of the shorter barrel which is tested to be successful on same system. Assuming both systems are identical except their barrels, the comparison will be done on gun barrels' end displacements and vibration activity levels.

Table 2-1 Cont'd. *Compensations in direct fire engagements [2]*

Jump Dispersion	0.25	0.25	0.25	0.25
Earth Rate	0.02	0.02	0.05	0.05
NON-STANDART CONDITIONS				
Muzzle velocity	0.06	0	0.16	0
Air temperature	0	0	0.01	0
Air density	0	0	0.02	0
Crosswind	0	0.1	0	0.26
Range Wind	0	Na	0	Na
Angle of site	0	Na	0.01	Na
OWN VEHICLE MOTION				
Cross Range	Na	13.8	Na	13.8
Down Range	0.08	0	0.22	0

Table 2-2. *Effects of system error on single shot hit probability.*

SYSTEM ERROR, mil	Single-shot Hit Probability P_{ss} dimensionless	
	1000 m	3000 m
0	0.99	0.74

Table 2-2 cont'd. *Effects of system error on single shot hit probability.*

0.2	0.99	0.57
0.3	0.98	0.45
0.4	0.97	0.34
0.5	0.92	0.26
0.6	0.86	0.20
0.8	0.69	
1.0	0.55	

For our case at 1000 meters;

Table 2-3. *Accuracy Table for the present system*.

Super elevation	0.1 mil
Traverse rate	Na
Elevation rate	0.1 mil
Bore sight alignment	0.1 mil
Earth rate and cross range:	Na
Non-standard conditions other than muzzle velocity is under control	0 mil
Tube bend, parallax and trunnion cant	0 mil
Stab accuracy & synch error	0.5 mil

2.1.6 EFFECT OF MUZZLE TIP DISPLACEMENT ON ACCURACY

Since it is the control of muzzle tip displacement we are interested in this thesis, it is important to know how it affects the accuracy calculations. Looking at the Table 2.1 in previous section 2.2.5 it can be seen that tube bend and super elevation have the highest effect on accuracy. In Table 2, tube bend is assumed to have no effect, this is because it represents the static deflection of the gun tube and is measured

with the help of MRS. MRS namely muzzle reference system is a simple reference device located at the end of the barrel. The aim is to maintain accuracy of fire, compensating thermally-induced inaccuracy in modern tank barrels, and the thermally induced inaccuracy may be due to wind, snow, and long term repeated firing. The system consists of a light projector which bounced light off a mirror at the muzzle end of the barrel and back into the gunner's sight. The deflections at the muzzle could be checked by the movements in the reflected light spot back into the gunner's sights and the gunner could alter his sight co-alignment with the barrel end by adjustment of 'x' & 'y' of his zero aiming point.

In our case we are interested in tube bend while the tank is on move. The deflection of the gun tube increases while the tank is on move due to random base excitation and MRS has no control on that situation. Another important factor is the jump dispersion. It is known that increased muzzle tip displacement increases the jump dispersion which lowers the accuracy drastically.

According to Eric Kathe the increased system receptance due to longer barrel, decreases weapon accuracy during live-fire bump-course test [1]. The accuracy is particularly sensitive to the traversing speed of the tank over the bump-course, and increases for system configurations that have utilized a shorter barrel. This decrease of accuracy is absent for live-fire testing of the same gun system from a stationary mount where the developmental system outperforms the shorter barrel system. According to article an effect relating to gun performance as well as accuracy is the yaw state of the bullet as it leaves the muzzle where yaw is the angle between the momentum vector and the axial centerline of the projectile.

A longer gun tube is designed for M1A1 MBT in order to achieve higher velocity. Doing so, projectile impact dispersion is observed to be increased significantly. But the accuracy of the shots is found to be low; Peter L. McCall’s study [3] mentioned several possible reasons and the concluded that the reason behind low accuracy is

the effect of dynamic tube flexure error. Since the flexing of the tube is not a part of the feedback to the fire control system, muzzle actually points the gun in a different direction which the control system believes to be correct. This study focuses on the muzzle pointing errors, and tests are done for both short and long gun tubes. The pointing error is measured by a special device MRS, Continuous Muzzle Reference System which is capable of continuous measurement of muzzle motion in mill radians. Muzzle motion vs. Velocity of the tank is plotted in elevation and azimuth axes. In these plots long and short gun barrels are compared and amplifying effect of longer gun barrel can be observed. At the end of the paper it is mentioned that for the error analysis and increased shot accuracy; the muzzle motion must be used in predictive algorithms in order to determine when to allow the cartridge to fire.

2.2 MODELING THE PROBLEM

In the third category of literature survey the modeling of the problem is considered. It is not only the modeling of the gun barrel but also the type of excitation, analysis to be done are important. The frequency range of interest, important modes, frequencies and how to model the whole analysis is studied.

2.2.1. TYPE OF VIBRATION

The type of vibration considered in this study is random vibration with base excitation. Several attempts are also done in literature with step and impulse response [4]. In literature the barrel is modeled as fixed free and pinched-free positioned along its trunnion axis [1]. In this thesis more detailed gun barrel finite element model is done with more complex boundary conditions. In chapter 3, the details are discussed. It is known that vibrations are due to random motion of the tank while it is moving along a rough terrain, data taken from such a test can be used for random vibration input. In ***Figure 2-1*** input PSD data taken from such a field test done while the tank is on move is seen. The data seen below is taken from a position close to trunnion axis while the tank is on move with a constant speed of 40 km/hr.

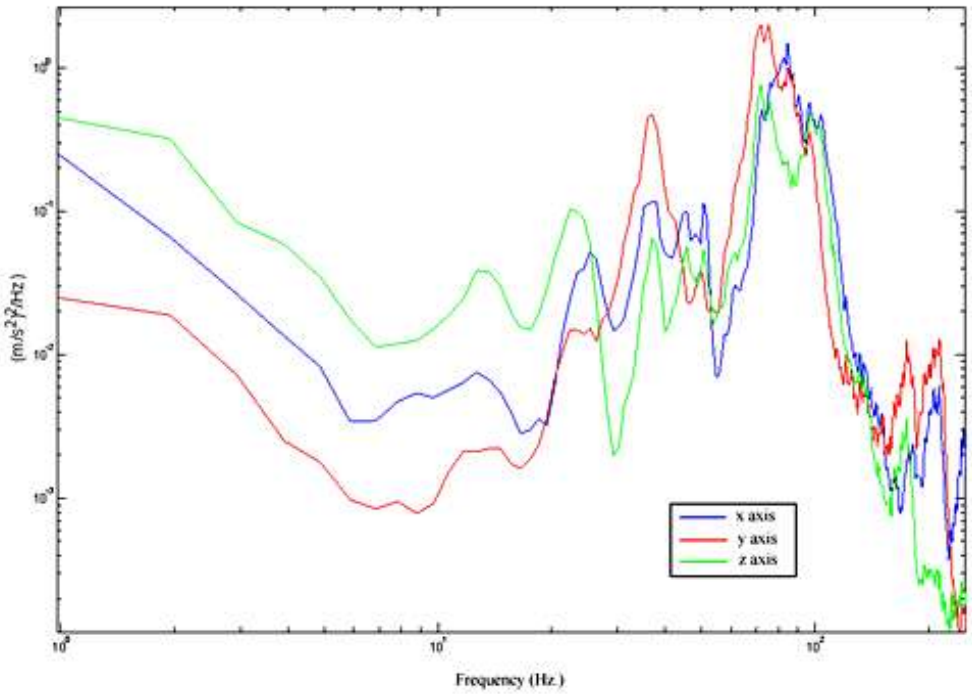

Figure 2-1. *Acceleration PSD vs. Frequency Plot, data taken from the field tests.*

(a)

(b)

Figure 2-2 *Photos taken from the field tests done in Koçhisar, ANKARA.* ***(a)*** *position of 3 axes accelerometer in large view.* ***(b)*** *Position of 3 axes accelerometer close to trunnion axis closer view.*

During the test the stabilization mode is turned on. The data below is used to simulate tank motion in analyses done in chapters 3-4-5 .In ***Figure 2-1*** x-axis is along the forward tank move direction, z-axis is downwards and y-axis is perpendicular to those axes according to right hand rule. Photos from the field test and position of accelerometer is seen in ***Figure 2-2***.

2.2.2 FREQUENCY RANGE OF RANDOM VIBRATION TO BE CONSIDERED

Using the input PSD data obtained from the field tests given in previous section 2.3.1 it is important to determine the frequency range of interest. Although according to MIL-STD-810F [5] vibration test levels for large ground vehicles are to be investigated between 0-500 Hz the PSD data taken during the field tests are taken between 0-250 Hz, for higher frequencies it is seen that amplitudes are negligible. In literature for barrel flexure first 3 modes of gun barrel are investigated [6]. During the analyses it is found that first three modes lie in the frequency range of 0-50 Hz. In this thesis study it is found in Chapter 4 and Chapter 5 that TVA should be tuned to first resonant frequency hence in the final part of the thesis work 0-25 Hz frequency range is investigated in detail since it is the first mode around 10 Hz is to be controlled.

2.2.3 MODELING THE GUN BARREL

According to M. Bundy et al. while the tank is on move the barrel vibrates both in horizontal (x-z) and elevation (x-y) planes [6]. From the input PSD data (Figure 2.1 and Figure 2.2) one can show that the vibration activities are much higher on elevation plane (x-y). It is shown in the article that the modes of barrel excited are the first three ones and first mode dominates the second and third mode shape amplitudes by ratio of 25:5:1. These results are verified by analysis in Chapter 4.

This being the case, it is possible to adequately characterize and model flexing of the barrel over this course by first mode shape. According to same article, gun barrel modes are occurred at around 10, 30 and 85 Hz.

Bundy et. al in their study focused on characterizing gun barrel flexure prior to firing [6]. Modeling is done as a system of point masses connected by spring-like forces. In this paper the effects of rigid-body or flexing mode motion on the projectile's flight path is not correlated but the dominant barrel flexing modes and, moreover, establish a methodology to ascertain the mode shape combinations that are most likely to occur prior to firing on the move. Fundamental barrel flexing modes are found are determined. First three mode shapes are found, and plotted.
Nadeem Ahmed, R D Brown, Amer Hameed developed a three dimensional finite element model of the barrel using ANSYS, and barrel motion during the fire was simulated [7]. In their study this simulation is verified with the SIMBAD data. Effects of various design factors on the dynamic response of the barrel are investigated. Some of the design factors are off axis masses and stabilization equipment on the barrel are discussed. Barrel's deflected shape during recoil with and without MRS is drawn at 1 millisecond intervals.

A finite element approach is used in Eric L Kathe's study [8]. The model is transformed in to MATLAB and optimized via scalar cost function. During the optimization mass is kept constant (20 kg) and Rayleigh stiffness proportional damping is varied. The optimum results are able to cut the peak amplitude by half. The barrel model is assumed to be an assembly of finite number of discrete elements. (7 elements) Between those elements nodes are formed and lateral displacements and slopes are equated as boundary conditions. For the inner motion of elements interpolation functions are used. The material properties are read from a MATLAB file and linear density from profile plots are obtained.

To form the finite element 3 locations in 7 elements are chosen to be imposed node locations where external constraints are applied. These are: elevation mechanism, trunnion bearing and the TVA. Gravity is neglected.

Since the barrel is steel damping coefficient is taken as zero and stiffness coefficient is taken to be 0.001 (N/(m/s))/(N/m) For the boundary conditions in trunnion bearings and elevation mechanism a force proportional to lateral displacement is applied and stiffness value is taken as 10e8 N/m. The forces are also applied at those degrees of freedom.

TVA is added as an additional of new energy storing degree of freedom. This increases the dimensions of system matrices 1by 1. The respective equation is constructed. In this equation M, C_D and K are the 17-by-17 mass, damping and stiffness matrices, respectively. The generalized coordinate vector q and force vector f (17-by-1 vectors) may be related to the nodal displacements.

The equation of motion is in 2^{nd} order symmetric form. By MATLAB this equation is converted to first order state space form. The method is explained in the study. After obtaining the relevant form, frequency response analysis is done in MATLAB. The input from elevation mechanism is only taken as linear compliance. The output is taken as muzzle pointing angle. For the SISO system the BODE diagram is drawn in MATLAB.

Vibration absorber optimization is done by using two variables; the stiffness and stiffness proportional damping coefficient. The mass is taken to be constant. A weighting function is used to emphasize the frequency of interest (Around 9 Hz). And a scalar cost function is quantitatively computed across the frequency range of interest to minimize the relative frequency response. For 2 dimensional cost function an optimization surface is obtained. It is seen that, for higher damping levels the TVA becomes insensitive. On the other hand for low damping values

TVA is highly sensitive. For low damping around 10000 N/m stiffness is the disturbance can be rejected by the TVA. The optimal value for that case is found to be 11400 N/m for a wide range of damping coefficient for 20 kg mass.

At the end of the study pole-zero comparison and mode shape comparison of unmodified and modified barrels are also done.

Finally it is also important to note that in this study, the modulus of elasticity is taken as: 29.5 $x10^6$ psi i.e. 203 GPa. In the analysis an impulse response applied from the trunnion axis and a step response applied at the same location is done. Static structural analysis is also done. The output to be investigated is the muzzle deflection.

2.2.4 MODELING THE ANALYSIS

During the literature survey several barrel modeling and analysis techniques are found [6] [7] [8], Most of the studies are corrected with the experimental results. The experiments are done as field tests while the tank is on move on a standard bump course with a predetermined constant speed. It is the barrel end deflection which is measured using experimental setups. In literature modeling the analyses, it is found that base excitation is applied at trunnion axis and response of the free end is investigated [7]. Moreover for the vibration analysis, modal frequencies and mode shapes are also found and compared [6] [7] [8]. Also barrel response to impulse and step functions are investigated [4].

2.3 VIBRATION ABSORBERS

2.3.1 ALTERNATIVE SOLUTIONS

In this thesis work tuned vibration absorber is used as a passive solution to the barrel vibration problem. During the literature survey several other solutions are also found:

First possible solution to decrease the barrel flexure effect is stiffening the barrel. This theoretically simple method bases on increasing the stiffness of the overall system. This results in increasing the mode frequencies. Although it is a certain method to achieve better results it requires a new design and reconstruction of a new barrel. For an already manufactured system this method is time consuming and cost inefficient.

Second method is the extended cradle mount. Theoretically extending a rotating beam towards opposite direction from the point of interest, mode frequencies increase and vibration activity tends to decrease. However for a main battle tank it is known that there is not enough free space for extension inside the turret. This lack of space in turret limits the availability of this solution.

Third method found during literature survey is using composite overwraps. This solution has the advantage of high stiffness and low weight solutions but composite technology is costly to adopt. Several attempts are done but composite-steel assemblage is found to be not successful yet. This solution still requires improvements.

The last possible solution is to adopt active control systems. Mentioned earlier in previous sections, the current active control systems receive data from gyros on the vehicle hull, turret, and sighting system. No input data is taken from the tip of the barrel. Although it would be an accurate solution, due to harsh environment at the barrel tip, it is hard to control the barrel vibration sensitively and healthy.

2.3.2 TUNED VIBRATION ABSORBERS

Today there are numerous ways of preventing unwanted vibrations in constructions and machines. One can change a construction’s rigidity and inertial parameters in order to tune them against their natural frequencies or one can use damping

treatments, increasing constructions damping capabilities, shifting and changing their dynamic behaviors. Different materials with different stiffness values, densities and geometries can be used to change the overall rigidity and mass properties of a system. Special coatings mostly made of visco-elastic materials (VEM) can be used as surface treatments for including damping to system. Another way of eliminating vibrations is to put barriers between the vibration source and affected body. This method is studied under vibration isolation techniques.

In this thesis another possible solution to unwanted vibrations is studied, namely vibration absorbers. Although every solution mentioned above is applicable for reasonable range of application, playing with system rigidity and inertial properties after construction stage is almost impossible. The main advantage of vibration absorbers is, their application is not limited to design or construction stage but also they can be added to the system during operation stage. Hence as in the case of already manufactured gun barrel, application of vibration absorber is meaningful.

By definition, Tuned Vibration Absorber is a device generating inertia, which reduces the vibration level of a protected structure [9]. Dynamic vibration absorber is also known as anti-vibrator, dynamic damper, vibration absorber, shock absorber etc. In most cases TVA consists of an additional mass, connected by means of an elastic and damping element to the structure needing protection or directly to the source of vibrations. Generally elastic and damping elements are connected in parallel to system. Vibration absorber invention is associated with the name of Frahm, who in 1909 first patented vibration absorber design the design was in simplest form and does not use any damping property [10]. The idea behind vibration absorbers is to reduce the vibration amplitude of a selected mode or modes. Single vibration absorber or multi vibration absorbers can be used for various cases.

Early types of vibration absorbers are undamped and tuned to the frequency of the disturbing force. The disturbing force may be a rotating motor etc. This kind of absorber is narrow-band type since it is unable to eliminate structural vibration after a change in the forcing frequency. In order to widen the frequency band damping is applied to vibration absorbers mostly in parallel to elastic members.

Since applying a TVA requires additional space and increases overall weight of the system, the mass used in TVA is chosen to be relatively small when compared with the mass of the vibrating system. The basic principle of operation of a TVA is vibration out-of-phase with the vibrating system; hence by applying a counteracting force vibration amplitude of the vibrating system can be reduced.

During literature survey several TVA application examples are investigated;
In his study Eric Kathe [1] studied the effects of vibration absorbers on cannon stabilization. The case is very similar to our problem; during the tests of M1A1 MBT, it was seen that the extended gun barrel increases the receptance of the system and shot accuracy decreases due to increased barrel flexure at the free end of the barrel. Several alternatives are discussed as a solution to change system's dynamic properties and vibration absorber application is chosen as a passive way of vibration control. In the study numerical modeling of the absorber is not mentioned but the test results and data processing done are revealed. The vertical and azimuth mount angles are measured via resolvers at the trunnion and turret ring, respectively; while the muzzle angles are measured optically by a system (the CMRS) that bounces a source beam from the turret off of a mirror mounted to the muzzle of the barrel and measures the deflection of the returned beam. The deflection of the returned beam correlates to the angular deflection of the muzzle. Performance in vertical and horizontal bending and vertical and horizontal pointing errors are compared.

At the end of the study it is found that applying vibration absorbers has two main benefits; reducing the receptance of the system and dissipation of vibration energy via damping property. To apply vibration absorbers; Euler-Bernoulli finite element technique is used to build the finite element model (second order DE). The model consists of varying section beams. Other types of TVAs found in literature survey are given in next section with their possible physical design solutions.

2.3.3 TYPES OF TVA

2.3.3.1 An Application to Gun Barrel

In this patent 2 types of vibration absorber applications are investigated. The first one simply consists of a spring and a mass element [11]. The second application makes use of the front thermal shroud and connects the shroud to the barrel via spring elements.

In the first design the solution is such that the vibration absorber is only made of a mass and a spring hence it can be put anywhere along the barrel, but it is preferred to put it where the vibration activity is important to control. In ***Figure 2-3*** sketch for first design is seen. The springs absorb the potential energy and also couples the kinetic energy stored in the mass. Type of springs used in this solution is compression springs constructed of flat wire with ground ends. The material properties, spring constants and dimensions are given in the patent. The spring is pre-compressed state when it is fitted to the barrel. And the mass is fixed to the spring and weights between 5-25 kg.

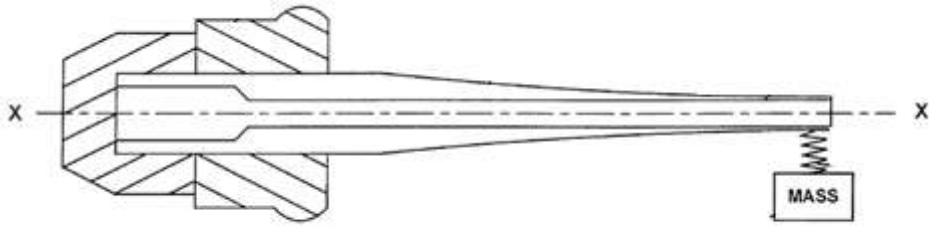

Figure 2-3. *First type of TVA discussed in US Patent, 6,167,794 [11].*

In the second design, thermal shrouds are used as inertia sources to control vibrations. The free end of the thermal shroud is fixed to the barrel via springs. A dynamically tunable spring collar is attached to the free end of the thermal shroud to tune the distance the thermal shroud to the barrel. Doing this muzzle reference system (MRS) can work. The spring number can vary up to 8 or even more. It is mentioned that due to present friction there is always some amount of damping in the system. A sketch for second design is seen in ***Figure 2-4***.

In the patent application of snubber liner to collar is mentioned, the aim for this is distributing the contact load to a wider area. Also spring pack caps are used to preload the springs. The caps may be screwed in to the collar. Moreover to prevent spring buckling push pins are used.

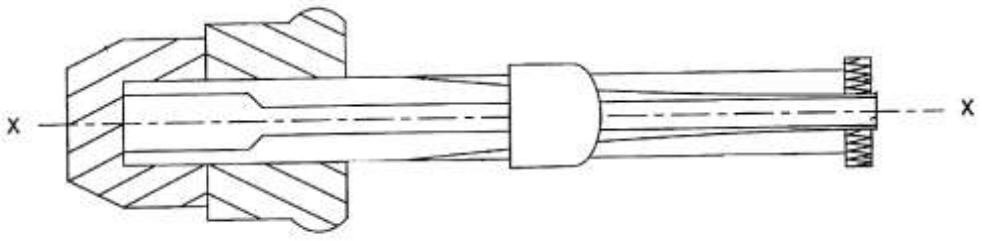

Figure 2-4. *Second type of TVA discussed in US Patent, 6,167,794 [11].*

2.3.3.2 An Application to piecewise linear beam system

An archetype piecewise linear beam when used in practice make uses of rubber snubbers to prevent panels striking to each other. If the pre-stress of snubbers is lowered to lose contact a piecewise linear beam system is seen as in ***Figure 2-5***. To reduce vibration amplitudes of such a system a tuned vibration absorber is used [12]
.

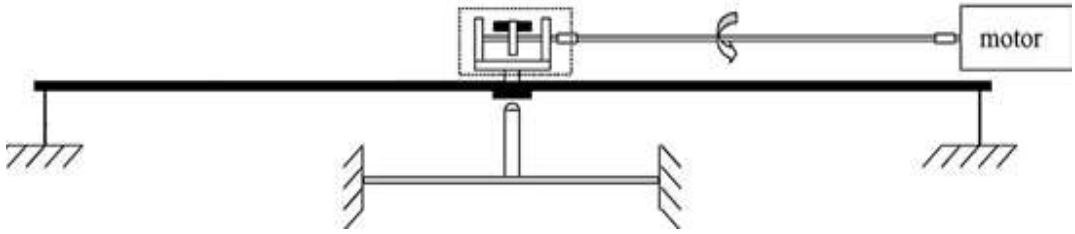

Figure 2-5. *A sketch of archetype piecewise linear beam system [12].*

The TVA is tuned to rotational frequency of the motor. Main mass of the TVA is 0.9 kg and on two sides two attached masses of 0.5 kg can slide to tune the TVA (See Figure 2.6 and Figure 2.7). When the undamped TVA is applied to system, it is seen that a stable anti-resonance occurs at the frequency of motor itself. New harmonic resonances occur at left and right of the anti-resonance. There are also many additional resonances occur at higher and lower frequencies due to new harmonic resonance. When the mass of the TVA is increased it is seen that two new resonance frequencies are further apart.

In the second part of the study a damped TVA is applied with 1kg mass and 38.2 Ns/m damping. Calculations show that damped TVA is able to suppress the harmonic resonance and also the newly formed harmonic resonances. Sketch for modified system with TVA is seen in ***Figure 2-6*** and physical design of such TVA is seen in ***Figure 2-7***.

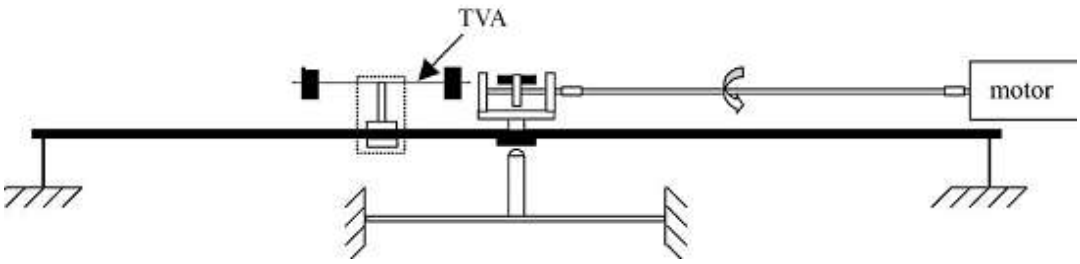

Figure 2-6. *A sketch of archetype piecewise linear beam system modified with TVA [12].*

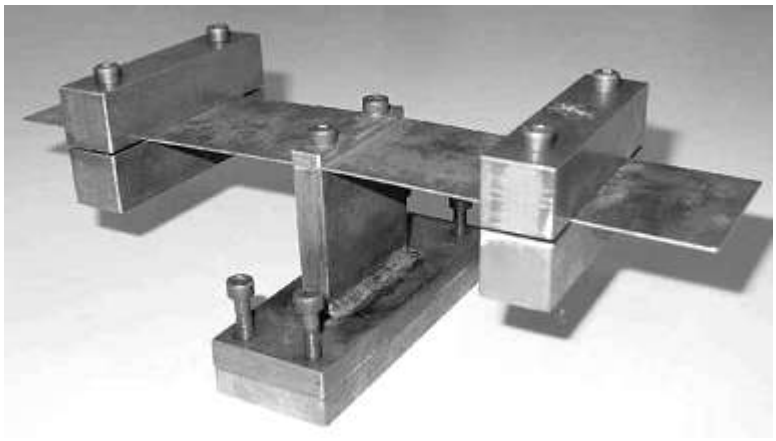

Figure 2-7. *Physical design of TVA applied to archetype piecewise linear beam system [12].*

2.3.3.3 An application to motorcycle handles

Another application of TVA is not because of improving dynamic properties but due to comfort issues. Motorcycles when operating vibrates to and higher vibration amplitudes may affect the drivers comfort badly. Since the driver holds and drives the motorcycle from handles, vibration amplitudes in handles are important and if can be controlled may help increasing the comfort of driver.

In their study Alessandro Fasana and Ermanno Giorcelli applied TVA to motorcycle handle and decrease the vibration amplitudes [13]. The design of TVA

is done according to first damping mode of the handle. The handle itself is modeled as a fixed-free straight beam whose characteristic properties are its length the area moment of inertia of the cross section and the material elastic modulus. (See Figure 2-8). The TVA is designed so that the stiffness and mass is able to be dismounted and changed. A sketch for modified system is seen in ***Figure 2-8***, 3-D model of applied absorber and its components are seen in ***Figure 2-9***.

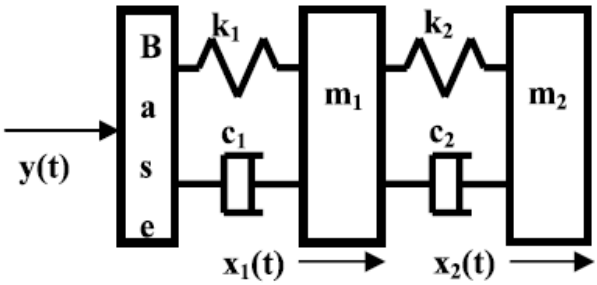

Figure 2-8. *Modeling of the handle and TVA system [13].*

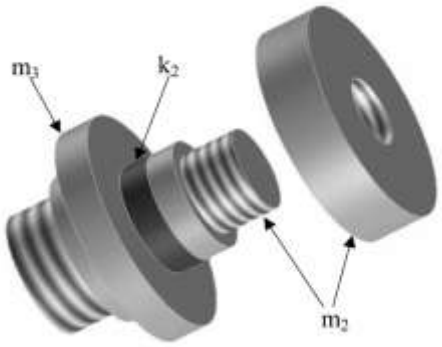

Figure 2-9. *Physical design of TVA [13].*

It is seen from the results that the presence of the absorber is positive and decreases the vibration amplitudes of handle than the original one. It is found that it is better not to tune the absorber on frequency of highest amplitude but to choose a lower frequency. Although the elastic modulus of rubber type materials used to include damping to system decreases with temperature, but it is found that its variation is

usually not so remarkable to lead to a complete mistuning of the absorber. To confirm material has been tested in an environmental chamber and in fact its resonant frequency varied less than 10% in the temperature range 0–30°C.

2.3.3.4 An application under point harmonic excitation

In their study M. Najafi, M.R. Ashory, E. Jamshidi studied two types of vibration absorbers; translational and rotational [14]. The finite element clamped-clamped beam model is obtained and this model is excited by a harmonic forcing a sketch for the setup is seen in ***Figure 2-10***. The best position for mounting the translational and rotational absorbers has to be found in an optimization procedure conducted for two cases: firstly when the translational and rotational absorbers are mounted at the same location, secondly when the translational and rotational absorbers are mounted at different locations on the beam.

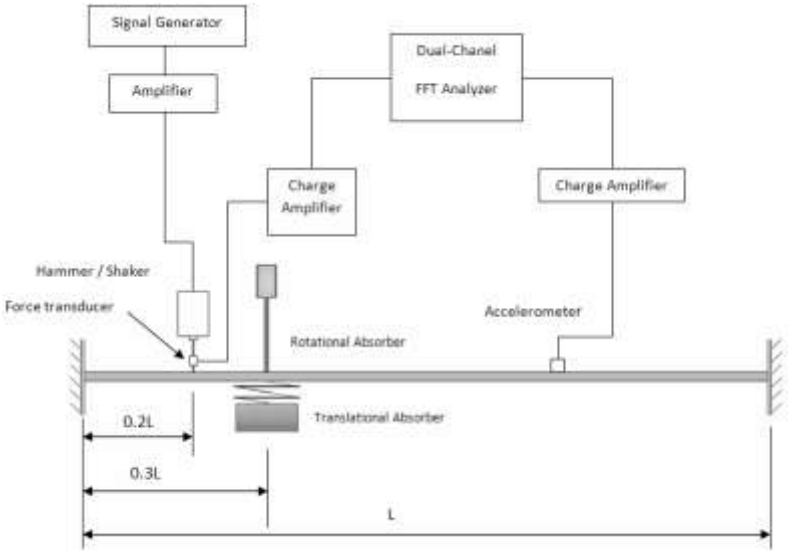

Figure 2-10. *Experimental setup sketch [14].*

The translational absorber was made of a cylindrical steel with a translational spring of stiffness 7500 N/m is seen in ***Figure 2-11***. The mass of the translational absorber is tuned by adding or removing the steel cylinders which is seen in Figure 2.11. The

rotational absorber is made of a steel beam with the added masses on its top the design allows that the location of the added masses and so the moment of inertia of absorber could be changed. The absorbers were fixed to the beam with glue.

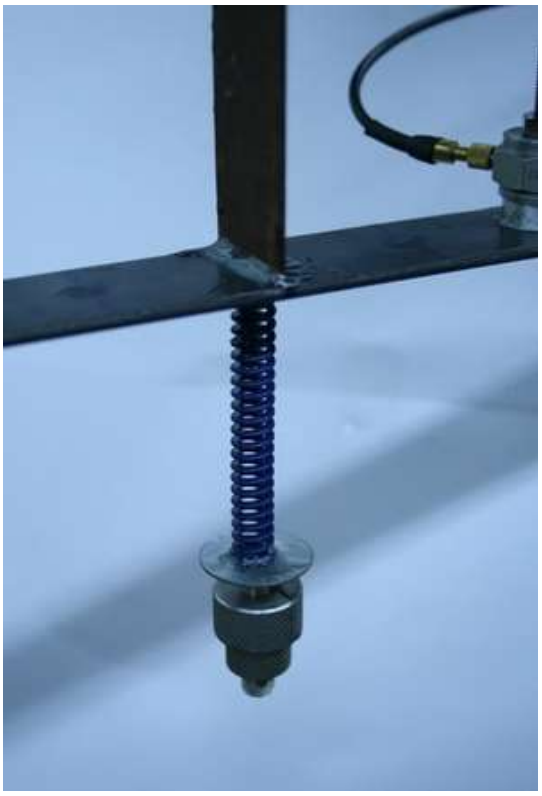

Figure 2-11. *Courtesy of translational absorber [14].*

In the end of the study it is found that minimum displacement is obtained when the combined translational and rotational absorbers are used in different positions along the beam.

2.3.3.5 An adaptive vibration absorber design for controlling multi modes

In their study Simon Hill, Scott Snyder and Ben Cazzolato studied a TVA that can be tuned to more than one modes of interest [15]. A successful example of this type of device is The Dog Bone vibration absorber which consists of a clamping device

and a rod with masses on each end. 3-D model of Dog Bone Vibration absorber is seen in ***Figure 2-12***. Although the design resembles the Stockbridge type vibration absorbers, It is found that by using an offset weight the manufactures claim that a torsional vibration mode can be induced and can be combined with its normal bending modes, and can control vibration modes beyond those available with the usual Stockbridge damper design.

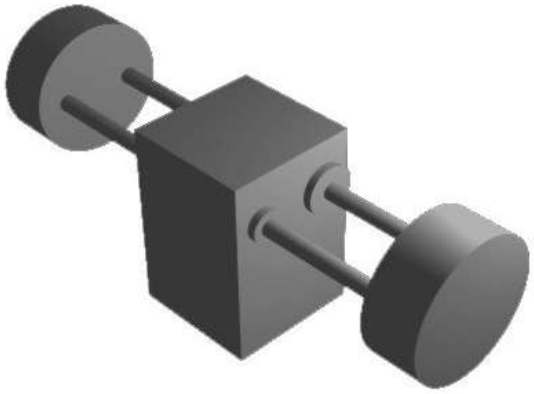

Figure 2-12. *3D model of dog-bone type vibration absorber [15].*

In this design the absorber consists of two rods supporting two equal masses on either side of a centre section. The absorber is attached to main structure from the centre section. One of the two rods is smooth and the other is threaded, with a stepper motor used to rotate the threaded rods masses are able to move And the absorber resonances are changed by this movement. Parameters such as the mass and dimensions of the bells, rod thickness and material, and the separation distance between the supporting rods are also affecting the tuning frequency. A valuable characteristic of this absorber is that the resonances can be modified independently. For the first two modes; rod diameter, mass and rod length can be played. The same applies for modes 3 and 4, however here the distance between the support rods is an additional factor affecting the stiffness of these modes. Since modes 5 and 6 are torsional, the moment of inertia becomes important. This is affected by the dimension of the masses. In ***Figure 2-13*** the mode shapes of TVA can be seen.

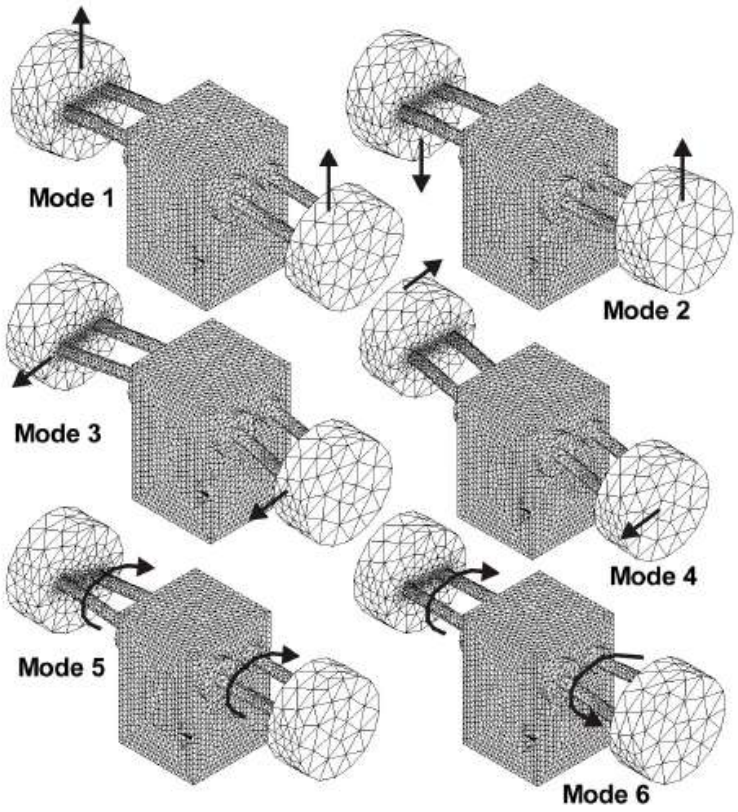

Figure 2-13. *Mode shapes of tuned vibration absorber. [15]*

2.3.3.6 An application for damping of lively structures

For human activities such as walking or running it is known that the activity itself leads to dynamic forces with large frequency content around 2 Hz. Hugo Bachmann and Benedict Weber studied tuned vibration applications for footbridges that are highly subjected to dynamic forces resulting from human activities [16].

Since footbridges are most commonly lightly damped they generate high vibration levels so they are called "lively". For the design stage harmonic forcing is assumed. Although it is known that the dynamic force applied by human activity is random in nature this simplification is appropriate for design purposes because a harmonic force leads to the maximum response and it is usually the critical case.

The parameters of absorber are found through optimization equations and fine tuning is done after installation. Since there is no space limitation the absorber mass is taken greater than the required and results show a fine decrease in vibration amplitude levels. In ***Figure 2-14*** a modified footbridge with application of TVA can be seen.

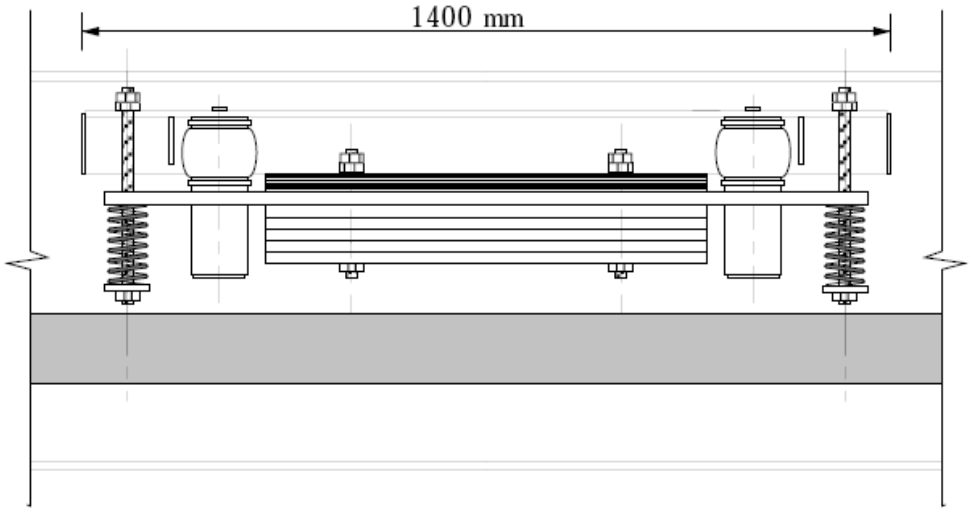

(a)

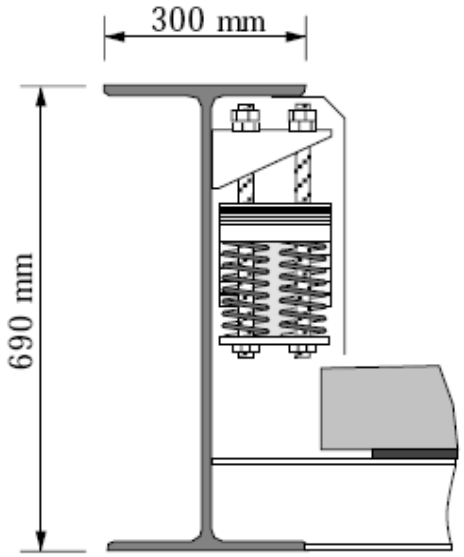

(b)

Figure 2-14. *Final design sketch of TVA applied to footbridge [16] (a) Front view. (b) Side view*

CHAPTER 3

VIBRATION ABSORBERS

In this chapter some basic expressions for tuned vibration absorbers are given. Most of the equations are for single degree of freedom (SDOF) systems hence for more detailed theoretical knowledge it is advised to check reference materials [9],[10] and [17]. In this thesis work TVA is planned to be used to suppress unwanted vibrations occurring at the free end of the gun barrel of a battle tank. In order to achieve such an objective, TVA parameters and their effects on system behavior must be well understood. In this chapter these parameters are studied for application to a generic vibration suppression problem.

As mentioned in Section 2.4, a TVA consists of a mass which is attached to system of interest through elastic and a damping element. Depending on the requirements of effective bandwidth for the specific vibration suppression problem, damper element may or may not be used. For example, for cases when the TVA should be effective in large bandwidth, largest possible damping should be present in the TVA design.

3.1 BASIC THEORY OF UNDAMPED TVA

The simplest form of TVA use for vibration control purposes consists of a mass (m_2) and a spring (k_2) attached to the main system (m_1 & k_1) can be seen in ***Figure 3-1***. Mass (m_2) and spring (k_2) represents the TVA while mass (m_1) and spring (k_1)

represents the dynamics of the structure on which the vibration suppression is required. .

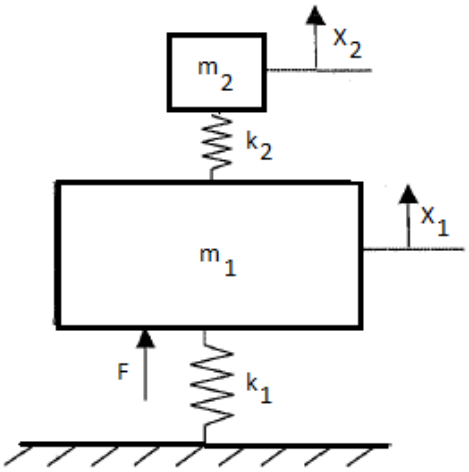

Figure 3-1. *Simplest form of TVA.*

For the system shown in ***Figure 3-1***, when the applied force is periodic with constant angular frequency ω_1 (F = Fsin ωt) and the natural frequency of the TVA ($\omega_2 = \sqrt{\frac{k_2}{m_2}} = \omega_1$) is chosen to be equal to that frequency ω_1; the system response i.e. x_1 becomes zero. To understand this phenomena and effect of parameters on the system response, equation of motion for the two DOF system is written down as follows [17]:

$$m_1\ddot{x}_1 + (k_1 + k_2)x_1 - k_2x_2 = F\sin\omega t$$
$$m_2\ddot{x}_2 + k_2(x_2 - x_1) = 0 \qquad \text{(Eq.3.1)}$$

Note that the system is undamped and the solution is of the form:

$$x_1 = a_1 \sin \omega t \quad \text{(Eq.3.2)}$$

$$x_2 = a_2 \sin \omega t \quad \text{(Eq.3.3)}$$

Substituting Equation 3.2 and 3.3 into Equation 3.1 and dividing both sides by sin ωt results in following algebraic equations:

$$a_1(-m_1\omega^2 + k_1 + k_2) - k_2 a_2 = F \quad \text{(Eq.3.4)}$$

$$-k_2 a_1 + a_2(-m_2\omega^2 + k_2) = 0 \quad \text{(Eq.3.5)}$$

Rearranging the above equations and defining some new variables results in the following expressions for vibration amplitudes [17]:

$$\frac{a_1}{x_{st}} = \frac{1 - \dfrac{\omega^2}{{\omega_2}^2}}{\left(1 - \dfrac{\omega^2}{{\omega_2}^2}\right)\left(1 + \dfrac{k_2}{k_1} - \dfrac{\omega^2}{{\omega_1}^2}\right) - \dfrac{k_2}{k_1}} \quad \text{(Eq.3.6)}$$

$$\frac{a_2}{x_{st}} = \frac{1}{\left(1 - \dfrac{\omega^2}{{\omega_2}^2}\right)\left(1 + \dfrac{k_2}{k_1} - \dfrac{\omega^2}{{\omega_1}^2}\right) - \dfrac{k_2}{k_1}} \quad \text{(Eq.3.7)}$$

Where, ω_i is defined as the natural frequencies of the TVA and the system modeled separately, i.e.

$$\omega_i = \sqrt{\frac{k_i}{m_i}} \quad \text{(Eq.3.8)}$$

and x_{st} is the equivalent static deflection of the mass of the system and defined as:

$$x_{st} = \frac{F}{k_1} = static deflection$$

Looking at the numerator of the Equation 3.6 in, vibration amplitude of the main system a_1 is zero when natural frequency of TVA is equal to the frequency of forcing (i.e. $\omega_2 = \omega$). If the absorber is designed to reduce the response amplitude of the system when it is excited at its resonance, then $\omega_1 = \omega_2$ and Equation 3.6 and 3.7 become: ($k_2 / k_1 = m_2 / m_1$)

$$\frac{a_1}{x_{st}} = \frac{1 - \frac{\omega^2}{\omega_1^2}}{\left(1 - \frac{\omega^2}{\omega_1^2}\right)\left(1 + \frac{m_2}{m_1} - \frac{\omega^2}{\omega_1^2}\right) - \frac{m_2}{m_1}} \qquad \text{(Eq.3.9)}$$

$$\frac{a_2}{x_{st}} = \frac{1}{\left(1 - \frac{\omega^2}{\omega_1^2}\right)\left(1 + \frac{m_2}{m_1} - \frac{\omega^2}{\omega_1^2}\right) - \frac{m_2}{m_1}} \qquad \text{(Eq.3.10)}$$

For this simple undamped case TVA is tuned to only exciting frequency thus absorbs all vibration energy of that mode to itself. The main system resonant frequencies are shifted from the original case. Assuming the excitation is only at the a single frequency main system does not vibrate at this tuning frequency; this is due to loss of damping and changed dynamic characteristics of the main system. Newly formed peak positions depend on mass ratio. Increasing the TVA mass increases the separation between the newly formed two peaks. In ***Figure 3.2*** one can see that the response amplitude of the system at the exciting frequency ω_1 is practically zero while as two new resonant peaks are formed with infinite amplitudes. If the excitation frequency of interest is ω_1, response at the new resonant frequencies is not of concern. In the figure mass ratio is denoted as μ.

$$\mu = \frac{m_2}{m_1} \qquad \text{(Eq.3.11)}$$

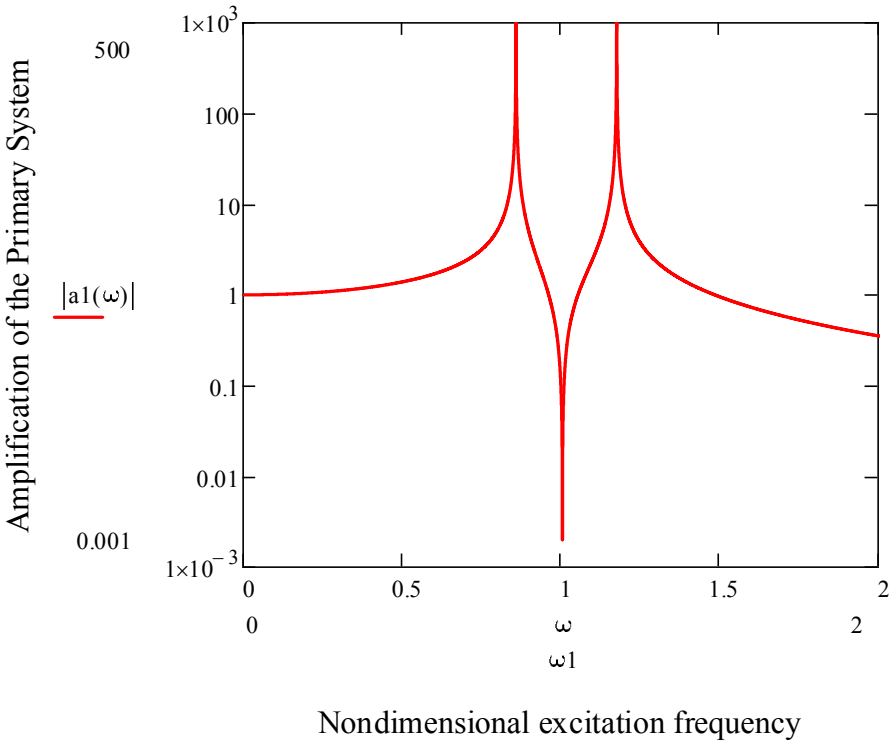

Figure 3-2. *Amplification of the primary system vs. nondimensional excitation frequency.*

The position of newly formed peaks seen in ***Figure 3-2*** is important since they represent the new resonant frequencies. The location of these peaks should be controlled for cases where excitation is not at a unique frequency but through a wider frequency band. If the frequency band is wide shifted peaks can still lie in the excitation frequency band and result in resonant response of the system. For further information one can refer to [17].

3.2 BASIC THEORY OF DAMPED TVA

It is known that if the frequency range of interest for vibration suppression using a TVA broadband, a damping element should be added to the TVA which may be

represented by a viscous damping element with constant damping coefficient c. Such a TVA is called a damped tuned vibration absorber. Equation of motions includes new damping terms as below:

$$m_1\ddot{x}_1 + c(\dot{x}_1 + \dot{x}_2) + k(x_1 - x_2) - k_1 x_1 = F\sin\omega t \quad \text{(Eq.3.12)}$$

$$m_2\ddot{x}_2 + c(\dot{x}_2 + \dot{x}_1) + k_2(x_2 - x_1) = 0 \quad \text{(Eq.3.13)}$$

The forced solution of this set of equations will be of the form:

$$x_1 = a_1\sin(\omega t - \phi_1) \quad \text{(Eq.3.14)}$$

$$x_2 = a_2\sin(\omega t - \phi_2) \quad \text{(Eq.3.15)}$$

With the newly added damping terms in order to make calculations and simplifications easier solutions are written in complex form:

$$x_1 = X_1 e^{j\omega t} \quad \text{(Eq.3.16)}$$

$$x_2 = X_2 e^{j\omega t} \quad \text{(Eq.3.17)}$$

$\boldsymbol{X_1}$ and $\boldsymbol{X_2}$ are complex amplitudes of responses of the TVA and system masses (of which the absolute values are $\boldsymbol{a_1}$ and $\boldsymbol{a_2}$ and phase angles are $\boldsymbol{\phi_1}$ and $\boldsymbol{\phi_2}$). Substituting the complex forms of the response terms in the equations of motion (Equations 3.12 and 3.13)

$$-m_1\omega^2 X_1 + j\omega c(X_1 - X_2) + k_2(X_1 - X_2) + k_1 X_1 = F \quad \text{(Eq.3.18)}$$

$$-m_2\omega^2 X_2 + j\omega c(X_2 - X_1) + k_2(X_2 - X_1) = 0 \quad \text{(Eq.3.19)}$$

Eliminating $\boldsymbol{X_2}$ from Eq. 3.19 and converting the equation 3.18 into an expression for $\boldsymbol{X_1}$ and taking the absolute value of the result, the harmonic amplitude of the main system mass to forcing amplitude ratio can be found as:

$$\frac{a_1}{F} = \sqrt{\frac{(k_2 - m_2\omega^2)^2 + \omega^2 c^2}{\left[(-m_1\omega^2 + k_1)(-m_2\omega^2 + k_2) - m_2\omega^2 k_2\right]^2 + \omega^2 c^2(-m_1\omega^2 + k_1 - m_2\omega^2)^2}} \qquad \text{(Eq.3.20)}$$

In order to decrease the number of variables, static deflection (x_{st}) mass ratio (μ), frequency ratio (f), forcing frequency ratio (v) and critical damping coefficient (C) terms are introduced, which converts Equation 3.20 into:

$$\frac{a_1}{x_{st}} = \sqrt{\frac{(2\frac{c}{C}v)^2 + (v^2 - f^2)^2}{(2\frac{c}{C}v)^2(v^2 - 1 + \mu v^2)^2 + \left[\mu f^2 v^2 - (v^2 - 1)(v^2 - f^2)\right]^2}} \qquad \text{(Eq.3.21)}$$

where,

$$f = \frac{\omega_2}{\omega_1}\ frequency ratio (tuning ratio)$$

$$v = \frac{\omega}{\omega_1}\ forcing frequency ratio$$

$$C = 2m_2\omega_1$$

Equation 3.21 depends on 4 main variables; 1) tuning ratio ***f***, 2) damping ratio of the TVA when it is taken as a SDOF system ***c/C***, 3) mass ratio $\boldsymbol{\mu}$, and 4) forcing frequency ratio ***v***. For different damping ratios of TVA response amplitude of main system vs. forcing frequency ratio is plotted in ***Figure 3-3***.

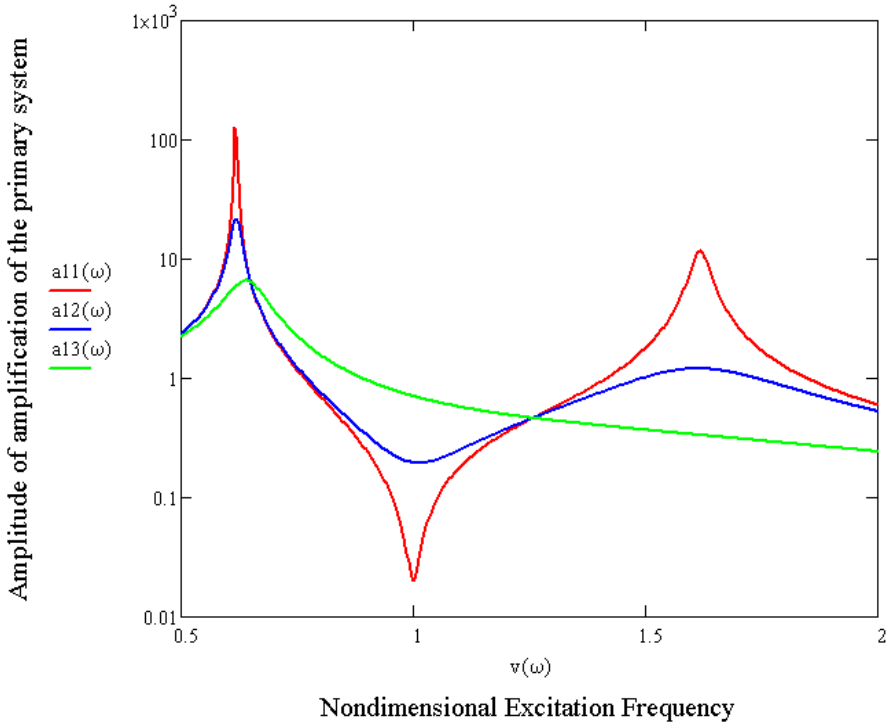

Figure 3-3. *Amplitude of amplification of the primary system vs. nondimensional excitation frequency. For different damping ratios: a11:* ***c/C=0,*** *a12:* ***c/C=0.1,*** *a13:* ***c/C=0.5***

It is shown in undamped case that assembling TVA increases the number of peaks, theoretically absorbing the all vibration at the single excitation frequency. Response amplitudes at the new resonant peaks go to infinity but since they are either not excited or not of concern, only the response at tuning frequency is investigated. In case the response in a broader frequency range was of concern, damping should be added to the TVA such that the newly formed resonances are damped as well as response is reduced in broader range that lies in between the resonant peaks.

Increasing the damping increases the energy dissipation of the system hence decreasing the system response in a different manner. As in the case of undamped case mass ratio has similar effect, they define the position of new resonant peaks. For a system where the excitation frequency is narrow applied damping can be

optimized. For infinite damping the system behaves like undamped SDOF system with a mass of 21/20 and k=k1. For damping ratio equal to zero undamped TVA properties can be seen. Optimum damping occurs in between. For the cases where excitation is wider in frequency domain increasing damping, decreases the main system response but this must be in physical limits. Amount of damping that can be introduced to TVA depends on physical properties of damping materials, TVA and available damping solutions. This subject is studied in detail in Chapter 5.

For the case of such systems where the excitation frequency is not narrow but spread over a wider frequency range, TVA is tuned not to excitation frequency but to first resonant frequency of the main system. Considering the case of white noise input excitation, first resonant frequency of TVA can be tuned to first resonant frequency of main system. This is due to lack of existence of a specific frequency of excitation dominating the response characteristics of the system.

In conclusion it is important to note one more time that for the case of broad band excitation in order to minimize the amplitude of system response, damping of TVA is at high importance. Increasing TVA damping leads lower response levels of the main system. The behavior of the TVA under such a condition is investigated in detail in Chapter 5. It is also important to note that for such broad band excitation increasing the TVA mass has almost negligible effect on system behavior. This is due to similar behavior of main system around the resonant peak, when new peaks are introduced to system due to TVA these peaks are also excited and similar responses are seen.

CHAPTER 4

FINITE ELEMENT MODELING OF GUN BARREL

Mentioned earlier in previous chapters, the objective of this thesis is to keep the vibration response of the free end of a long gun barrel used in a modern battle tank same as the vibration response level of the free end of the short gun barrel used in the same tank platform. In its original design, long gun barrel tends to respond more to dynamic displacement inputs coming from the base structure compared to the short barrel. It is planned to modify the long barrel at the free end using a properly tuned vibration absorber such that necessary vibration suppression is achieved. the motivation behind this design modification activity is the fact that the first round hit probability (accuracy) of gun systems is dependent on the vibration levels at the tip of the barrel thus with a new and long barrel should have a similar vibration response at its tip compared to the short barrel that it is replacing.

In order to properly design the TVA needed for this design modification the gun barrel must be modeled correctly so that correct tuning of TVA can be done. For tuning we need accurate representation of modal characteristics of both gun barrels such that their frequency response characteristics can be accurately represented. This chapter is reserved for building and validating a a proper structural dynamics model (specifically finite element based model) for a gun barrel which may be used for modeling both the short and long gun barrels. The design of the TVA is done in Chapter 5 accordingly.

In the first part of Chapter 4, a finite element model of the short gun barrel is prepared, where the 3D solid model is prepared using data available in the manufacturer catalogues. In the next part of the chapter, the finite element model of the short gun barrel model is verified by comparing the analysis results of the FEA to the results of the experimental modal analysis performed on a physical model of the short gun barrel. Comparison is made between both the modal frequencies and the mode shapes. In the third part, basing on the verified short gun barrel model, long gun barrel finite element model is constructed. In the final part of Chapter 4 part several analyses which are also specified mentioned in Section 2.3.4 are done on both models. At the end results are tabulated and summarized.

4.1 MODELING OF SHORTER GUN BARREL

The solid model of shorter gun barrel is constructed using data obtained from 3D scanner. The 3D scanner data is in the form of point cloud and converted to 3D solid model using Pro/E software. The accuracy of the solid model is verified with direct measurements done on barrel i.e. outer diameter of several regions of gun barrel and length of components are measured and compared with the solid model. The verified solid model is imported to ANSYS software to construct the finite element barrel model. For the finite element model, several element types are used for modeling different parts of the barrel.

In the construction of the finite element model, the component named elevation actuator, modeled in two different ways. . In the first one, the elevation actuator is modeled as a linear stiffness member with cylindrical joint that allows linear motion. In the second way, the elevation actuator is modeled as a stiffness member without any linear motion allowance. Both models are constructed using ANSYS software and results are verified with experimental modal analysis. The effect of actuator stiffness is also investigated.

For the geometry and material properties of the gun barrel factory catalogues and literature survey is also used.

4.1.1. BARREL STRUCTURE AND COMPONENTS

Before constructing the finite element model of the long barrel solid model taken from scanner data is constructed. The gun barrel consists of mainly the gun tube, gun breech, cradle, shielding, thermal shrouds and bore evacuator. 3-D Pro/E model of gun barrel is seen in ***Figure 4-1***.

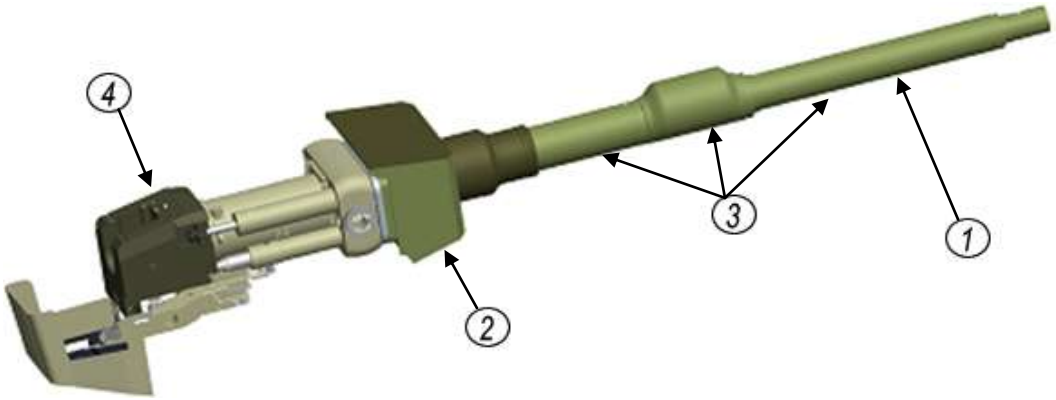

Figure 4-1 *Overall view of gun barrel.1) Gun Tube. 2)Shielding and add-on armor. 3)Bore evacuator and thermal shrouds. 4)Rear Components.*

According to factory data and literature survey, gun tube properties are given in ***Table 4-1***, 3-D Pro/E model of gun tube is seen in ***Figure 4-2***.

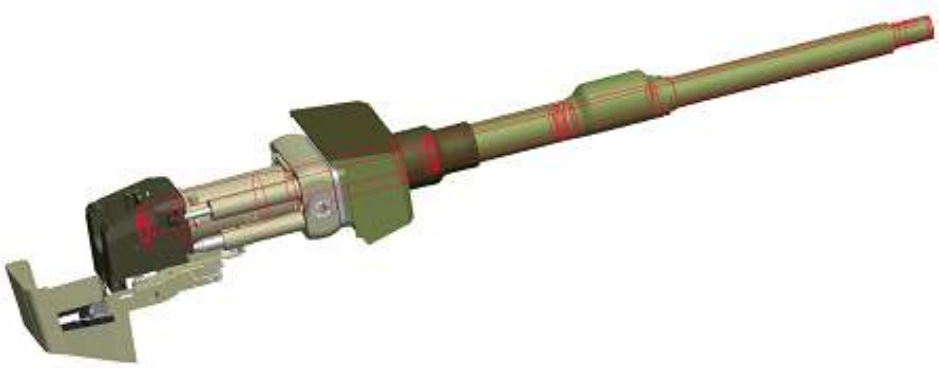

(a)

(b)

Figure 4-2 (a) *gun tube assembled to gun barrel. (b) Overall view of gun tube.*

Table 4-1 *Properties of gun tube.*

Weight (kg)	1165
Geometry, inner diameter (mm)	120 (smoothbore).
Length (m)	5.3
Material properties	Added vanadium carbon steel (0.4% Carbon)
Modulus of elasticity (Gpa)	207

The 3-D Pro/E model and location of shielding is seen in ***Figure 4-3***. For modernized main battle tanks as in the case of this study additional protection is provided by add-on armor. Although add-on armor properties are not defined

clearly, during the analyses and tests it is taken as 200kg. . Mechanical properties of shielding is given in ***Table 4-2***.

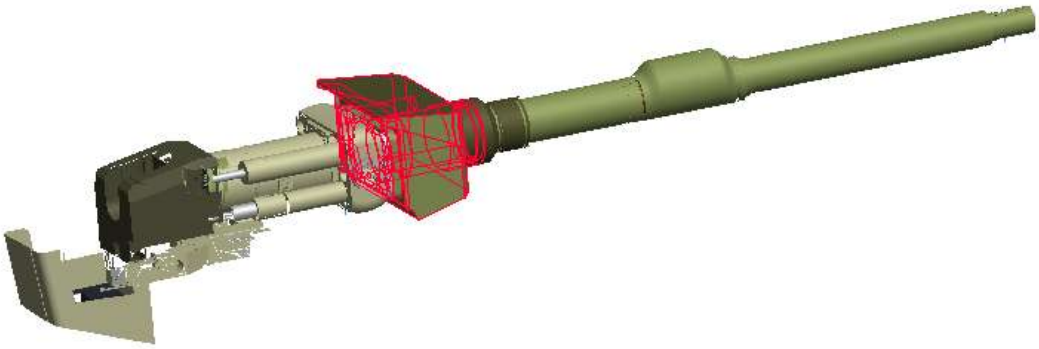

(a)

(b)

Figure 4-3. *(a) Shielding assembled to gun barrel. (b) Shielding solid model.*

Table 4-2. *Properties of shielding.*

Weight (kg)	650
Position of center of gravity w.r.to trunnion axis (m)	0.383
I_{zz} (kgm^2)	29.6

The 3-D Pro/E models of the bore evacuator and front thermal shroud can be seen in ***Figure 4-4***. The starting position of rear thermal shroud with respect to the trunnion axis is 0.8 meters. The length of rear shroud is 1 meter. Front thermal shroud is located 1.8 meters away from trunnion axis and it is 0.64 meters long. Bore evacuator is located in between and it is 1.46 meters long. Mechanical properties of thermal shrouds are given in ***Table 4-3***.

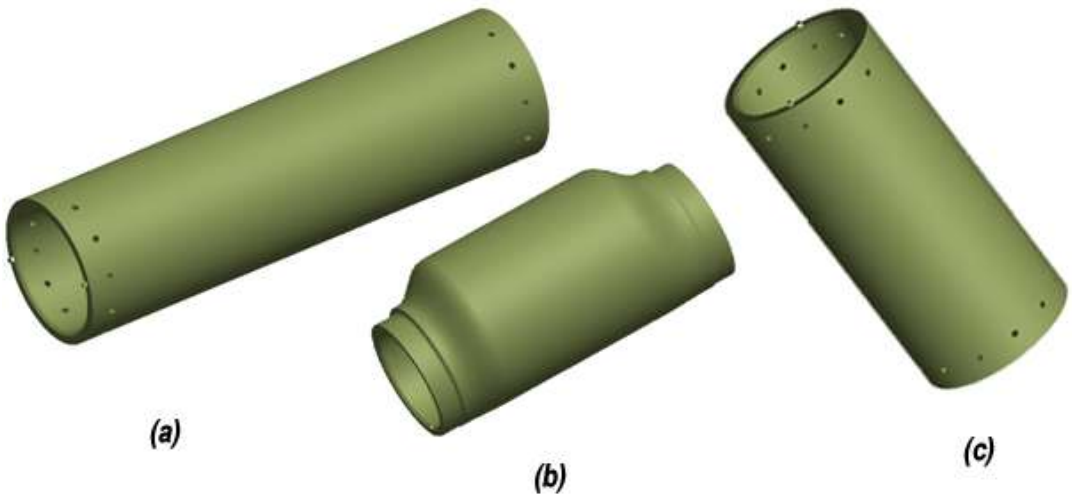

Figure 4-4. *(a) Front Thermal Shroud,(b)Bore Evacuator. (c) Rear thermal shroud.*

Table 4-3. *Properties of thermal shrouds.*

Weight of rear thermal shroud (kg)	13
Weight of front thermal shroud (kg)	14
Weight of bore evacuator (kg)	13.5

In ***Figure 4-5***, the 3-D model of rear components can be seen. Mechanical properties of the rear components are listed in ***Table 4-***4. The rear elements are assumed to be rigidly connected, total mass and position of center of gravity is determined using Pro/E software.

***Table 4-4**. Properties of rear elements.*

Total Weight (kg)	1845
Position of center of gravity w.r.to trunnion axis (m)	-0.515
I_{zz} (kgm^2)	667

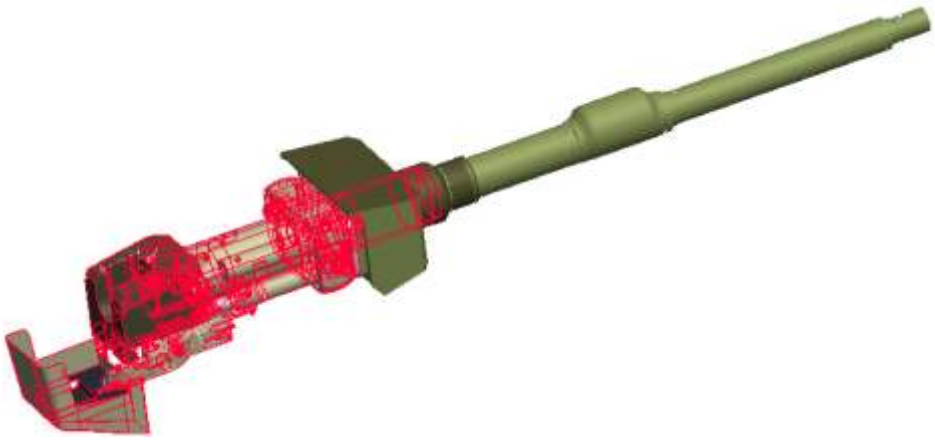

(a)

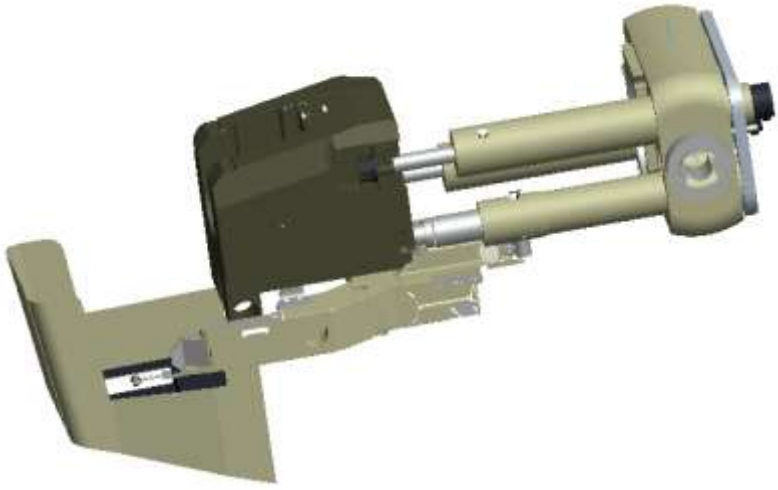

(b)

***Figure 4-5,** (a) Rear components assembled to the gun barrel. (b) Solid models of breech, cradle and rear components.*

4.1.2 MECHANISM ON THE ELEVATION PLANE

When the barrel is at zero position (parallel to tank body) the distance between the trunnion axis and the revolute joint of elevation motor is found to be -0.963 m along x-axis and -0.42 m. along y-axis. The length of the elevation motor at that position is 0.811 m. The 3-D model and representative view of gun barrel at that position is seen in ***Figure 4-6***.

The stiffness value of the actuator is taken from the manufacturer and it is $140 \cdot 10^6$ N/m. The moment of inertia of the motor shaft and gear assembly with respect to trunnion axis is 264 kg·m^2. Using the formulation below, this value is converted to be used along spindle axis. From the work-energy principle translational mass along spindle axis resembling the moment of inertia can be found. If amount of work is same for translation and rotation of the actuator if angular to translational velocity ratios are known inertia to mass ratio is also known. Using kinetic energy equations of translation and rotation translational mass of actuator can be found using equations 4.1, 4.2, 4.3 and 4.4.

$$Work = F \times d = m \times \ddot{s} \times s = m \times \frac{\dot{s}}{t} \times \frac{\dot{s}}{2} \times t = \frac{1}{2} \times m \times \dot{s}^2 \quad \text{(Eq.4.1)}$$

$$Work = \eta \times \theta = I \times \ddot{\theta} \times \theta = I \times \frac{\dot{\theta}}{t} \times \frac{\dot{\theta}}{2} \times t = \frac{1}{2} \times I \times \dot{\theta}^2 \quad \text{(Eq.4.2)}$$

$$\frac{1}{2} I(\dot{\theta})^2 = \frac{1}{2} M(\dot{s})^2 \quad \text{(Eq.4.3)}$$

$$for\, \theta = 0° \Rightarrow \dot{\theta} \big/ \dot{s} = 2.5127 \Rightarrow M = 1667kg \quad \text{(Eq.4.4)}$$

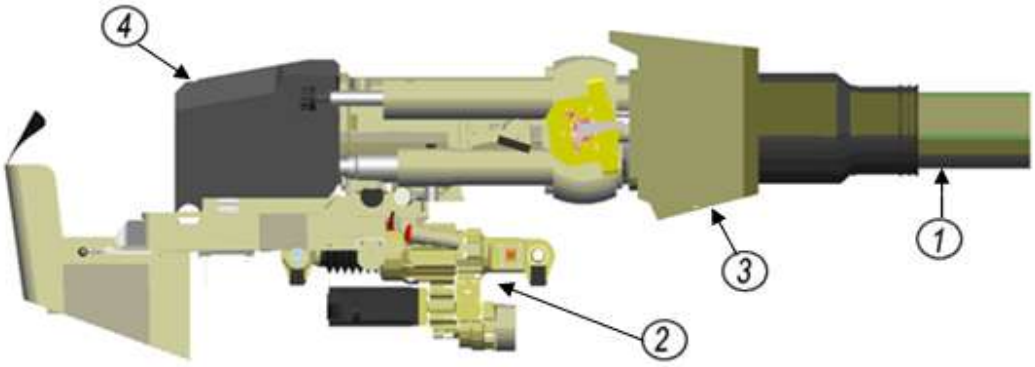

Figure 4-6. *Gun, elevation motor and the mechanism. 1) Gun Tube. 2)Elevation motor. 3)Shielding. 4)Rear Components.*

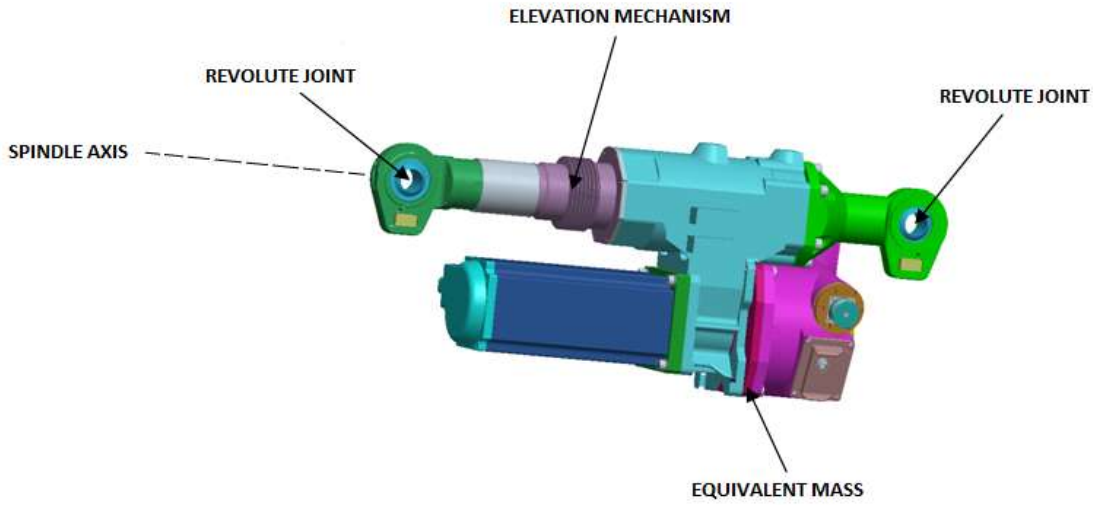

Figure 4-7*. View of elevation motor and its sub components.*

4.1.3 FINITE ELEMENT MODEL

As mentioned in the introduction of this chapter, ANSYS software is used to build the finite element model of the gun barrel. Gun tube is modeled as if it is made of

hallow cylinder beam elements of equal inner diameter and different outer diameters.

Prior to meshing steel is assigned as material with total weight difference from the catalogue value is less than 3%. The components at the back of the barrel (breech, elevation actuator, cradle, execution and suppression cylinders are considered to be rigid and all of them assigned as a point mass at the center of gravity of those components with defined equivalent moment of inertia with respect to trunnion axis. Both position of center of gravity and moment of inertia are found from 3-D model [18]. In order to simulate the rigid links of barrel to actuator connection, rigid beam elements are used.

Elevation actuator is modeled in two ways. Firstly elevation actuator is modeled as a spring element with revolute joints at both ends. Secondly it is modeled as if it has a slider joint in addition to spring element. In modeling following both ways equivalent mass and stiffness of the elevation motor is added. The whole elevation motor elements are connected to rigid tank turret with a revolute joint as it is the real case.

Thermal shrouds bore evacuator, breech, cradle and shields are modeled as point masses along the gun tube at their joint locations. During the trials of analyses it's seen that shrouds and evacuator have almost no effect on overall behavior of the system.

The global element edge length is taken as 0.05 m, which is found to be enough for accurate results after several runs of analyses. The results are verified to be healthy.

Not only the beam elements are used in modeling the gun barrel. For different parts of gun barrel different element type are used. Element types used in the finite element model of the gun barrel are given in ***Table 4-5*** [19].

The final model has a total of 116 nodes. Some important nodes are the node where the axis of rotation of the barrel is located. Another one is the free end of the barrel and the displacement and vibration energy level is recorded at that node. Another one is representing the rigid turret body where the actuator is connected from one end. The final gun barrel finite element model is given in ***Figure 4-10***.

Table 4-5. *Element types used in modeling of gun barrel [19]*.

Name of the element	***Definition***
BEAM 188	Used in 3D modeling of the gun tube 3D with cylindrical beam elements.
MPC 184	Used for defining rigid beam elements, revolute joints, and slider joint.
COMBIN 14	Used in modeling of stiffness of the elevation motor.
MASS21	Used to define point masses; one for the rear components of the barrel and one for the equivalent mass of elevation motor. Moment of inertia values are also assigned to MASS21 element.

After modeling the short gun barrel in ANSYS, modal analysis is done for verification of the model. Since the behavior of the elevation motor is not easily predictable, two different scenarios for the motor are tried out:

1 - Modal analysis with locked slider mechanism.
2 - Modal analysis with included slider mechanism.

For the first case, the slider mechanism and the mass effect of elevation motor is neglected since the motor mass that slides on the joint becomes a rigid part of the tank turret. Elevation motor behaves as it is a stiffness member only, at the end of the study for the first case first mode frequency vs. different stiffness values are plotted. In ***Figure 4-8*** representative view of locked slider-crank mechanism is seen.

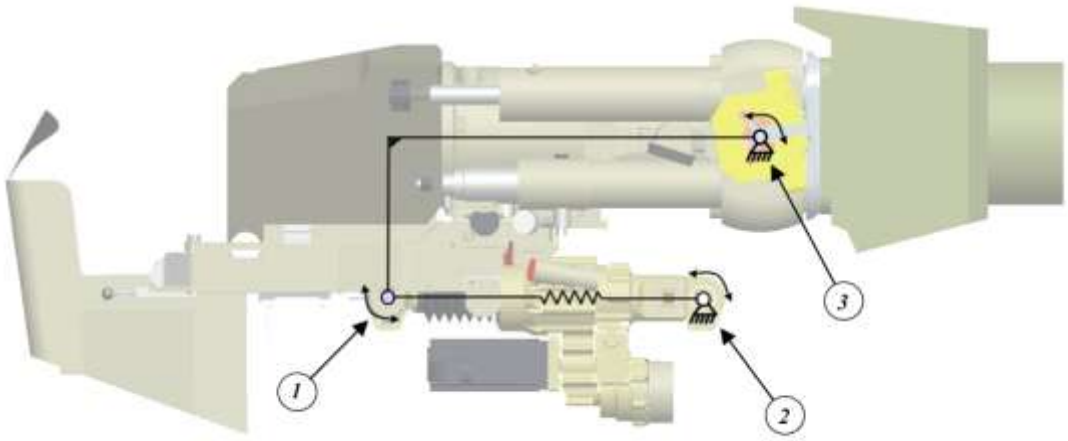

Figure 4-8. *Representative view of joints and links of locked slider mechanism model. 1) Revolute joint between the actuator and the barrel. 2) Pinned joint between the actuator and the turret. 3) Pinned joint between the barrel and the turret.*

For the second case the elevation motor is considered to be consisting of a spring and equivalent mass that slide on the slider mechanism. Due to natural effect of the slider mechanism the spring effect is lost and the gun barrel behavior becomes pinned-free. An additional degree of freedom from the elevation motor itself is added to the system. This degree of freedom is due to equivalent mass-stiffness of the motor and has little effect on gun barrel behavior. In ***Figure 4-9*** representative view of included slider-crank mechanism is seen.

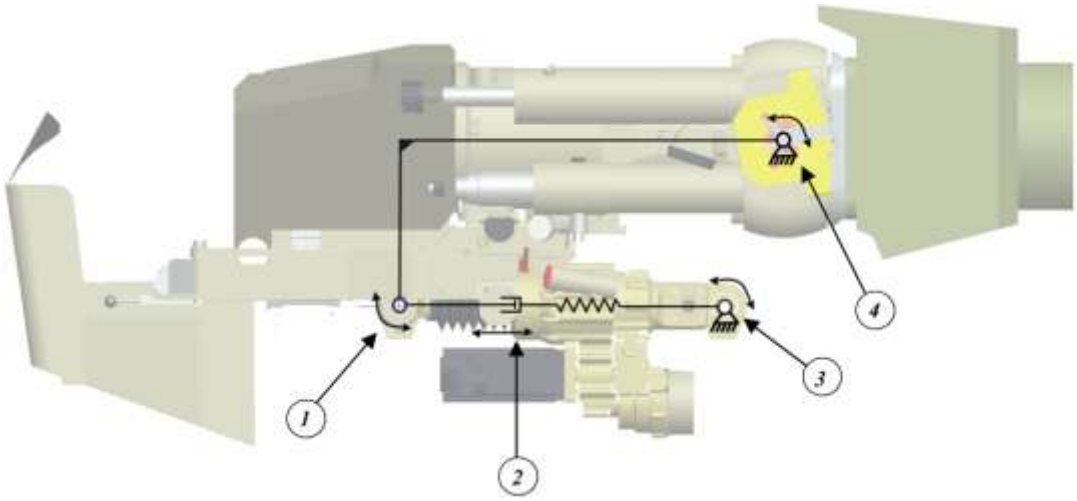

Figure 4-9. *Representative view of joints and links of included slider mechanism model. 1) Revolute joint between the actuator and the barrel. 2) Slider joint inside the actuator. 3) Pinned joint between the actuator and the turret. 4) Pinned joint between the barrel and the turret.*

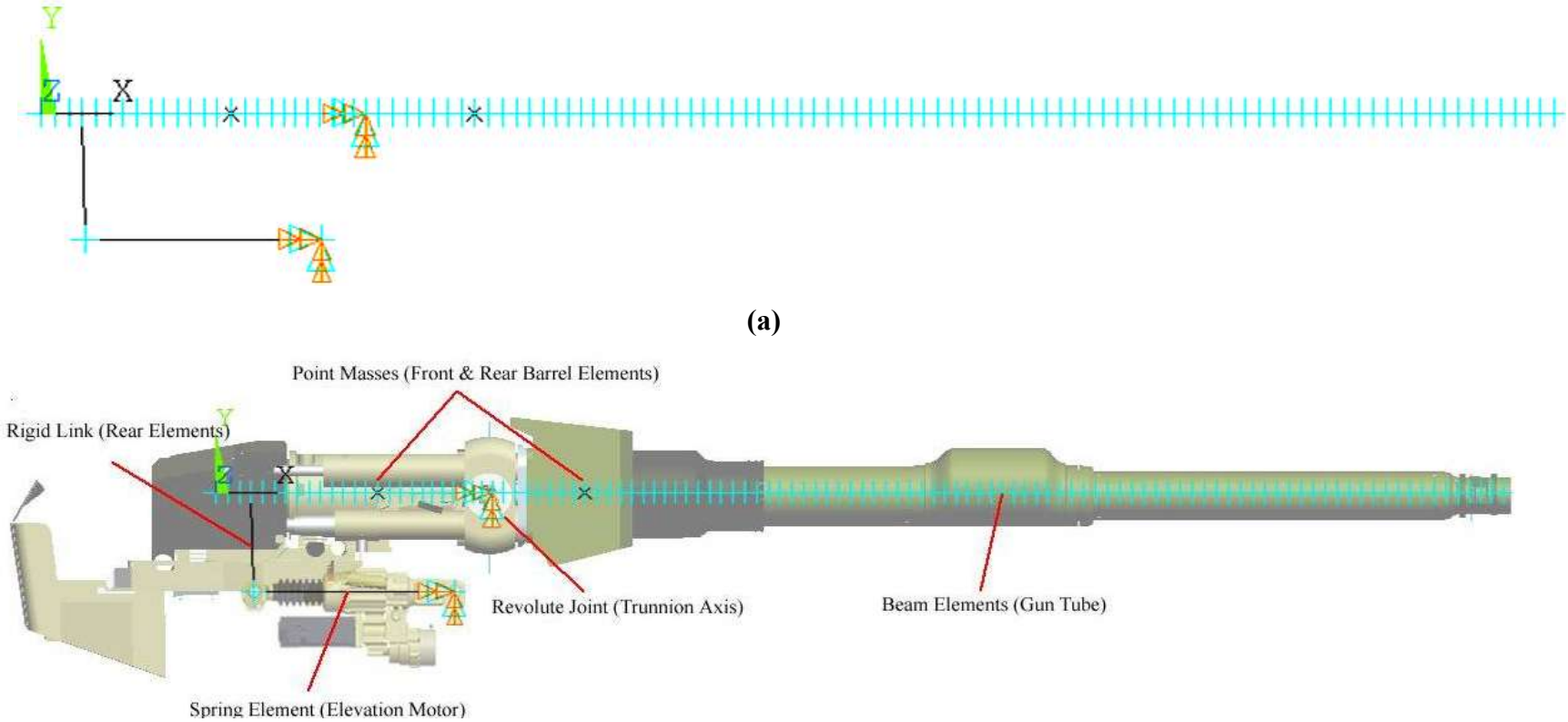

***Figure 4-10**. (a) Gun barrel finite element model. (b) Gun barrel solid and finite element model.*

4.1.3.1 Modal Analysis with Locked Slider Crank Mechanism

If the slider mechanism is fixed as seen in ***Figure 4-8***, the equivalent mass of the elevation motor is eliminated since it becomes a part of rigid tank turret. For this case the elevation motor behaves as it is a stiffness member that connects the rear of the barrel to the rigid tank turret (See ***Figure 4.9***). For different stiffness values, the natural frequencies and corresponding mode shapes are found. In ***Figure 4-11*** finite element model of the locked slider crank mechanism gun barrel is seen.

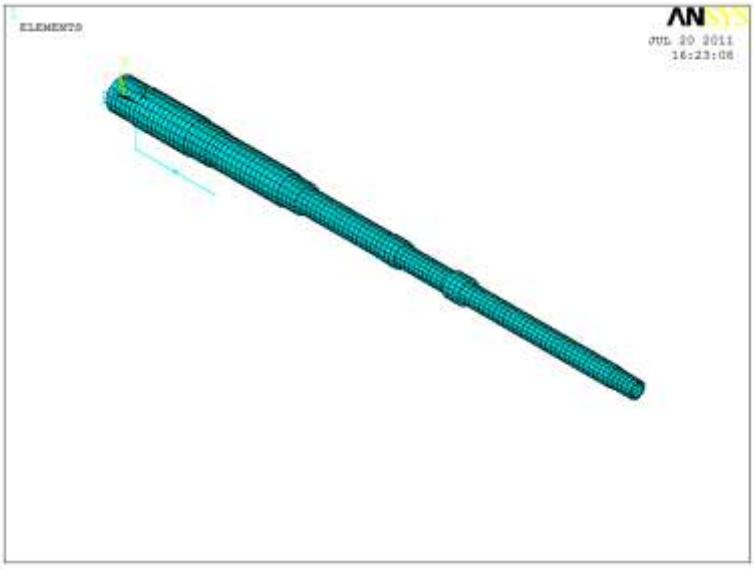

Figure 4-11. *Shorter gun barrel finite model with the elevator actuator mechanism modeled as a fixed slider mechanism.*

For the case of very low actuator stiffness, stiffness of the actuator is taken to be 140 N/m. It is found that for very low stiffness values, first mode frequency is 0 Hz hence the barrel behaves as it is pinned free from the trunnion axis. Mode shapes of gun barrel are given in ***Figure 4-12*** to ***4-14***. Resonant frequencies of mode shapes are tabulated in ***Table 4-6***.

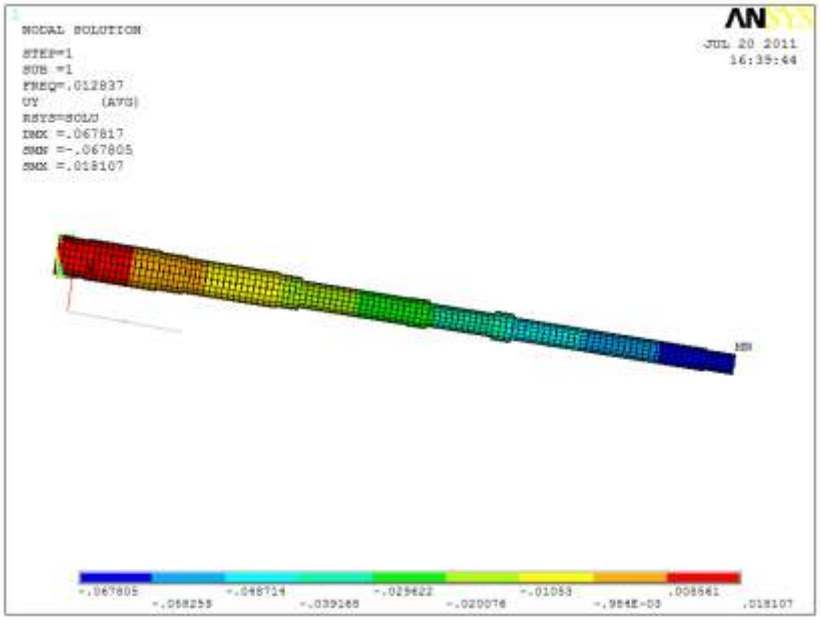

Figure 4-12. *Relative modal displacement distribution in y direction wrt. global coordinate system, 1st mode shape of short gun barrel for very low actuator stiffness (Scaled 10 times).*

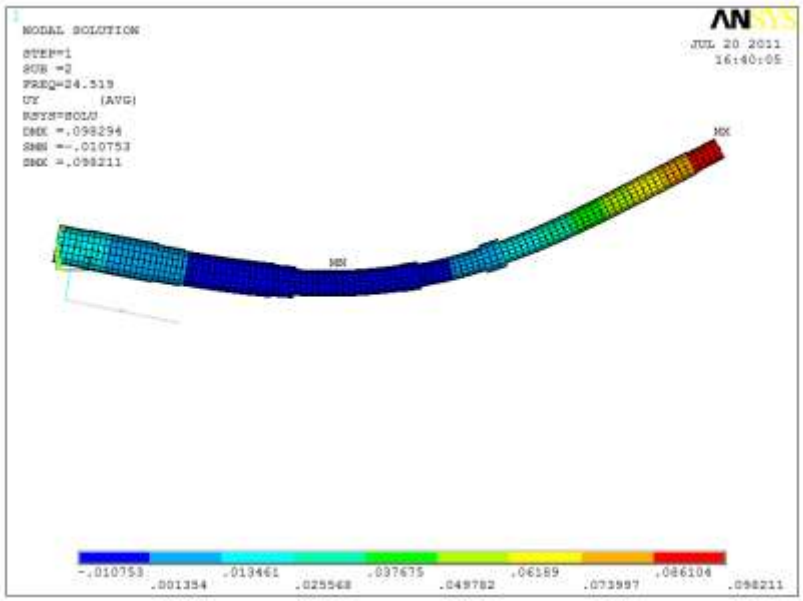

Figure 4-13. *Relative modal displacement distribution in y direction wrt. global coordinate system, 2nd mode shape of short gun barrel for very low actuator stiffness (Scaled 10 times).*

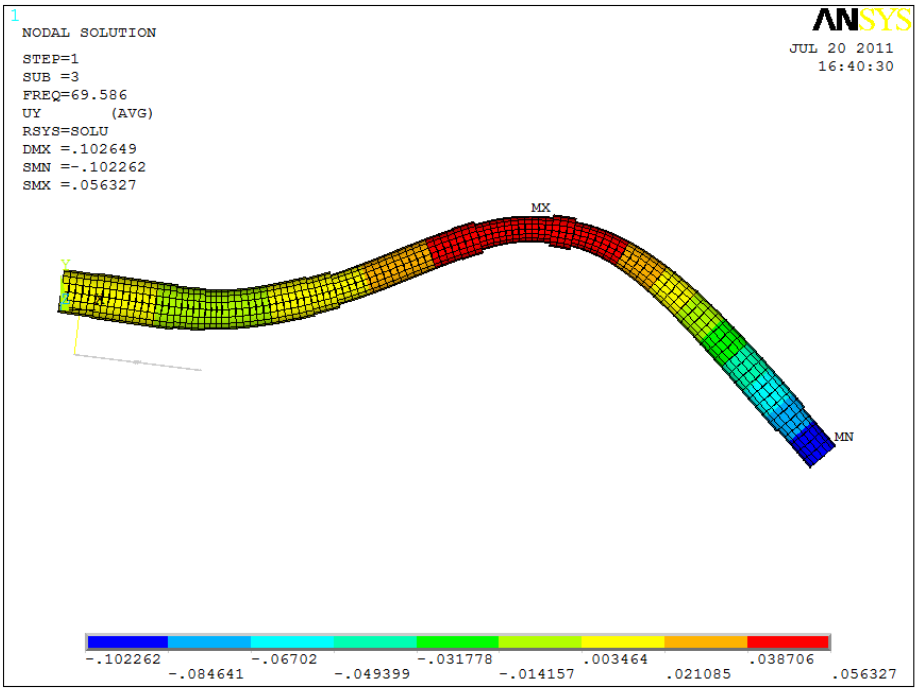

***Figure 4-14**. Relative modal displacement distribution in y direction wrt. global coordinate system, 3rd mode shape of short gun barrel for very low actuator stiffness (Scaled 10 times).*

***Table 4-6**. Resonant frequencies of barrel when actuator stiffness is very low.*

Mode Number	***Resonant Frequency (Hz)***
1	0
2	24.5
3	69.6

When the elevation motor is modeled with a high stiffness value i.e 2.5 e17 N/m gun barrel behaves as if it is fixed-free. In practice, this situation can be simulated by fixing the gun barrel to the roof of the turret. This connection is rigid and can give same results. It is seen that for higher mode number the effect of changing stiffness on resonant frequencies are getting less. Mode shapes are given in ***Figure 4-15*** to ***4-17***. Resonant frequencies of mode shapes are tabulated in ***Table 4-7***.

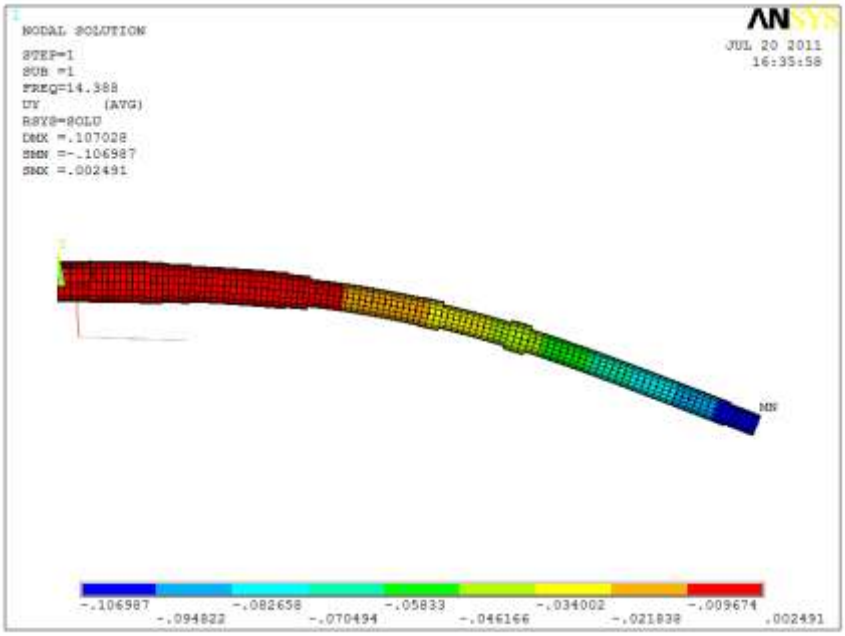

Figure 4-15. *Relative modal displacement distribution in y direction wrt. global coordinate system,* 1st mode shape of shorter gun barrel for very high actuator stiffness (Scaled 10 times).

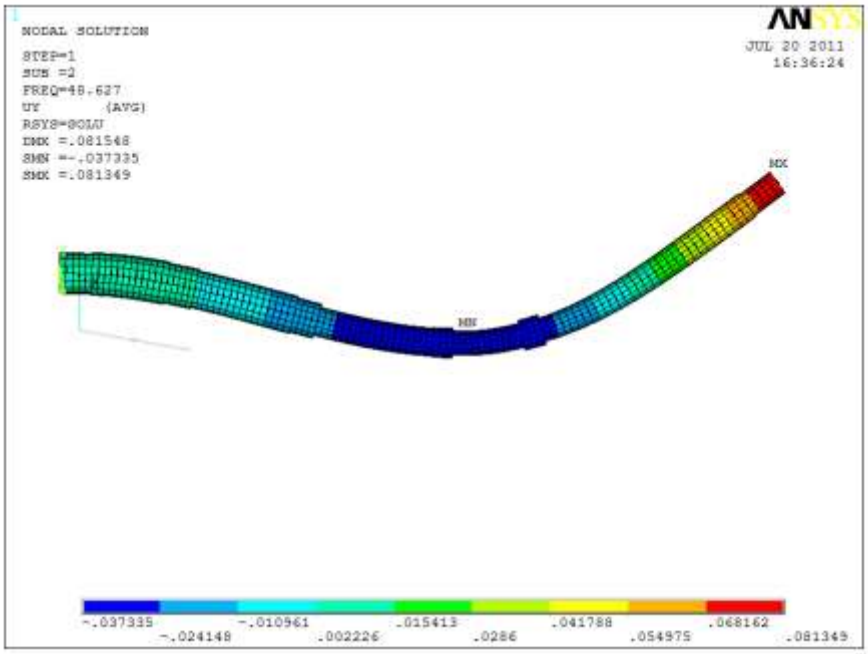

Figure 4-16. *Relative modal displacement distribution in y direction wrt.global coordinate system, 2nd mode shape of shorter gun barrel for very high actuator stiffness (Scaled 10 times).*

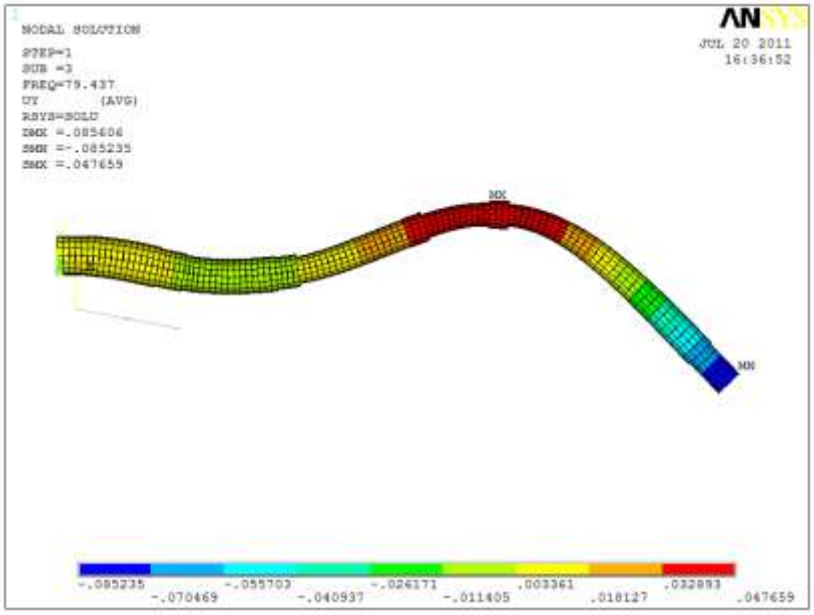

Figure 4-17. *Relative modal displacement distribution in y direction wrt. global coordinate system, 3rd mode shape of shorter gun barrel for very high actuator stiffness (Scaled 10 times).*

Table 4-7*. Resonant frequencies of barrel when actuator stiffness is very low.*

Mode Number	***Resonant Frequency (Hz)***
1	14.4
2	48.6
3	79.4

For the third case, the stiffness of the elevation actuator is assigned as its real value which is 140e6 N/m as obtained from the manufacturer. The results are in between the first 2 cases as it is waited. Change of stiffness value mostly affects the first mode frequency Mode shapes of gun barrel are given in ***Figure 4-18*** to ***4-20***. Resonant frequencies of mode shapes are tabulated in ***Table 4-8***.

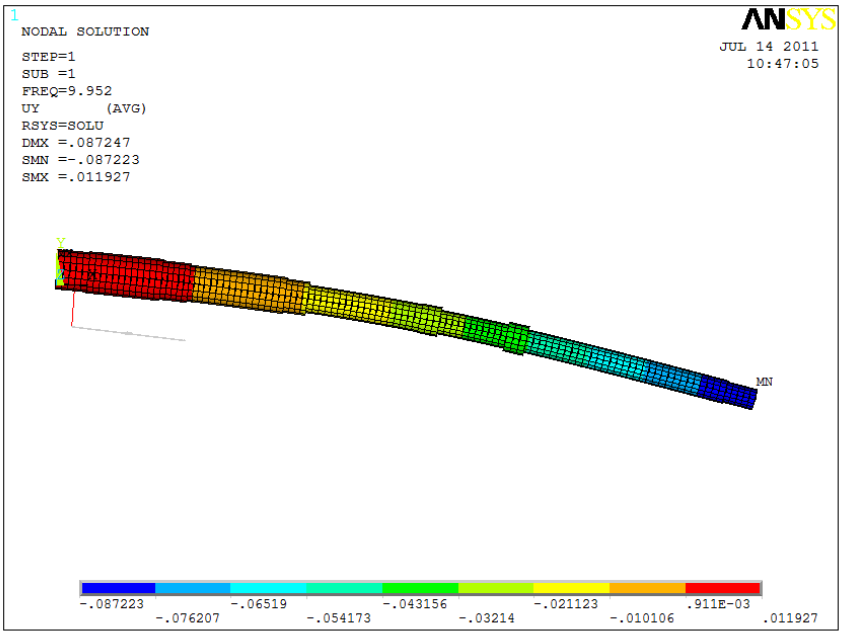

Figure 4-18. *Relative modal displacement distribution in y direction wrt. global coordinate system, 1st mode shape of shorter gun barrel for actual (medium) actuator stiffness (Scaled 10 times).*

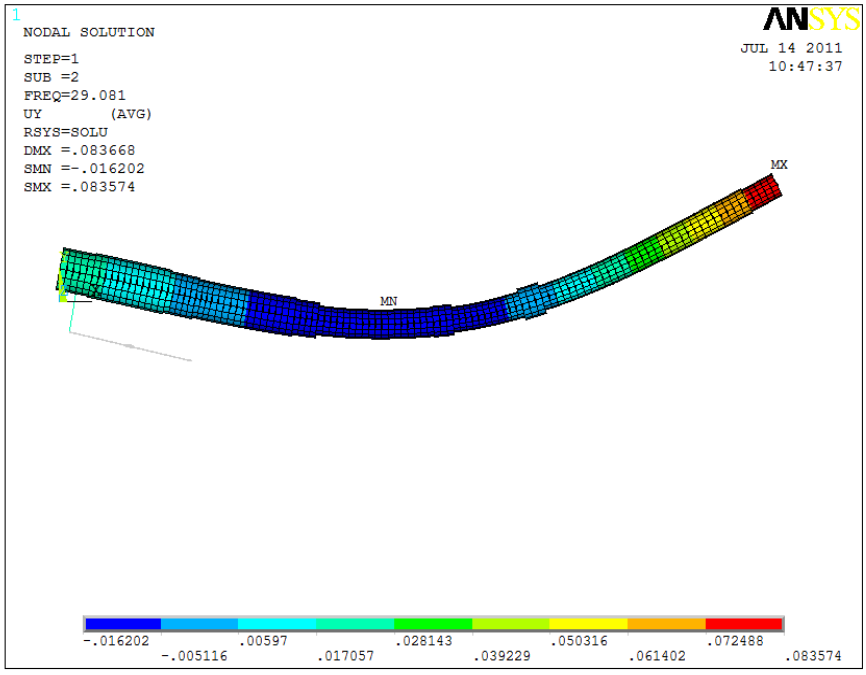

Figure 4-19. *Relative modal displacement distribution in y direction wrt. global coordinate system, 2nd mode shape of shorter gun barrel for actual (medium) actuator stiffness (Scaled 10 times).*

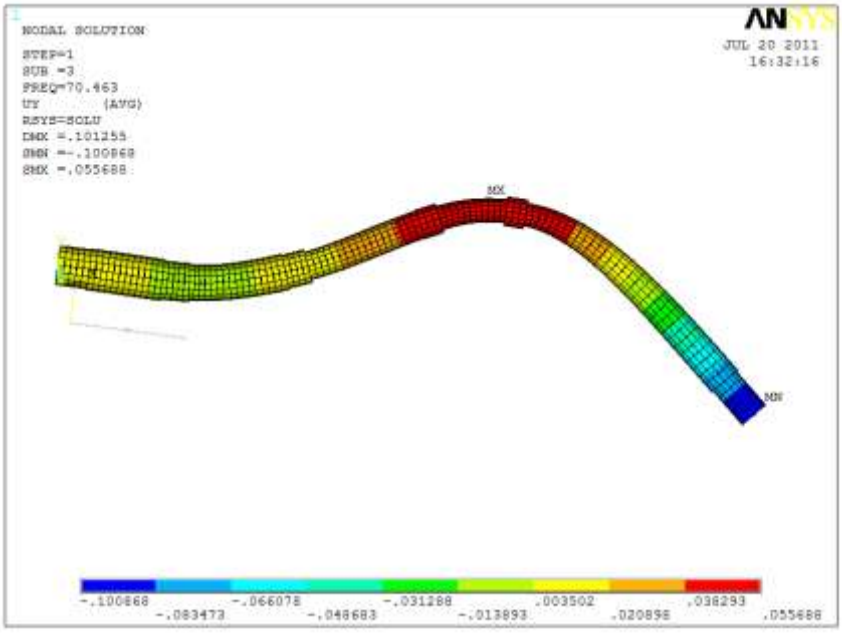

Figure 4-20. *Relative modal displacement distribution in y direction wrt. global coordinate system, 3rd mode shape of shorter gun barrel for actual (medium) actuator stiffness (Scaled 10 times).*

Table 4-8*. Resonant frequencies of barrel when actuator stiffness is very low.*

Mode Number	***Resonant Frequency (Hz)***
1	9.95
2	29.08
3	70.46

Dependency of first mode resonant frequency to stiffness value of the actuator motor is studied in ***Figure 4-21***. It is well seen that after very high stiffness values first mode frequency converges to its limit i.e. fixed-free case. For very low stiffness values first mode natural frequency converges to zero, i.e. the pinned-free case behavior found in plot is already verified with analyses done with different stiffness values.

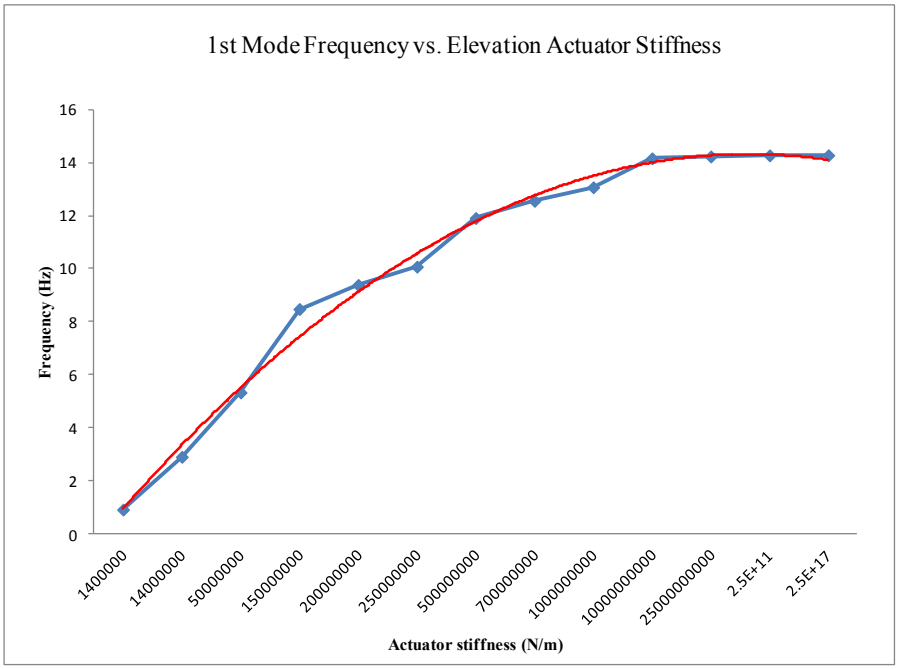

Figure 4-21. *1st Mode Frequencies vs. Elevation Actuator Stiffness*

4.1.3.2 Modal Analysis with Included Slider Mechanism

As the second alternative for assigning boundary conditions to finite element barrel model, time slider mechanism and mass of the actuator is included. Modal analysis are repeated and the modal frequencies and mode shapes are found. In this case the slider mechanism adds a degree of freedom along the spindle axis of the actuator and the behavior of the barrel is as if there is a very small or zero actuator stiffness which is already studied in previous chapter. The barrel is found to act like pinned free. When the elevation motor is being actuated and gun stabilization mode is on, the slider mechanism is assumed not to give such a freedom.

In ***Figure 22*** a detailed view of finite element model of the gun barrel is seen. M_o is the actuator mass and K_o is the stiffness of the actuator. M_o can slide along the direction of K_o and the actuator is connected to fixed turret with a revolute joint denoted as R1.

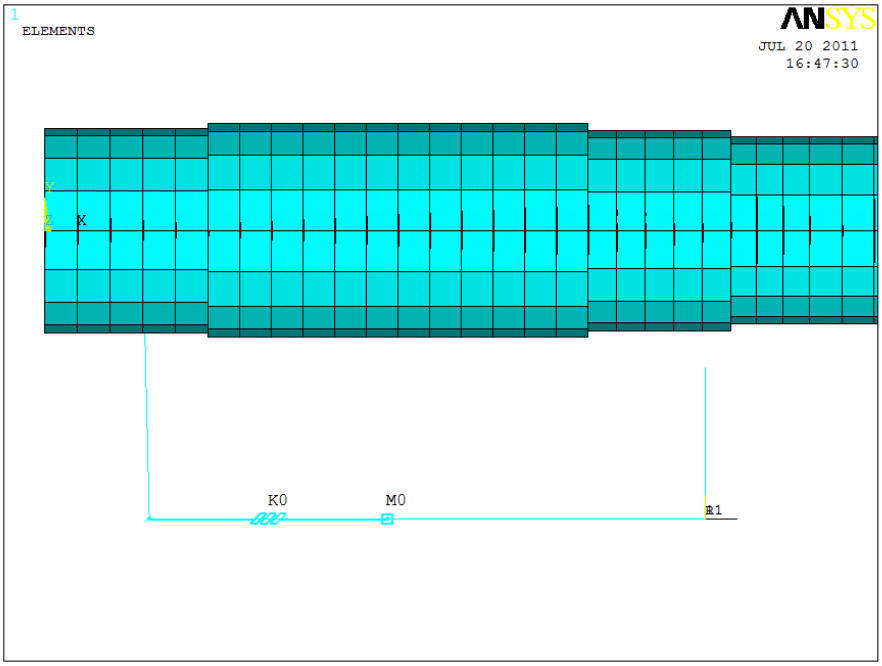

***Figure 4-22**. Finite Element model of gun barrel with included slider mechanism.*

In ***Figures 23*** to ***26***, resonant modes of gun barrel is seen. Due to additional degree of freedom coming from the sliding mechanism first mode is a rigid body mode which is seen in pinned-free beams. The results are also found to be very similar to low stiffness value analysis done in Case 1 presented in Section 4.1.4. It is also important to note that elevation actuator mass acts as an additional degree of freedom to system and at 46.392 Hz. there exists a local mode shape dominated by the actuator. In ***Table 4-9*** resonant frequencies are given.

***Table 4-9**. Resonant frequencies of barrel when slider-crank mechanism is included*

Mode Number	***Resonant Frequency (Hz)***
1	0
2	21.51
3	46.39
4	69.44

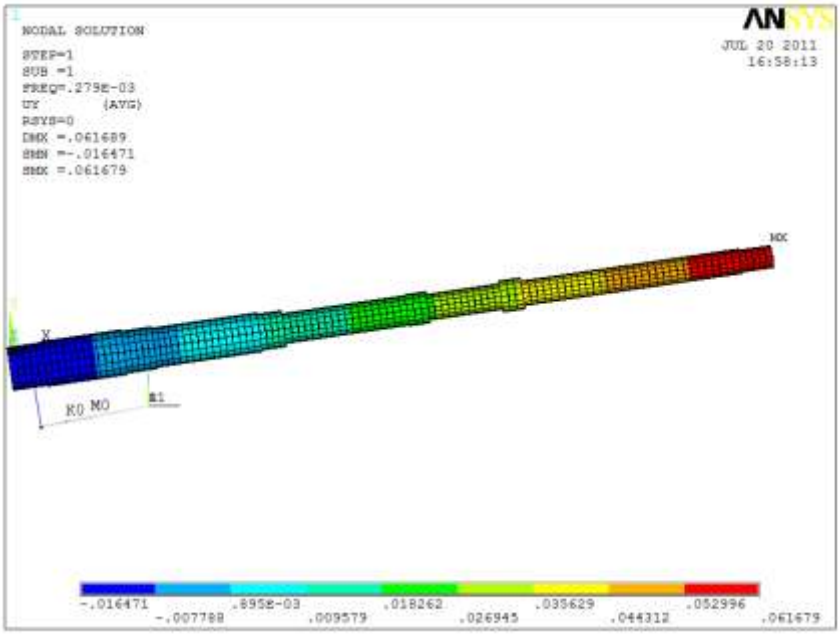

Figure 4-23 *Relative modal displacement distribution in y direction wrt. global coordinate system, 1st mode shape of shorter gun barrel with included slider mechanism (Scaled 10 times).*

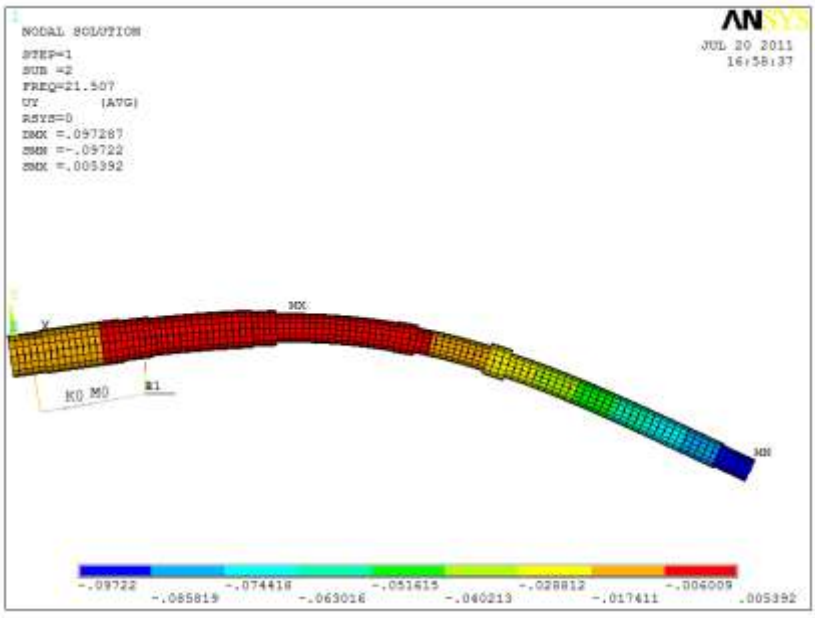

Figure 4-24. *Relative modal displacement distribution in y direction wrt. global coordinate system, 2nd mode shape of shorter gun barrel with included slider mechanism (Scaled 10 times).*

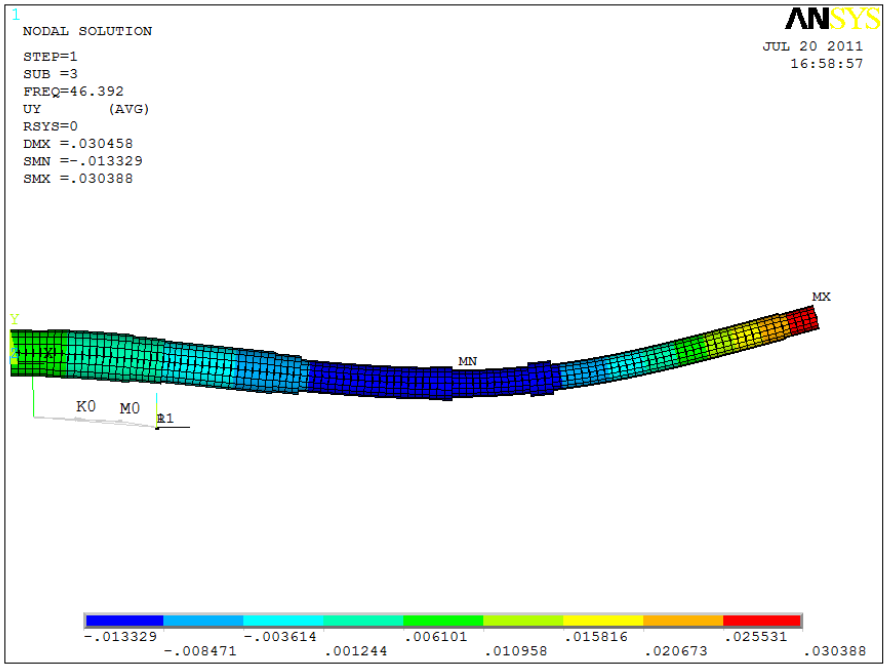

Figure 4-25. *Relative modal displacement distribution in y direction wrt. global coordinate system, 3rd mode shape of shorter gun barrel with included slider mechanism (Scaled 10 times).*

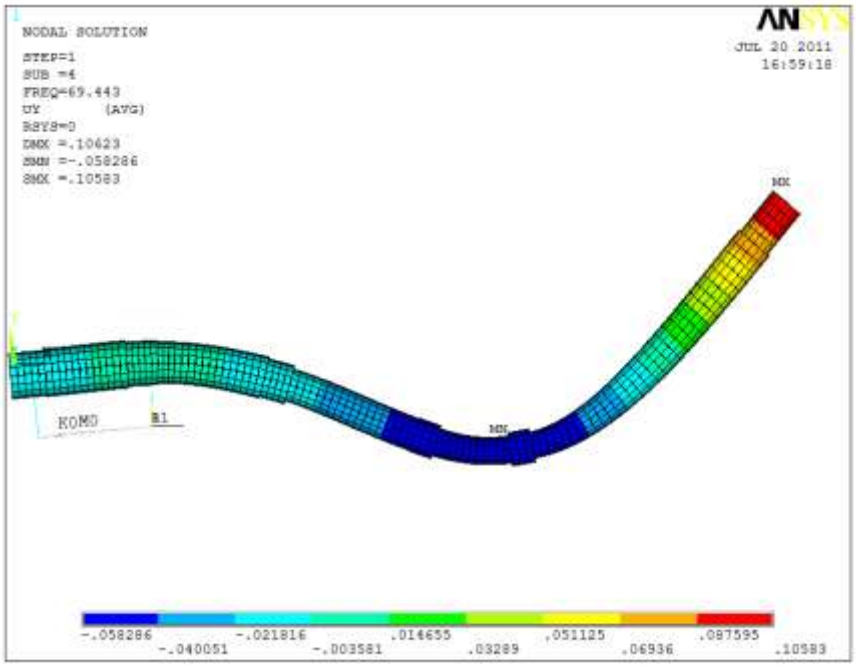

Figure 4-26. *Relative modal displacement distribution in y direction wrt. global coordinate system, 4th mode shape of shorter gun barrel with included slider mechanism (Scaled 10 times).*

4.2 VERIFICATION OF SHORTER GUN BARREL MODEL WITH MODAL TEST

Before modeling the longer gun barrel which is not yet manufactured the methods using in finite element modeling of short gun barrel must be verified. In previous sections short gun barrel is modeled with and without a slider mechanism and for different stiffness values the dynamic behavior of the short barrel is investigated. The verification of the true modeling is done on already manufactured short gun barrel using ASELSAN facilities. Experimental modal testing is done on the short gun barrel in lab environment. Test results are compared with the analyses results in order to verify the modeling technique.

Experimental modal testing of gun barrel is done by a single shaker fixed to ground. Shaker is directly connected to the force transducer. Pulse software is used for controlling, signal generating and analyzing the data.

Response is measured at 5 points by single axis accelerometers located along the barrel in downwards direction. Location of shaker and accelerometers are seen in ***Figure 4-27***. Sweep sine signal is generated by the software and signal is amplified using power amplifier. Although the test can also be done with random signal sweep sine signal is preferred since it can generate higher energy to excite the modes easily. During the test barrel is assembled to turret with trunnion axis. The actuator breaks are activated and holding the barrel. The turret is assembled to the main body of the tank (hull) which is standing on a suspension system.

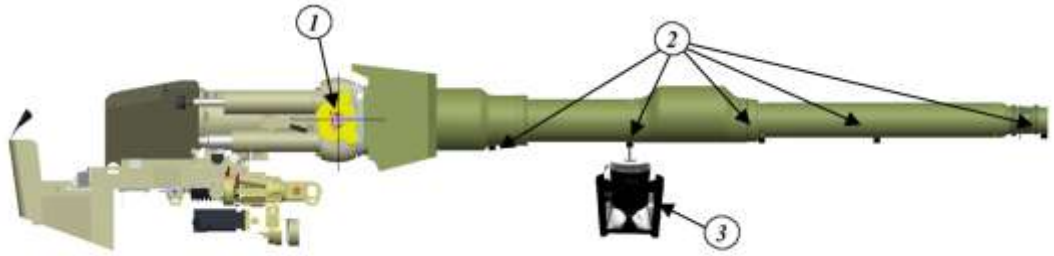

(a)

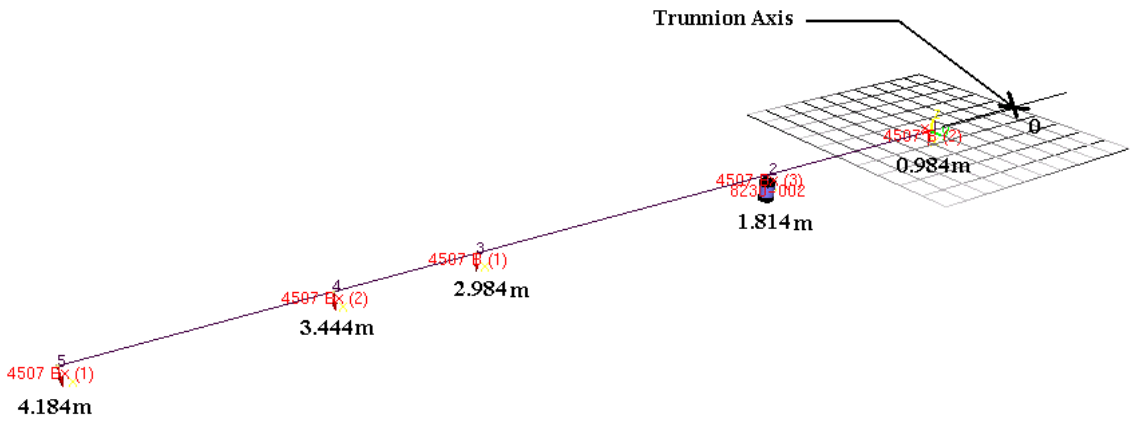

(b)

Figure 4-27. *Position of accelerometers used in experimental modal test with respect to trunnion axis.* ***(a)*** *Solid model 1) Trunnion axis. 2) Accelerometers. 3) Shaker.* ***(b)****Distances of accelerometers and shaker from trunnion axis.*

Figure 4-28 *Accelerometers are fixed to the gun barrel on several positions.*

Figure 4-29 *Shaker is located around the second accelerometer.*

Due to software and test safety issues elevation actuator brakes, kept active during the test. It is seen that active breaks simulate directly the locked slider-crank mechanism case studied in previous section.

A sample FRF and its coherence function obtained from the accelerometer at the free end of the barrel are given in ***Figure 4-30*** and ***4-31***. After obtaining FRFs, they are directly imported to ME'Scope (modal analysis software) for identifying the modal frequencies and the mode shapes.

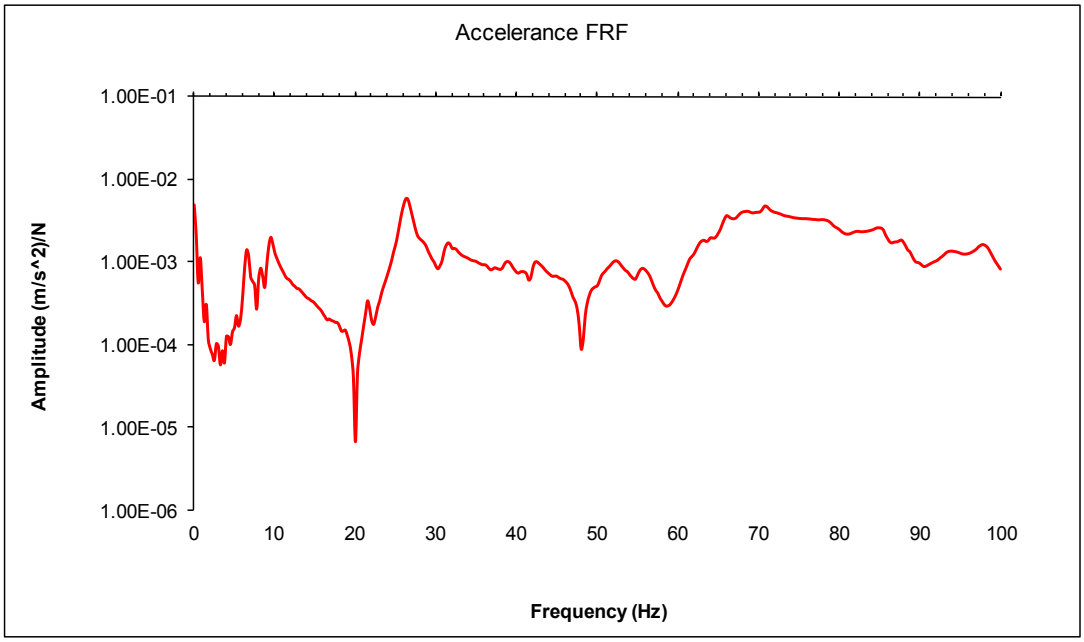

Figure 4-30. *Accelarance FRF obtained from the accelerometer at the free end of the barrel during modal testing.*

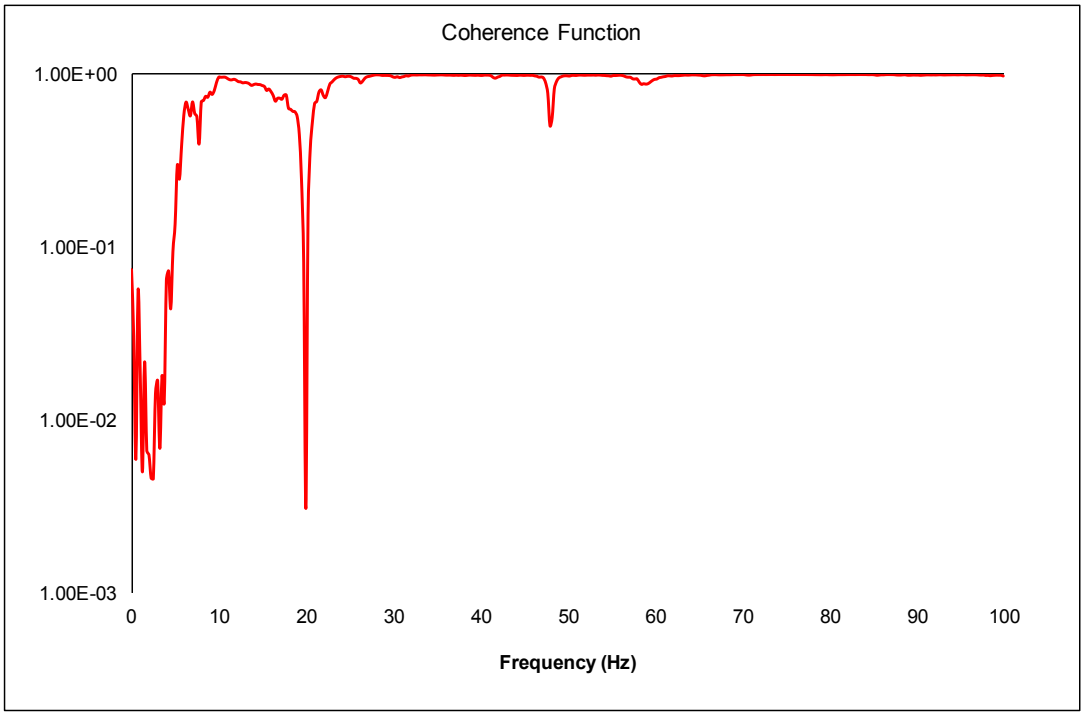

Figure 4-31 *Coherence function obtained from the accelerometer at the free end of the barrel during modal testing..*

From ***Figure 4-30*** resonant peaks are seen at around 6 Hz, 9 Hz, 25 Hz. The peak positions are relevant with analysis results. ME'Scope software gives mode frequencies and mode shapes in detail. A small resonant peak at around 20 Hz seen but looking at coherence function there is a drastic drop at that region. From the mode frequencies found from the software no resonant mode is seen at around 20 Hz. Coherence function is close to unity after around 20 Hz which proves the test results are healthy. Between 0-5 Hz coherence function is low and this is due to suspension effect coming from the hull of the tank. Looking at the mode shapes and frequencies it is seen that rigid body mode without bending dominates the modes at those regions. In ***Figure 4-32*** mode shapes found from experimental modal test is seen. In ***Table 4-10*** mode frequencies and damping properties are tabulated.

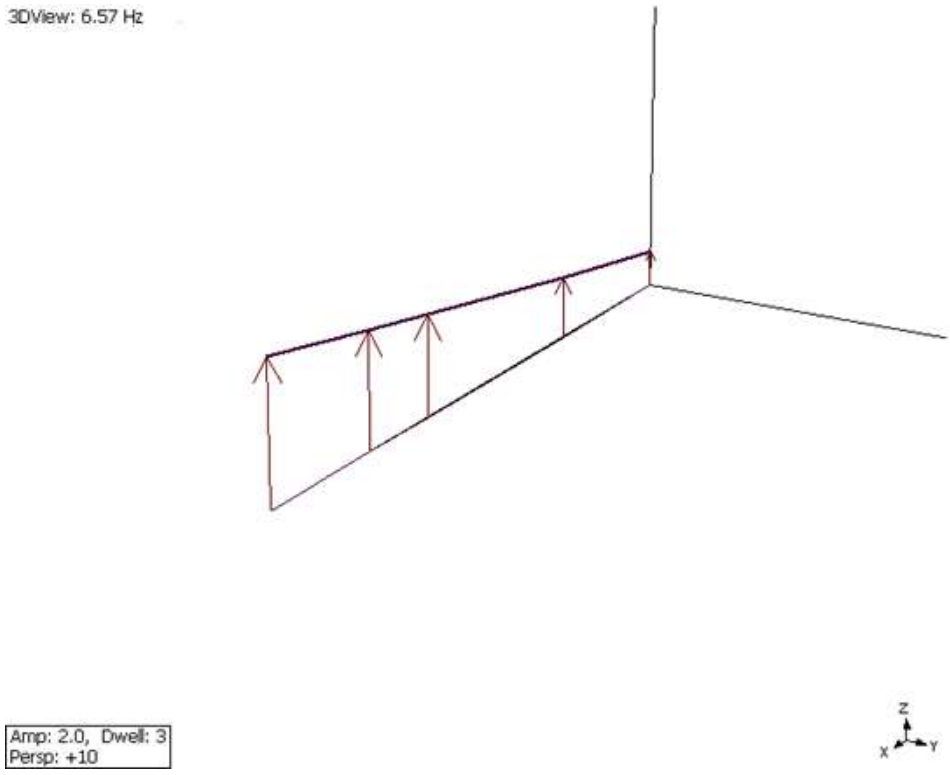

(a)

Figure 4-32.*Mode shapes obtained from modal testing.* ***a)*** *Mode at 6.57 Hz.* ***b)*** *Mode at 8.23 Hz.* ***c)*** *Mode at 9.39 Hz.* ***d)*** *Mode at 26.34 Hz.* ***e)*** *Mode at 31 Hz.*

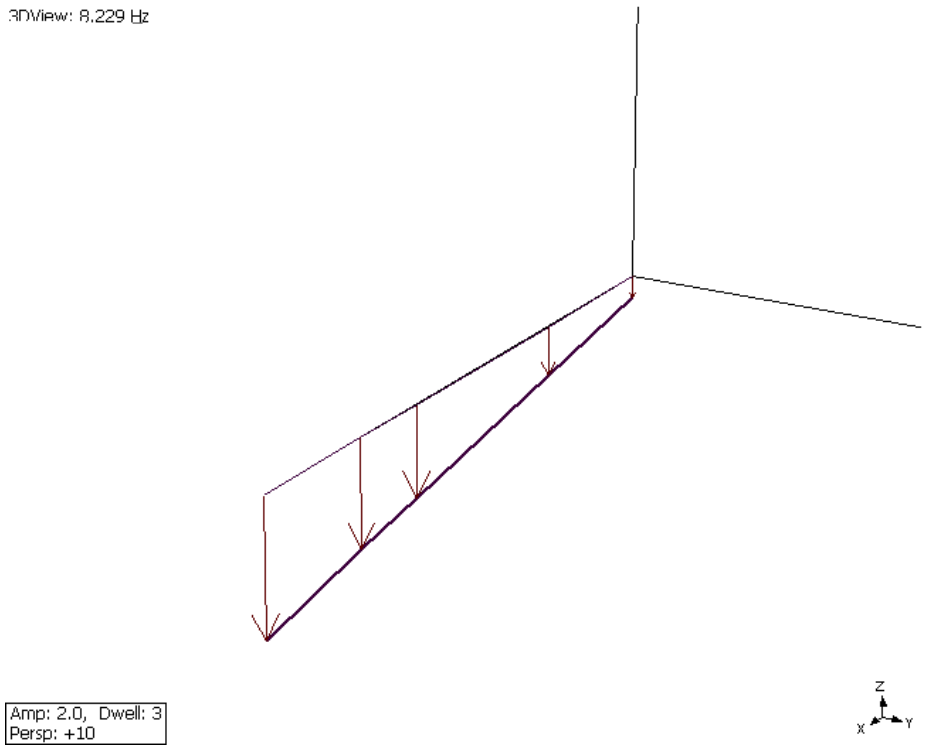

(b)

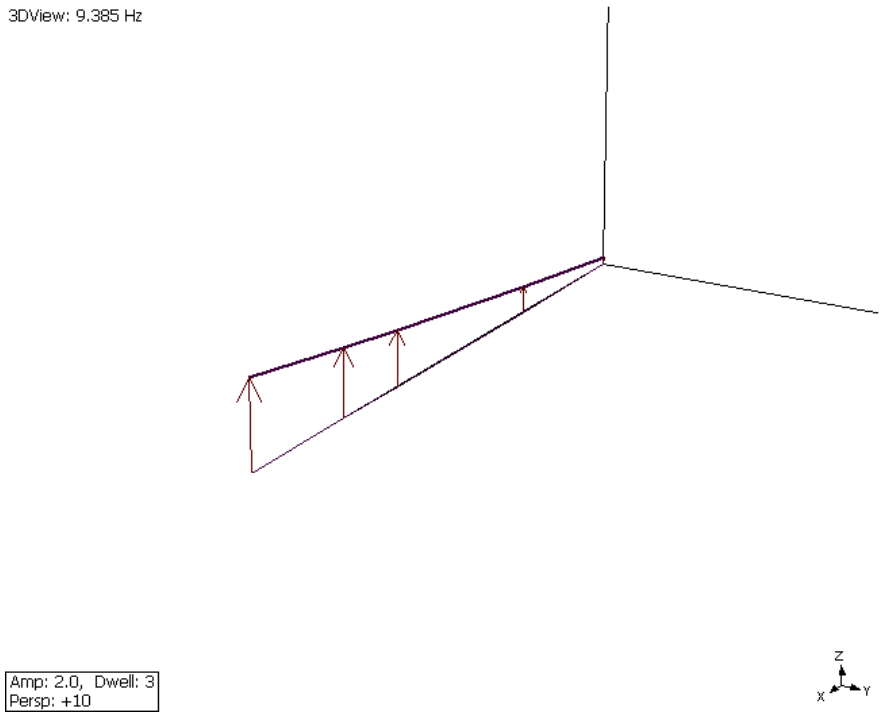

(c)

Figure 4-32. cont'd. *Mode shapes obtained from modal testing.* ***a)*** *Mode at 6.57 Hz.* ***b)*** *Mode at 8.23 Hz.* ***c)*** *Mode at 9.39 Hz.* ***d)*** *Mode at 26.34 Hz.* ***e)*** *Mode at 31 Hz.*

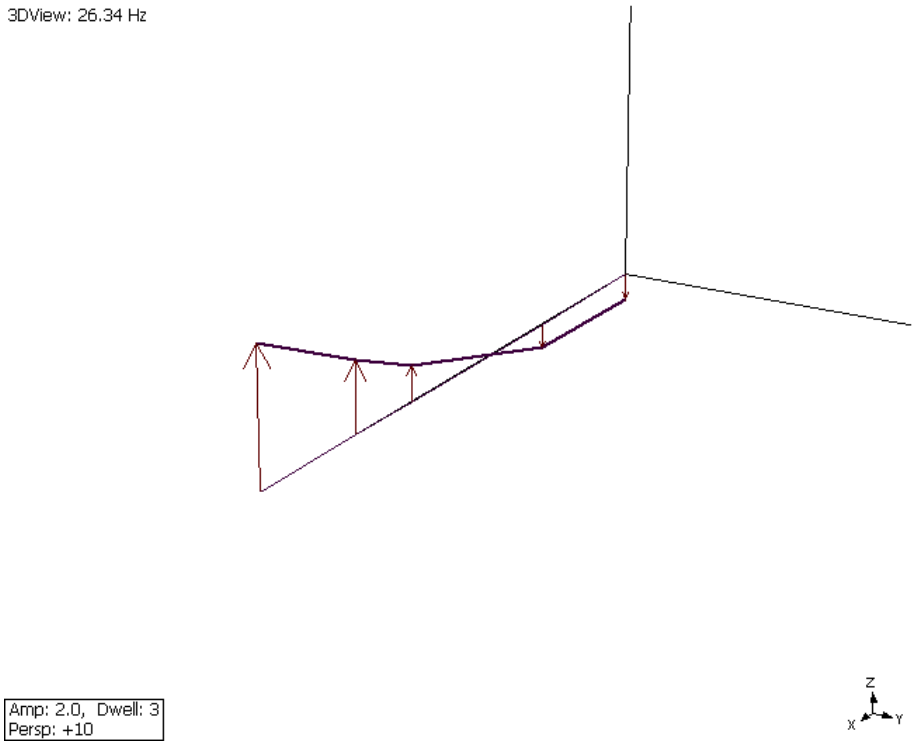

(d)

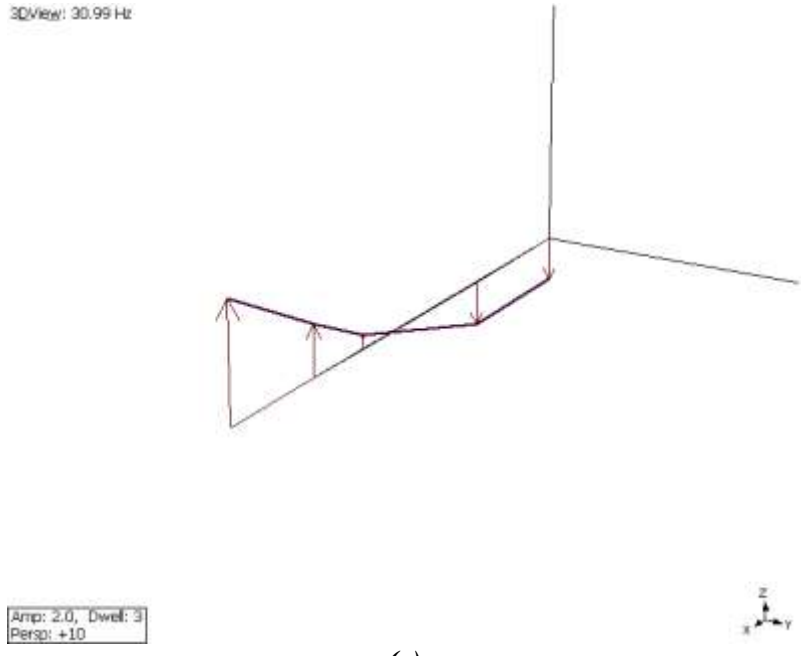

(e)

Figure 4-32. cont'd. *Mode shapes obtained from modal testing.* ***a)*** *Mode at 6.57 Hz.* ***b)*** *Mode at 8.23 Hz.* ***c)*** *Mode at 9.39 Hz.* ***d)*** *Mode at 26.34 Hz.* ***e)*** *Mode at 31 Hz.*

Table 4-10. Mode parameters found by modal testing.

Mode Number	Resonance Frequency	Damping %
1	6,57 Hz	4.94
2	8,229 Hz	2.642
3	9,385 Hz	3.163
4	26,34 Hz	1.985
5	30,99 Hz	1.96

The resonant frequency is the easiest parameter to be found. A resonance is identified as peak in frequency response function. Damping ratio is determined by using a frequency weighting function to isolate a single mode from the frequency response function SDOF impulse response function for that mode alone is produced. Using Hilbert transform facility incorporated in the analyzers damping of ratio of each mode is calculated [29].

Summarized in Table 4-9, mode around 6.57 Hz and second one around 8.229 Hz are assumed to be due to suspension of the tank. When mode shapes are investigated it is seen that rigid body mode is dominating and not much bending is seen. Also looking at the FRFs the amplitudes of those peaks are lower than the peak occurred at around 9.39 Hz. Although 4^{th} and 5^{th} mode resonant frequencies are very close from Table 4-9 when mode shapes are investigated in Figure 4-32 it is seen that mode shapes are very similar. Looking at the FRF vibration amplitude is much higher for the 4^{th} mode which actually resembles the second mode shape of the gun barrel. The fifth mode is again due to suspension of tank.

At 9.385 Hz first mode shape is seen and there is a difference of less than 1 Hz with the analysis results of Section 4.1.4 case 3 which assumes that slider mechanism is locked and actuator has only stiffness effect on overall behavior of the system. The second mode shape occurs at 26.34 Hz again with the same mode shape in section

4.2.1 case 3 "Barrel behavior for actual stiffness value of the elevation motor. In ***Table 4-11*** comparison of found resonant frequencies of analysis and experimental test is given and compared.

Table 4-11. *Comparison of test and analysis results*

Mode Number	Modal Test	FE Analysis	% Error
1	9.385 Hz	9.952 Hz	6 %
2	26.34 Hz	29.081	10%

It is found that resonant frequencies found from modal test and finite element analyses are compatible. In order to make sure that frequencies found from experimental modal test are referring to finite element analysis results another criteria which is called as Modal Assurance Criteria (MAC) is studied.

The function of the modal assurance criterion (MAC) is to provide a measure of consistency (degree of linearity) between estimates of a modal vector. This provides an additional confidence factor in the evaluation of a modal vector from different excitation (reference) locations or different modal parameter estimation algorithms [22].

If MAC number found from the analysis is 1 it means that mode shapes are perfectly matched. If MAC number is far from 1 it means that mode shapes of numerical analysis and modal test is inconsistent [22]. In Figure 4-35 positions of accelerometers used in modal testing is used. Although displacements in the figure is given with respect to trunnion axis, in finite element model starting point not the trunnion axis but the back-end of the barrel. Relative displacements of accelerometers in modal test setup and finite element model is given in ***Table 4-12***.

Table 4-12. *Position of accelerometers with respect to trunnion axis and finite element model.*

Accelerometer Number	Position wrt Trunnion axis (m)	Position wrt. FEM (m)	Node numbers in FEM
1	0.984	2.1	48
2	1.814	2.93	66
3	2.984	4.1	90
4	3.444	4.56	100
5	4.184	5.3	110

In order to do the MAC number analysis mode shape vectors of finite element model and modal test results is necessary. 1st mode shape vector obtained from the experimental modal test is already given as program output. For both modes, phases are found to be very close for each accelerometer and they are neglected.

From the experimental test first mode shape vector corresponding to 9.385 Hz is:

$$\vec{X}_{\text{exp,1}} = \begin{Bmatrix} 0.007 \\ 0.02 \\ 0.04 \\ 0.05 \\ 0.07 \end{Bmatrix}$$

Normalizing the first mode shape vector to unity:

$$\vec{X}_{\text{exp,1}} = \begin{Bmatrix} 1 \\ 3 \\ 6.3 \\ 7.7 \\ 10 \end{Bmatrix}$$

After finding the normalized 1st mode shape vector found from the experimental modal test, mode shape found from the finite element analysis is found. For the first mode shape vector found from the analysis, displacement data taken from the nodes

corresponding to 5 accelerometers are read. 1st mode shape vector found from relative displacements is found as:

$$\vec{X}_{analysis,1} = \begin{Bmatrix} 0.0134 \\ 0.0291 \\ 0.0558 \\ 0.0685 \\ 0.0872 \end{Bmatrix}$$

Normalizing the vector:

$$\vec{X}_{analysis,1} = \begin{Bmatrix} 1 \\ 2.17 \\ 4.16 \\ 5.11 \\ 6.507 \end{Bmatrix}$$

Finally modal assurance criterion formula below is used to calculate MAC number [22].

$$MAC = \frac{\left| \left\{ \vec{X}_{\exp,1} \right\}^T \left\{ \vec{X}^*_{analysis,1} \right\} \right|^2}{\left\{ \vec{X}_{\exp,1} \right\}^T \left\{ \vec{X}^*_{\exp,1} \right\} \left\{ \vec{X}_{analysis,1} \right\}^T \left\{ \vec{X}^*_{analysis,1} \right\}} \qquad \text{(Eq.4.5)}$$

$$MAC = 0.998$$

MAC number found as 0.998 for 1st mode shape which is almost unity. Next, calculations are done for comparison of second mode shapes which is occured at 26.34 Hz. Experimental mode shape vector for the 2nd mode is found as:

$$\vec{X}_{\exp,2} = \begin{Bmatrix} 0.039 \\ 0.035 \\ 0.053 \\ 0.11 \\ 0.2 \end{Bmatrix}$$

Normalizing the second mode shape vector to unity:

$$\vec{X}_{\exp,2} = \begin{Bmatrix} 1.11 \\ 1 \\ 1.36 \\ 2.82 \\ 5.13 \end{Bmatrix}$$

And for the mode shape vector found from finite element analysis displacements of nodes corresponding the accelerometer positions are used. Second mode shape vector found from relative displacements is found as:

$$\vec{X}_{analysis,2} = \begin{Bmatrix} 0.0152 \\ 0.0122 \\ 0.0234 \\ 0.047 \\ 0.0836 \end{Bmatrix}$$

Normalizing the vector:

$$\vec{X}_{analysis,2} = \begin{Bmatrix} 1.25 \\ 1 \\ 1.92 \\ 3.85 \\ 6.85 \end{Bmatrix}$$

Using same formulas as above MAC number is as 0.997

MAC number for the second mode is also found close to unity. For both modes, this is an indication that the modal vectors from FEA and experiments are consistent.

In conclusion finite element analysis done with actual stiffness value of the actuator motor is verified with the experimental modal testing for the first two modes obtained from FE Results are summarized in Table 4-8 and mode shapes are found to be consistent for analysis and test results. In the next section of Chapter 4 finite element modeling of longer gun barrel is done accordingly.

4.3 MODELING OF LONGER GUN BARREL

Since the objective of this thesis is to increase the first hit accuracy of a tank barrel with a long gun barrel while the tank is subjected to random vibration from the ground, the longer gun barrel must be modeled correctly and correct analyses should be done accordingly. Long barrel itself is not manufactured yet, hence the details of subcomponents are not very clear. The gun tube geometry is known and also it is known that the length of the long gun barrel is 1.3 meters longer than the short barrel. In addition, position of center of gravity with respect to trunnion axis is known to be 37 mm to the front. Although the barrel is not manufactured yet weight and design properties are already available with technical data from the manufacturer. Total weight of the gun barrel is known from catalogues obtained from the manufacturer is about 4133 kg.

In order to design an appropriate TVA , which is expected minimize the vibration response at the free end of the long barrel, dynamic characteristics of the barrel must be well known. In Sections 4.1 and 4.2 finite element modeling for already manufactured short gun barrel is done. Finite element model of the short gun barrel is verified by comparing the modal parameters from analysis to experimental ones (See Section 4.3). Using the knowledge of how to build the finite element model correctly for the short barrel, the long gun barrel is modeled in the same way using data given in the previous paragraph. It is assumed that sub-components mentioned in Section 4.1 have same properties with the short gun barrel. Gun tube is remodeled and finite element model is reconstructed as seen in Figure 4-36.

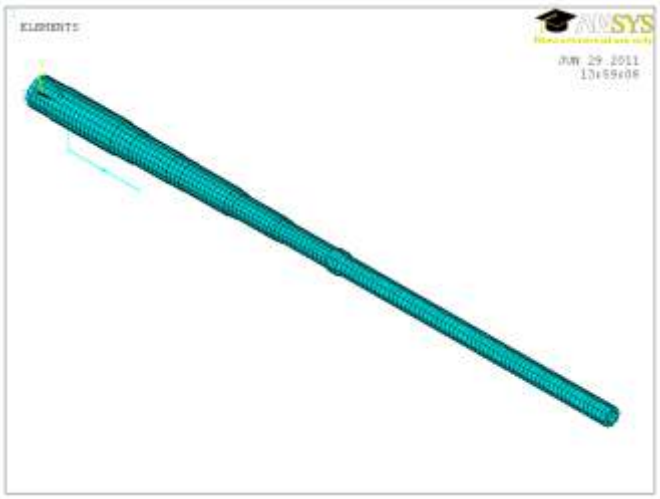

Figure 4-33. *Finite Element Model of Longer Gun Barrel*

During the modeling same global element edge length of 0.05 m is used. Several runs are repeated with smaller element edge lengths and resonant frequencies are found to be not changed. The results are seen to be not changed much for smaller edge lengths. Total number of 140 nodes is defined in the FE model. The important node locations are determined to be the trunnion axis and the free end of the barrel.

Same element types as mentioned earlier in Section 4.1.3 are used in the longer gun barrel model.

4.4 FINITE ELEMENT ANALYSES OF LONG AND SHORT GUN BARRELS

Since now the FE models for both barrels are available, now we can proceed with the analysis of the barrels so that their vibration response characteristics at the free end are compared. In order to compare the properties and static/dynamic responses of two barrels, static structural, modal, harmonic and spectrum analyses are done. All analyses are done using ANSYS software, using finite element barrel models constructed in Sections 4.1 through 4.3. At the end of the analyses, results are tabulated and compared. Since the aim of the thesis is to control vibrations of longer

gun barrel such that the vibration response of the long gun barrel is same as the response level of the short gun barrel under random excitation from the base, spectrum analysis results are more seriously considered and modification of longer gun barrel based on its harmonic response to a specified input spectrum respectively.

Below are the analyses results of shorter and longer gun barrels. All the results are summarized in Section 4.5 at the end.

4.4.1 FINITE ELEMENT ANALYSES OF THE SHORT GUN BARREL

Static structural, modal and spectrum analysis are done on the short gun barrel. Static deflection of the short gun barrel under its own weight is analyzed in fixed-free boundary condition. Although the effect of static deflection is prevented by MRS as described in Section 2.2.6, it is important to compare the deflection magnitudes of both barrels under static earth gravity to obtain know-how on that subject. To do the analysis correctly, and find a stable solution, fixed free boundary condition is held by keeping trunnion axis fixed; spring element representing the elevation actuator prevents a unique solution when it is included in static analysis. In ***Figure 4-34,*** ANSYS figures of short gun barrel modeled for static structural analysis and displacements of nodes is seen. The maximum deflection is found to be 1.83 mm, which is observed at the free end of the barrel.

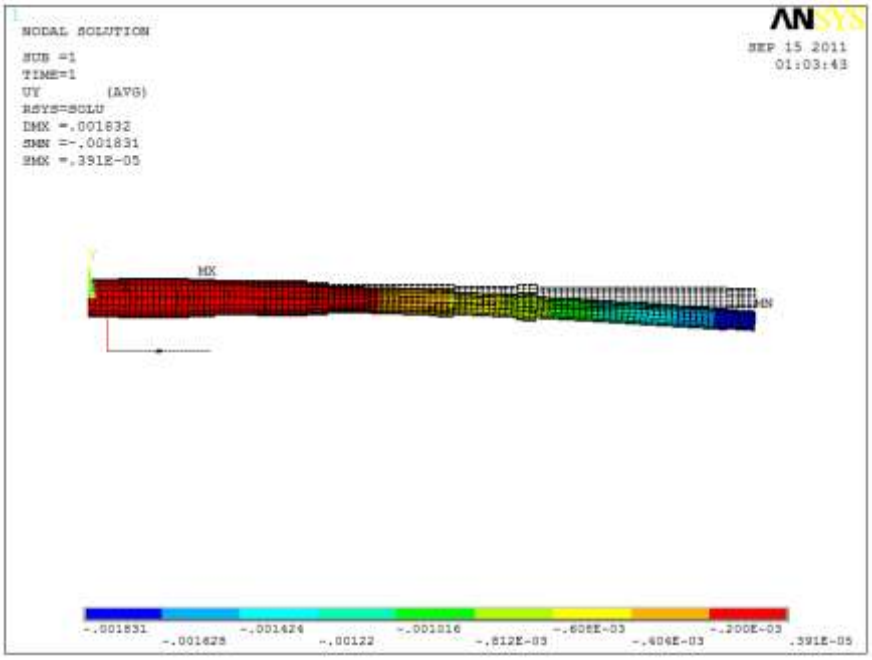

Figure 4-34. *Relative displacement distribution wrt.trunnion axis which is held constant, Resultant static deflection of shorter gun barrel under effect of gravity is 1.83 mm.*

After finding static deflection of shorter gun barrel modal analysis is done in order to study the dynamic characteristics of the short barrel. By doing the modal analysis, mode shapes and modal frequencies of the short gun barrel are found. And Modal frequencies for the short barrel are tabulated in ***Table 4-9***. Mode shape Results for the first two modes are given in ***Figure 4-35*** and ***4-36***. For ground vehicles, frequency range of interest for structural vibration response is generally around 0-250 Hz [5]. It is also known that for system response amplitudes of barrels first mode dominates the second and third mode as a ratio of about 25:5:1 [6]. As a result it is the first two mode shapes and frequencies focused on this thesis. In the case of gun barrel it is seen from the analysis that important frequency range is 0-50 Hz. In ***Figure 4-37*** to ***Figure 4-41*** results are seen for different frequency ranges. It is seen that when frequency range is taken as 0-50 Hz results are very close to the case of 0-250 Hz, hence modes that lie in that range are found the FE analysis.

In modal analysis of shorter gun barrel, first two modes are extracted and Block Lanczos solver of ANSYS software is used [19]. The solver allows extracting number of modes that is equal to number of degrees of freedom. At the end of the analysis the modal results i.e. mode shapes and frequencies of first two modes are expanded and written in the solver file in order to use them in spectrum analysis later on. The gun barrel is allowed to rotate along trunnion axis, and rear side is modeled as rigidly assembled to the gun tube. The connection to turret is modeled as spring due to nature of elevation actuator. ***In Table 4-13*** first 5 modal frequencies of short gun barrel is tabulated. Since we are interested in first two modes only first two mode shapes are plotted in ***Figure 4-35*** and ***4-36***.

Table 4-13. *Mode Numbers and modal frequencies of short gun barrel.*

Mode Number	Frequency (Hz)
1	9.9522
2	29.081
3	70.463
4	136.7
5	213.61

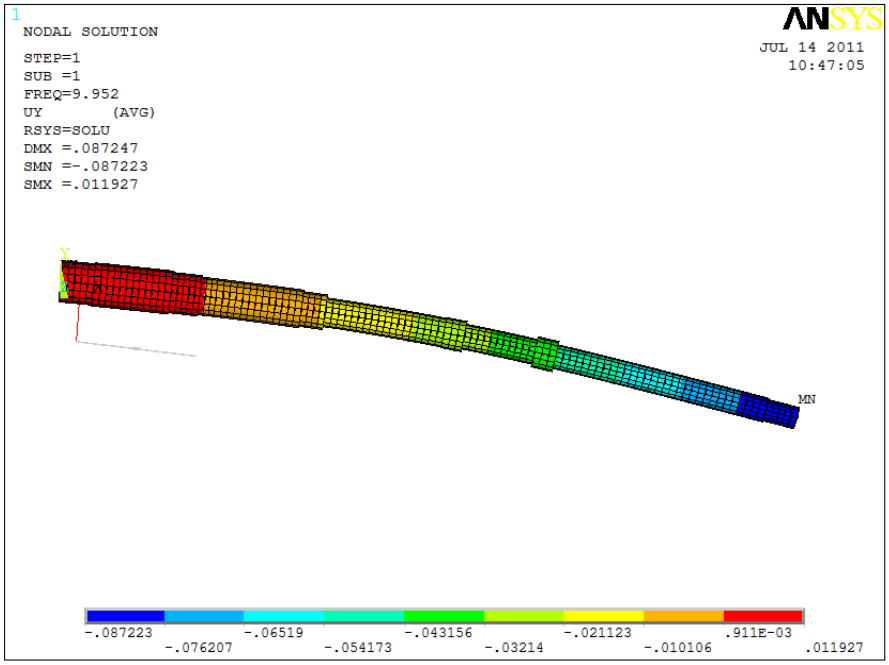

Figure 4-35. *Relative modal displacement distribution in y direction wrt. global coordinate system, 1st mode shape and frequency of shorter gun barrel (Scaled 10 times).*

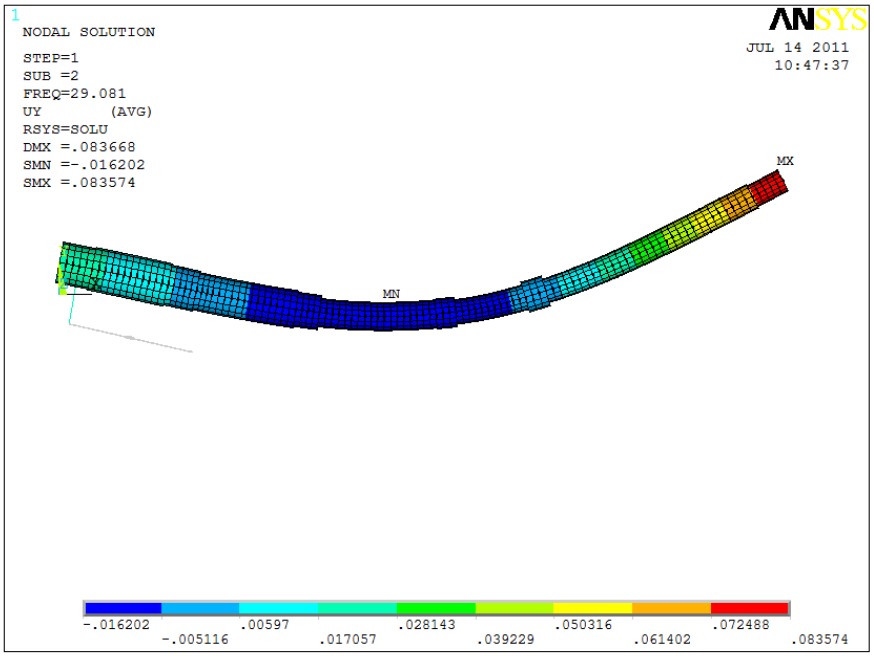

Figure 4-36. *Relative modal displacement distribution in y direction wrt. global coordinate system, 2nd mode shape and frequency of shorter gun barrel (Scaled 10 times).*

To see the response of shorter gun barrel under random vibration input, results of modal analysis and external excitation data are used to perform spectrum analysis. Power spectral density (PSD) function or the Spectrum function is a graph of spectral values vs. frequency that captures the intensity and frequency content of time history loads. The analysis is probabilistic in nature since both the input and output quantities represent only the probability that they take on certain values. Input vibration data is used in PSD format. PSD is a statistical measure defined as the limiting mean-square value of a random variable; it is used in spectrum analysis because the input and response magnitudes of the analysis can be specified with probability distribution. A PSD spectrum is statistical measure of the input and/or response of a structure due to random dynamic loading. The PSD may be of type, displacement, velocity or acceleration. The data in this study is recorded from a point close to trunnion axis during field tests of a main battle tank with shorter gun barrel, using ASELSAN Inc. facilities. It is in acceleration form. In finite element model this load is applied at trunnion node i.e. the connection of the tank turret to the gun barrel.

Firstly first 7 modes are combined and 1σ displacement results are chosen to be computed. For 1 σ results output by the solver are one sigma or one standard deviation values (with zero mean value). These results follow a Gaussian distribution. The interpretation is that 68.3% of the time the response will be less than the standard deviation value [19]. The reason of combining first 7 modes is to increase the effective modal mass. The effective modal mass provides a method for judging the "significance" of a vibration mode. Some modes have higher effective masses than others. Those with relatively high effective masses can be readily excited by base excitation while others cannot. For finite element analysis a limited number of modes should be included in the analysis and effective modal mass determines required number of modes to be included in the analysis the number should be enough so that the total effective modal mass of the model is at least 90% of the actual mass. It is known that for fixed-free beams accounting first four modes

results in use of 90% modal mass [21], for Euler-Bernoulli beams, pinned free from both sides accounting first seven modes the effective mass reached is 95%. Being in the safe side in spectrum analysis for mode participation and mode combination, first seven modes are taken into account. Mode participation factor is the sensitivity of the mode. It is a good indication of the importance of the state to the mode. Participation factors can be positive, zero, or negative. A positive participation factor associated with a particular mode means that mode is contributing to the oscillation of the system. A negative participation factor indicates a generator that is dampening the system oscillation. In ANSYS analyses done in this thesis mode participation factors are taken to be 1 for all modes by default [19]. Mode combination determines the number of modes to include in the analysis. The output of spectrum analysis is a Response PSD graph of the chosen node and 1 σ deflections of the barrel. For the response PSD graph the node at the free end of the barrel is chosen. The response PSD plots of the free end when field data is applied at the trunnion (base) is seen in Figures 4-37 to 4-39. 1 σ deflections of the barrel when it is excited from trunnion is seen in Figure 4.40 and 4-41.

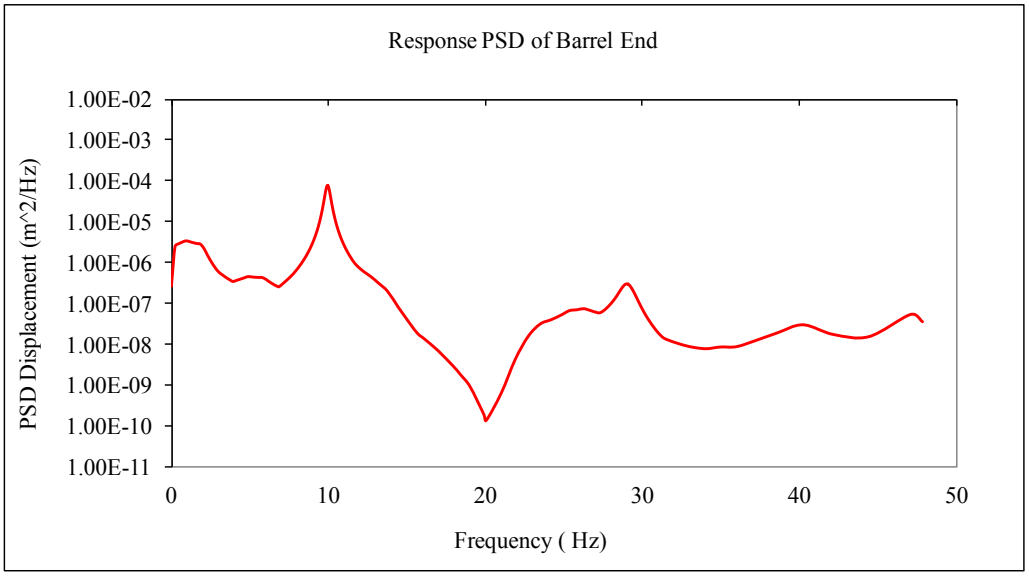

Figure 4-37. *Response PSD of short barrel end when experimentally measured base displacement spectrum is applied from trunnion axis.(0-50 Hz)*

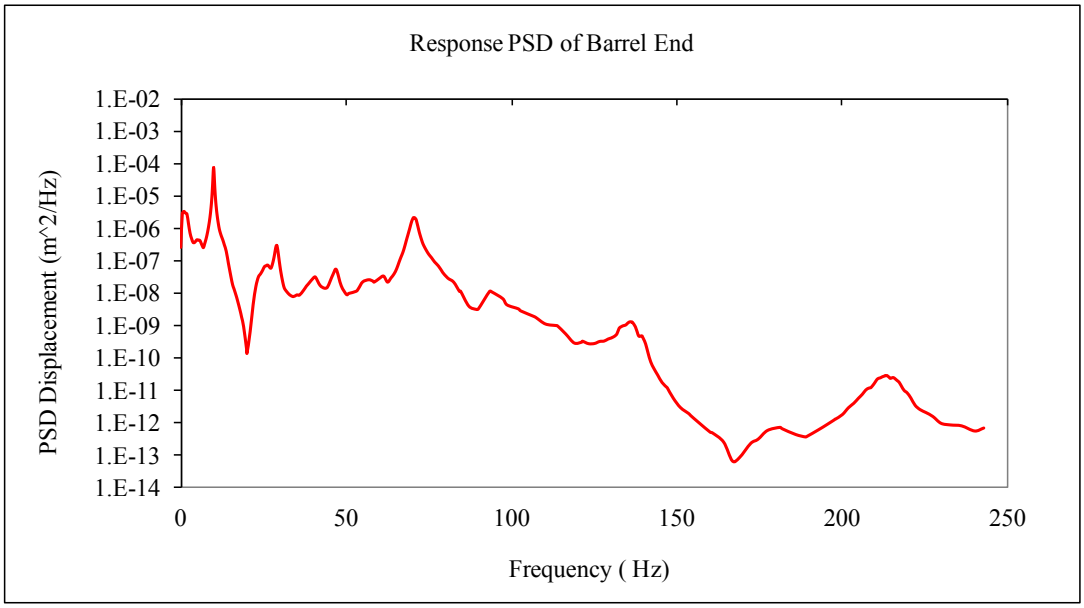

Figure 4-38. *Response PSD of short barrel end when experimentally measured base displacement spectrum is applied from trunnion axis.(0-250 Hz)*

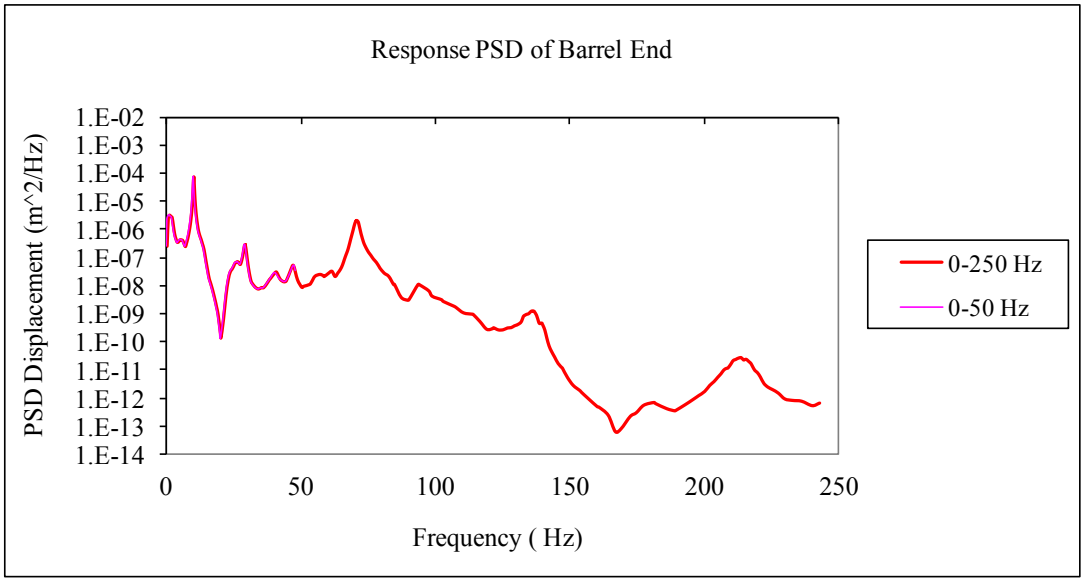

Figure 4-39. *Comparison of Barrel end responses of short gun barrel.*

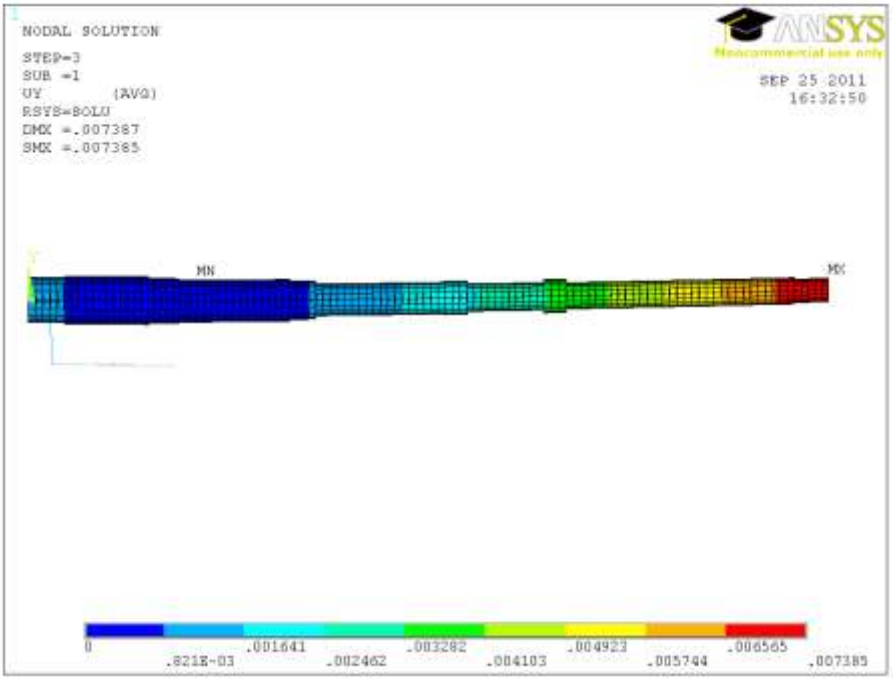

Figure 4-40. *Barrel deflection of short gun barrel when experimentally measured base displacement spectrum between 0-50 Hz is applied. Displacement is 7.385 mm.*

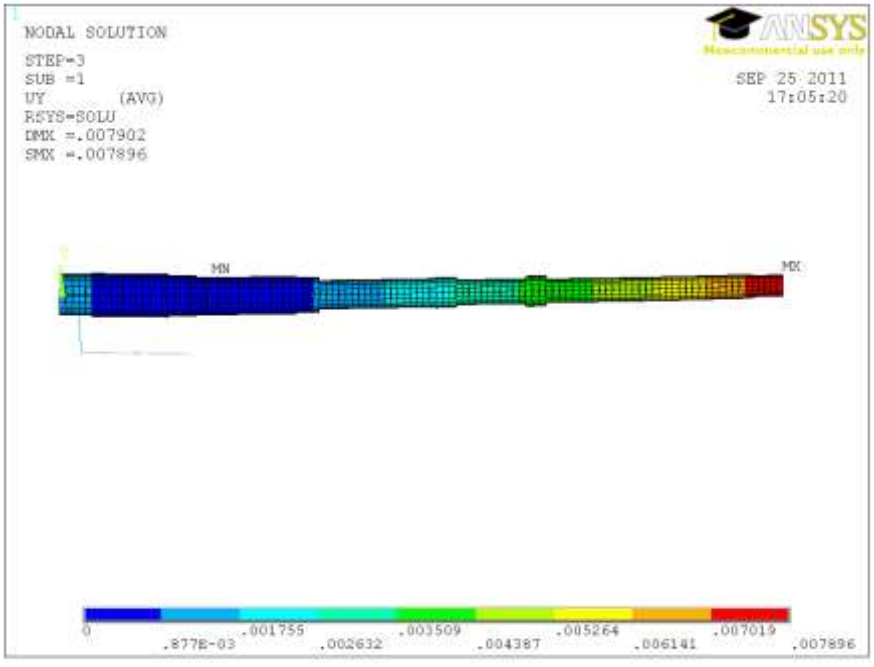

Figure 4-41. *Barrel deflection of short barrel when experimentally measured base displacement spectrum is applied. Maximum displacement is 7.896 mm. (0-250 Hz.)*

4.4.2 FINITE ELEMENT ANALYSES OF THE LONG GUN BARREL

As in the case of the short gun barrel, static deflection of the long gun barrel is analyzed for fixed free boundary condition. Although the deflection is larger due to increased free length of the long barrel, the effect of static deflection is prevented by MRS as described in Section 2.2.6. Static structural analysis is done under standard gravity. Static deflection at the free end when the long barrel is hold by a rigid support is found to be 5.617 mm. The undeflected and deflected barrel shapes are given in ***Figure 4-42***.

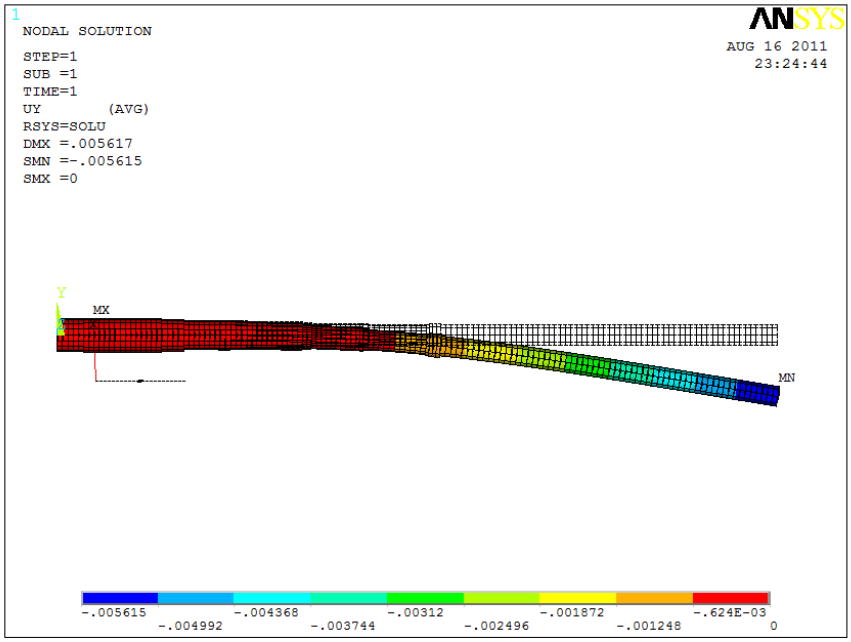

Figure 4-42. *Deflection at the end of the barrel when the barrel is fixed from trunnion axis. (Scaled 10 times)*

In order to study the dynamic characteristics of long gun barrel, modal analysis is done. The goal is to determine the mode shapes and modal frequencies of the long gun barrel during free vibration. As it is mentioned for the short gun barrel, for ground vehicles frequency range of interest for vibration response is determined to

be 0-250 Hz [5]. Modal frequencies lie in the range of 0-250 Hz are also tabulated in ***Table 4-14.*** Also it is found for the short barrel that a frequency range of 0-50 Hz is enough for accurate enough results. During the analysis modes of the barrel which lie in that range are found. From [6] and analyses it is also known that first mode dominates the second and third mode. Mode shapes lie in the range of 0-50 Hz is plotted in ***Figure 4-43*** to ***4-45.***

Table 4-14. *Mode Numbers and modal frequencies of long gun barrel.*

Mode Number	Frequency (Hz)
1	6.0715
2	19.752
3	45.547
4	93.573
5	145.12
6	178.49
7	191.85

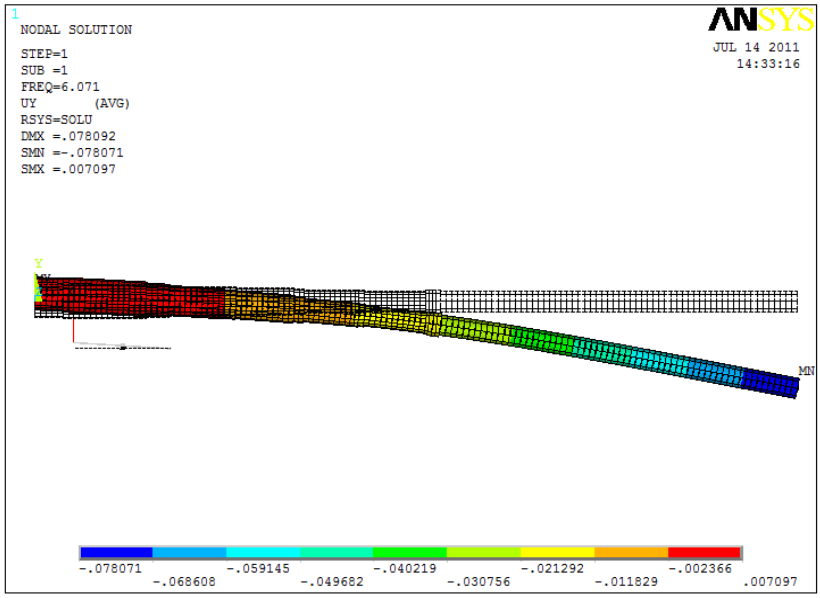

Figure 4-43. . *Relative modal displacement distribution in y direction wrt. global coordinate system, 1st mode shape and frequency of longer gun barrel (Scaled 10 times).*

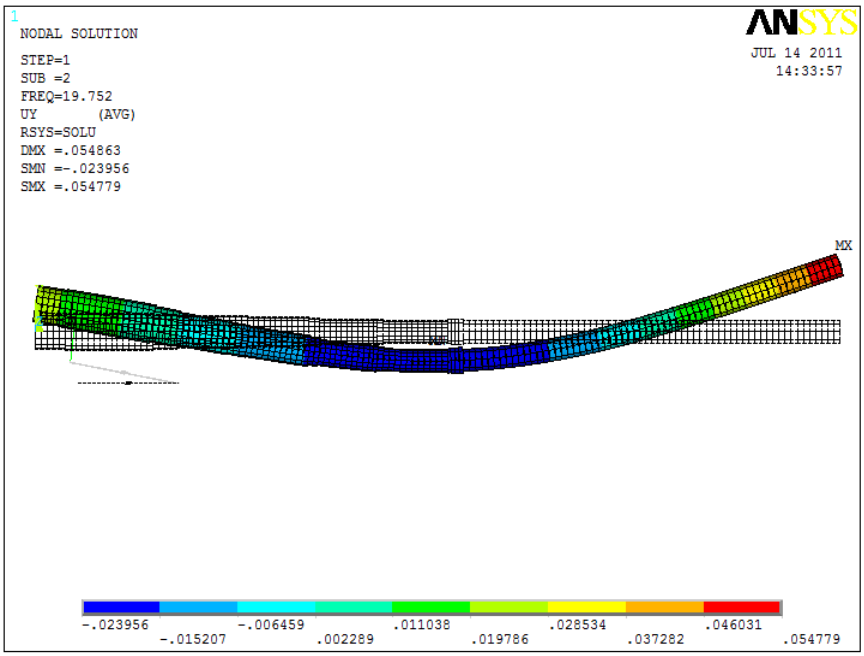

Figure 4-44. . *Relative modal displacement distribution in y direction wrt. global coordinate system, 2nd mode shape and frequency of longer gun barrel (Scaled 10 times).*

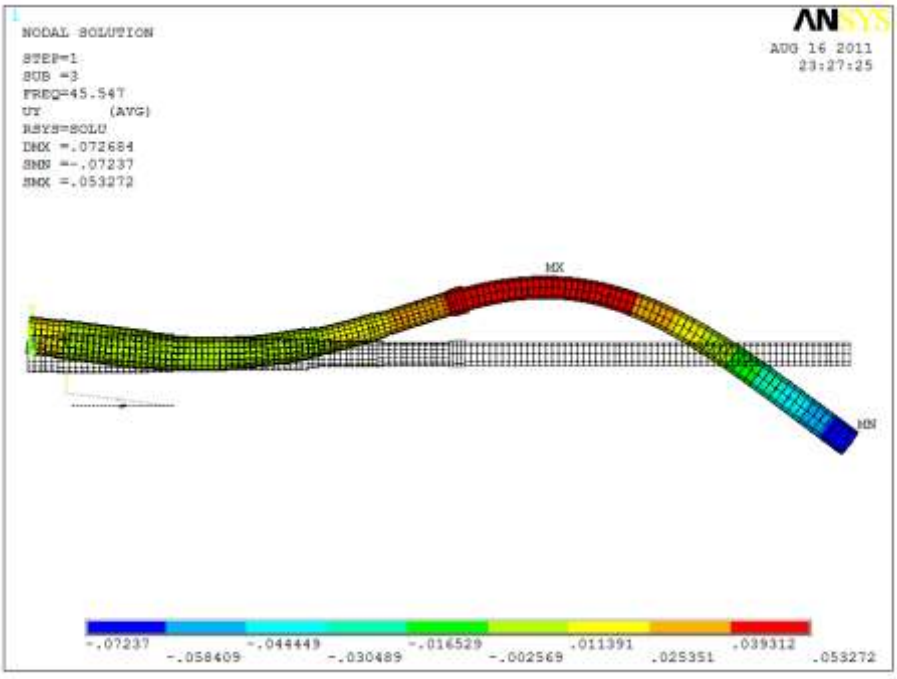

Figure 4-45. *Relative modal displacement distribution in y direction wrt. global coordinate system, 3rd mode shape and frequency of longer gun barrel (Scaled 10 times).*

Spectrum analysis is the final analysis to be done before determining the TVA properties for the long barrel. Since the objective of thesis is to minimize the vibration activity at the end of the long gun barrel with the help of passive vibration control ability of TVA, a combinative effect of dynamic characteristics of barrel and the type of excitation is important.

Same input PSD data used in the spectrum analysis of the short barrel is applied as input to the long gun barrel FE model. It is assumed that all other variables other than barrels are neglected for both tanks i.e. same hull and same turret are used for both tanks. Same excitation is applied to both the long and short gun barrels and the responses of two barrels are compared. As in the case of short gun barrel, structural damping is applied as constant damping ratio of 0.02 which is structural damping of steel that is the material of gun barrel. Input data is the power spectral density function of base acceleration with units of g^2/Hz. First seven modes are combined and 1σ displacement results are computed. Results of spectrum analysis of longer gun barrel to field data is seen in ***Figure 4-46*** to ***4-48***. In Figures 4-46 to 4-48 effect of frequency range of analysis is studied and it is found that results are very close for frequency ranges of 0-50 Hz and 0-250 Hz. It is due to fact that for both frequency ranges first three modes are dominating the response of the barrel. RMS amplitude of deflection occurs at the free end is found in ***Figure 4-49*** and ***4-50*** for different frequency ranges. It is seen that results are close and frequency range of 0-50 Hz is enough for analysis and maximum RMS amplitude of deflection of barrel is found to be 19.044 mm in ***Figure 4-49***. In ***Figure 4-51*** response PSD graph of long gun barrel in different planes are compared. It is found that the barrel vibrates more in elevation plane than in azimuth plane. In ***Figure 4-52*** maximum RMS deflection of long barrel in azimuth plane is found to be 3.95 mm which is 5 times smaller than the maximum deflection at the elevation plane. The comparison of maximum deflections of shorter and longer gun barrels can be found in next section.

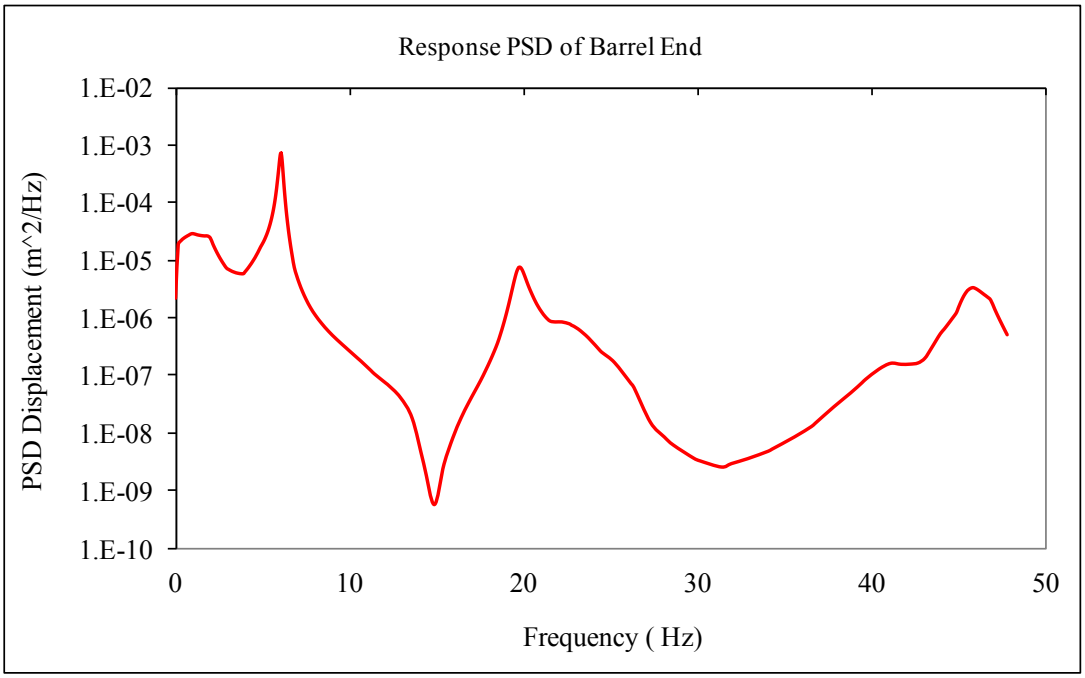

Figure 4-46. *Response PSD of long barrel end when when experimentally measured base displacement spectrum is applied from trunnion axis.(0-50 Hz)*

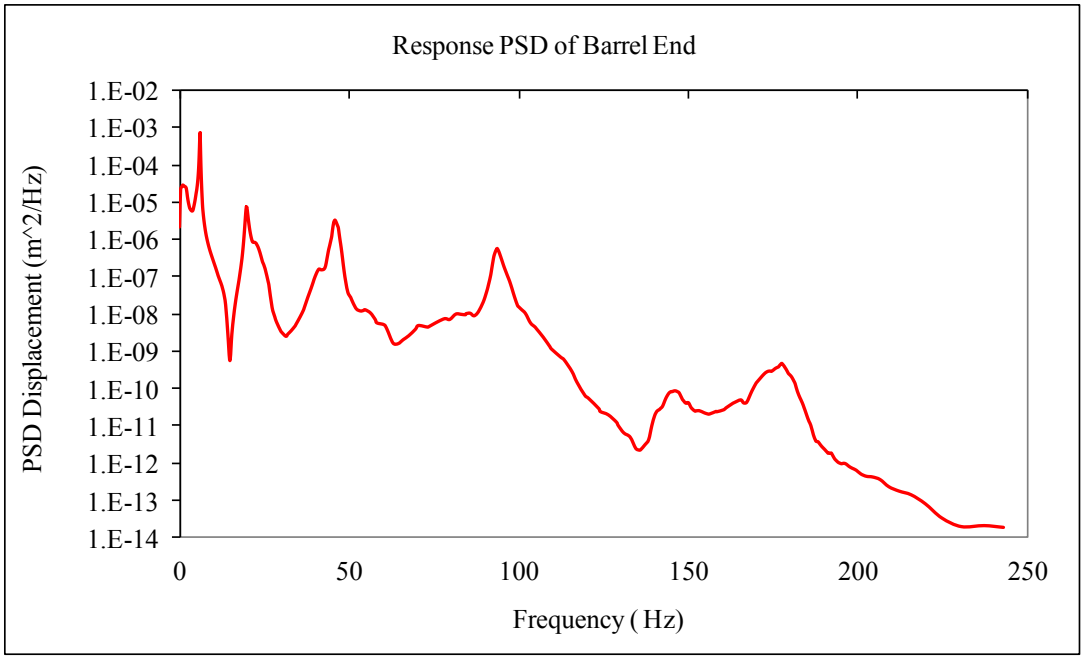

Figure 4-47. *Response PSD of long barrel end when experimentally measured base displacement spectrum is applied from trunnion axis. (0-250 Hz)*

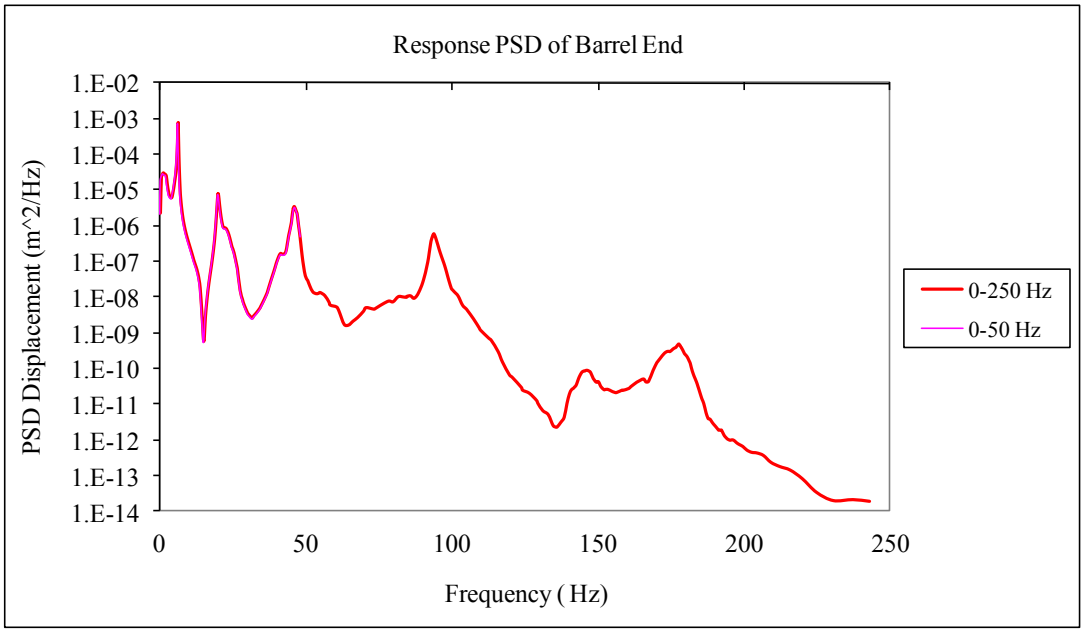

Figure 4-48. *Comparison of Barrel end responses of long gun barrel.*

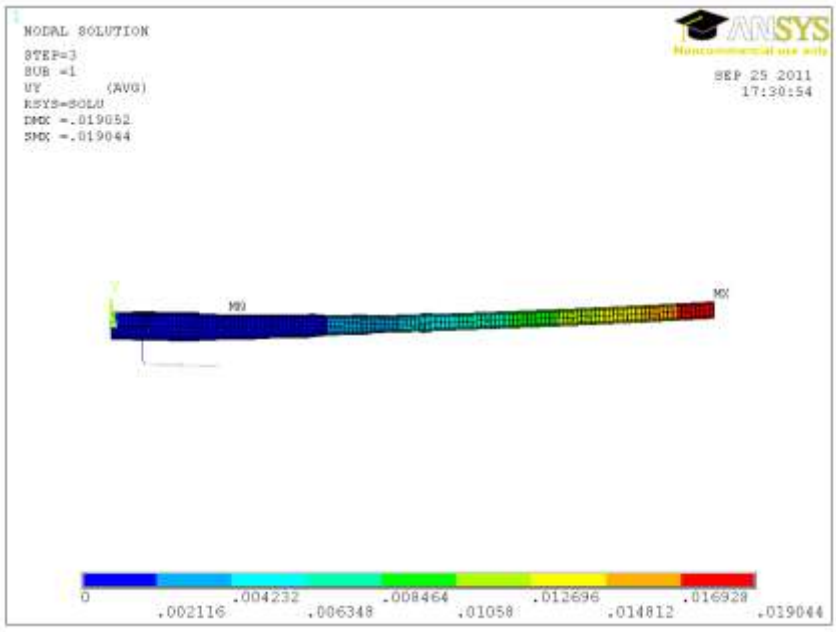

Figure 4-49. *Barrel deflection and response PSD of long gun barrel when experimentally measured base displacement spectrum is applied (0-50 Hz) is 19.044 mm.*

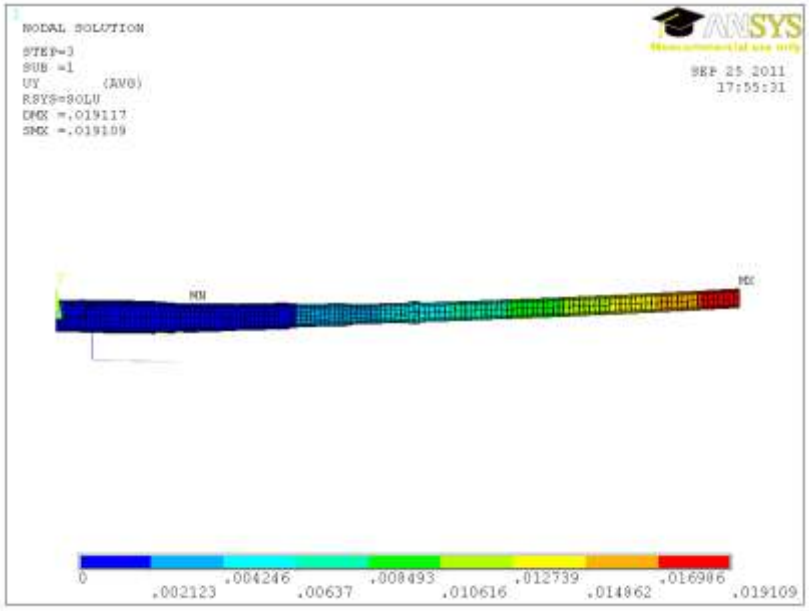

Figure 4-50. *Barrel deflection and response PSD of longer gun barrel when experimentally measured base displacement spectrum is applied (0-250 Hz) is 19.11 mm.*

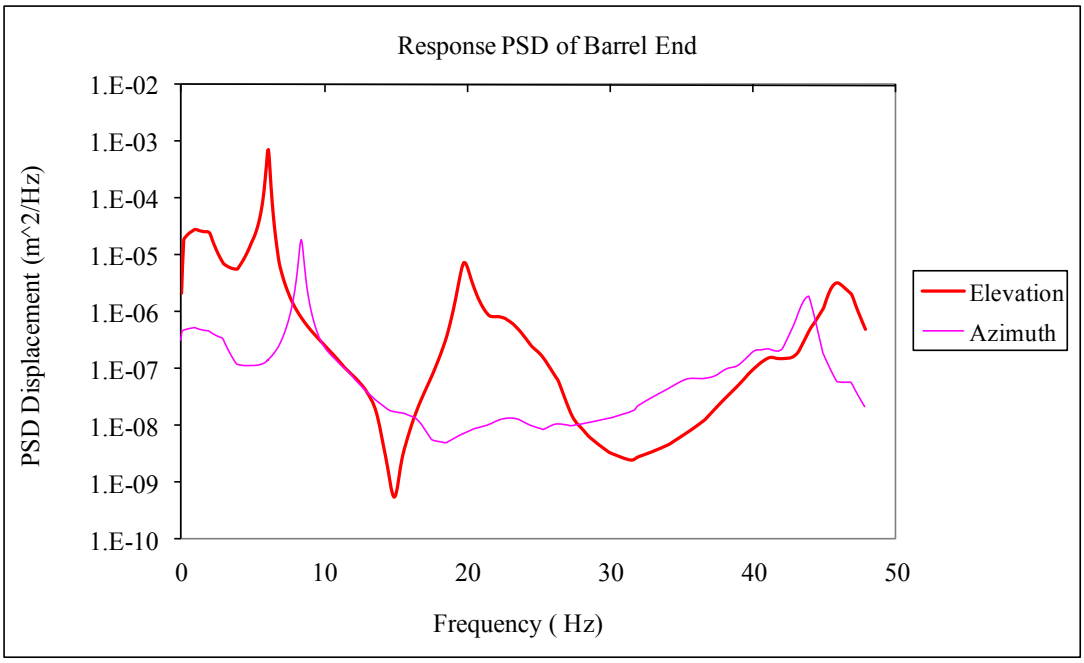

Figure 4-51. *Comparison of response PSDs of long barrel free end in different planes.*

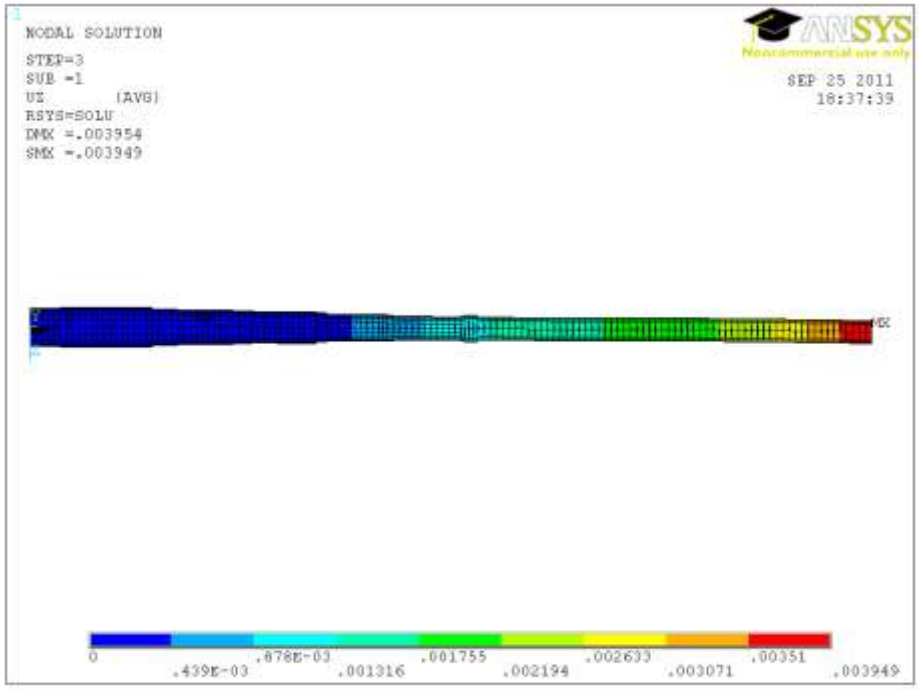

Figure 4-52. *Barrel deflection and response PSD of longer gun barrel when experimentally measured base displacement spectrum is applied in x-z plane z direction is 3.95 mm.*

4.4.3 COMPARISON OF ANALYSES RESULTS

In Sections 4.4.1 and 4.4.2 static structural, modal and spectrum analyses are done on short and long gun barrels. For static structural analysis, maximum deflections at the free end of the barrels are calculated and compared. For modal analysis resonance (modal) frequencies are found and compared. For the spectrum analysis barrel end displacements and response PSD plots are found and compared. Response PSD plot comparison is seen in ***Figure 4-53***. Finally harmonic response analyses are done on both barrels and barrel end displacements where a unit harmonic base displacement is applied and the responses are found as a function of frequency. These results for both barrels, which may be defined as the frequency response functions of the barrel free ends for a base displacement input, are compared in ***Figure 4-54***.

Results found in this chapter are summarized in ***Table 4-15***. Static deformations of both barrels under their own weights are given in ***Table 4-15*** it is seen that long barrel deflects more than the short barrel as expected. It deflects nearly 5 mm more statically under standard earth gravity. It is known that this static deflection is under control with the help of MRS and has no crucial effect on longer gun barrel's shot performance. Modal frequencies of both barrels are compared and it is seen that long gun gun barrel being less stiff than the short barrel has lower resonant frequencies.

Following the modal analyses, spectrum analyses give important results also. Firstly it is seen from the response PSD graphs that first mode dominates the latter two modes, the amplitudes are larger around the first mode. From response PSD plots, it is seen that vibration energy amplitude at the end of longer gun barrel is greater than the shorter barrel as a result higher deflection at the free end of the long barrel is seen. Vibration energy is directly related to the area under PSD plot.

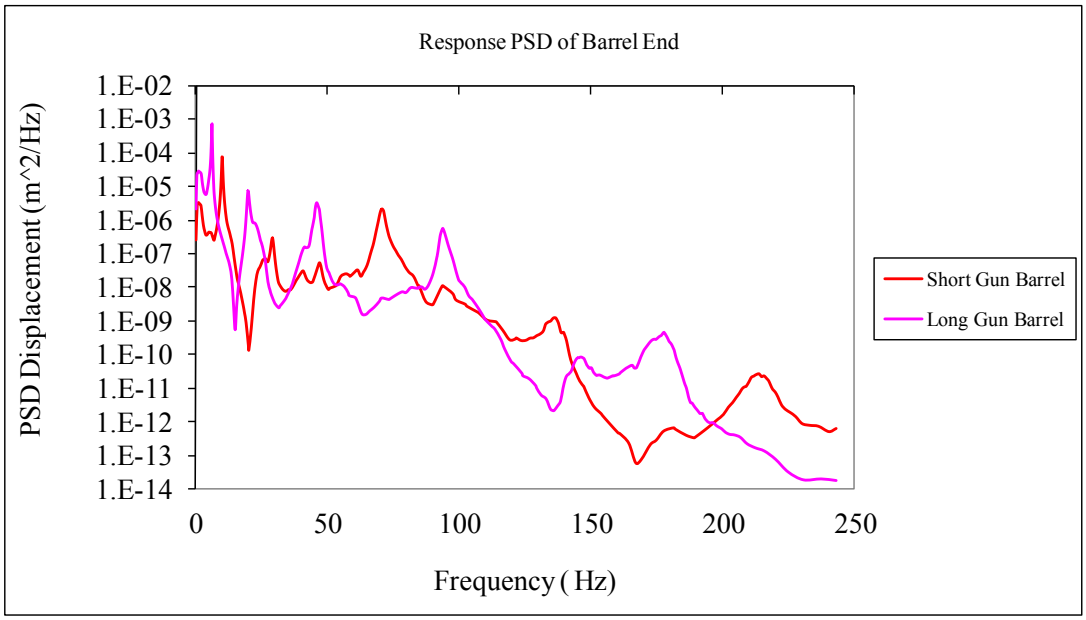

Figure 4-53. *Comparison of response PSDs of barrel ends of short and long barrels.*

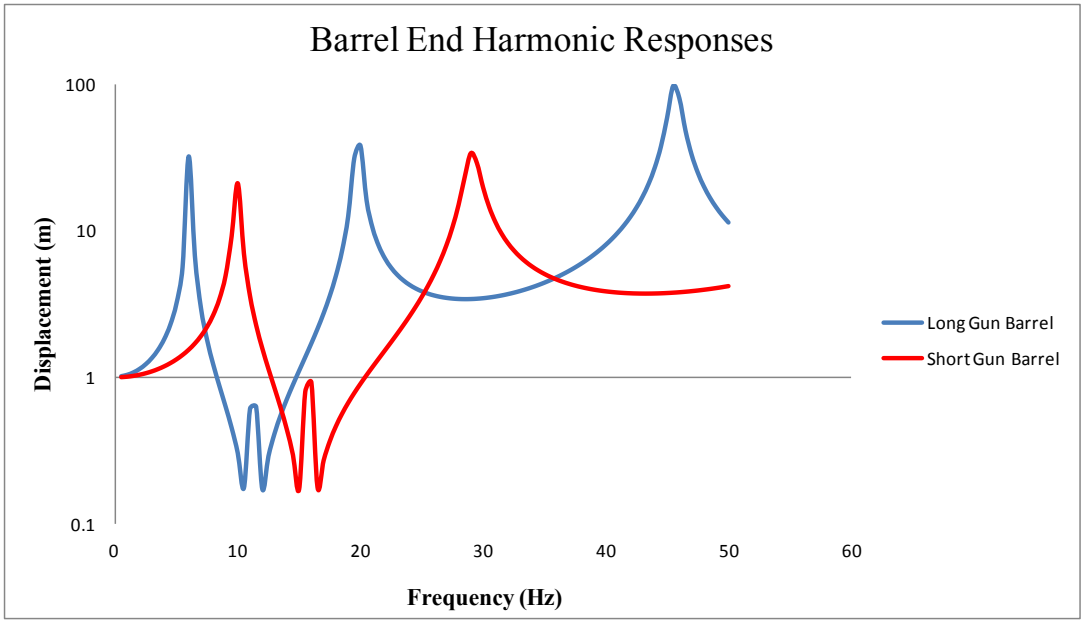

Figure 4-54. *Comparison of harmonic responses barrel ends of short and long barrels.*

From the results it is found that when it is subjected to random base excitation long gun barrel vibrates more than twice the amount short gun barrel vibrates. Increased vibration activity and deflection at the free end lowers the accuracy of the longer gun barrel. Also vibrations of long gun barrel in different planes are compared and it is found that long barrel vibrates more in elevation plane than the azimuth plane.

In the next chapter a detailed design of TVA is done to change the dynamic characteristics of long gun barrel as a passive vibration control technique. The ultimate goal is to reach vibration activity levels of short gun barrel at the end.

Table 4-15. *Comparison of static and dynamic analyses results.*

Static Structural Analysis Results	
Shorter gun barrel	Longer gun barrel
Max. deflection at the end: 1.83 mm.	Max. deflection at the end: 5.617 mm.
Modal Analysis Results	
Shorter gun barrel	Longer gun barrel
First mode occurs at: 9.952 Hz. Second mode occurs at: 29.081 Hz.	First mode occurs at: 6.071 Hz. Second mode occurs at: 19.752 Hz.
Spectrum Analysis Results	
Shorter gun barrel	Longer gun barrel
Max. RMS amplitude of deflection due to field data in y direction: 7.385 mm.	Max. RMS amplitude of deflection due to field data in y direction: 19.044 mm In z direction 3.95 mm

CHAPTER 5

DESIGN OF TVA

In this chapter design parameters of tuned vibration absorber for controlling the vibrations of longer gun barrel are determined. The aim is to minimize the end displacement of the long gun barrel by applying an appropriate TVA so that the displacement amplitude is kept as low as the short gun barrel.

In the beginning of Chapter 5, TVA parameters namely its mass, stiffness and damping ratios are determined with the help of ANSYS software. A representative single degree of freedom spring damper mass model is attached at the free end of the barrel. The free end of the barrel is chosen to be the application point since largest vibration activity occurs there as seen in ***Figure 5-1***.

After determining the properties of TVA and verifying the results with spectrum analysis, detailed design of TVA is studied in the second part. Appropriate physical TVA design that fulfills the requirements is done by considering possible space and assembling restrictions.

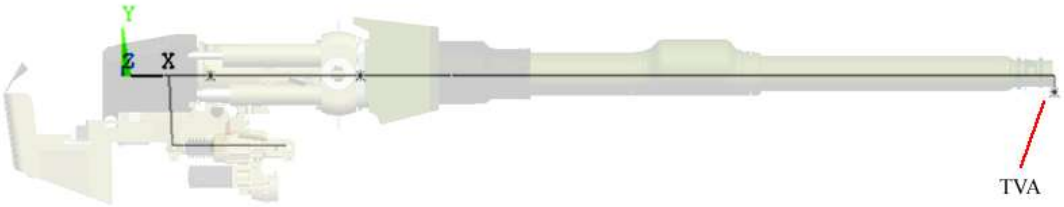

(a)

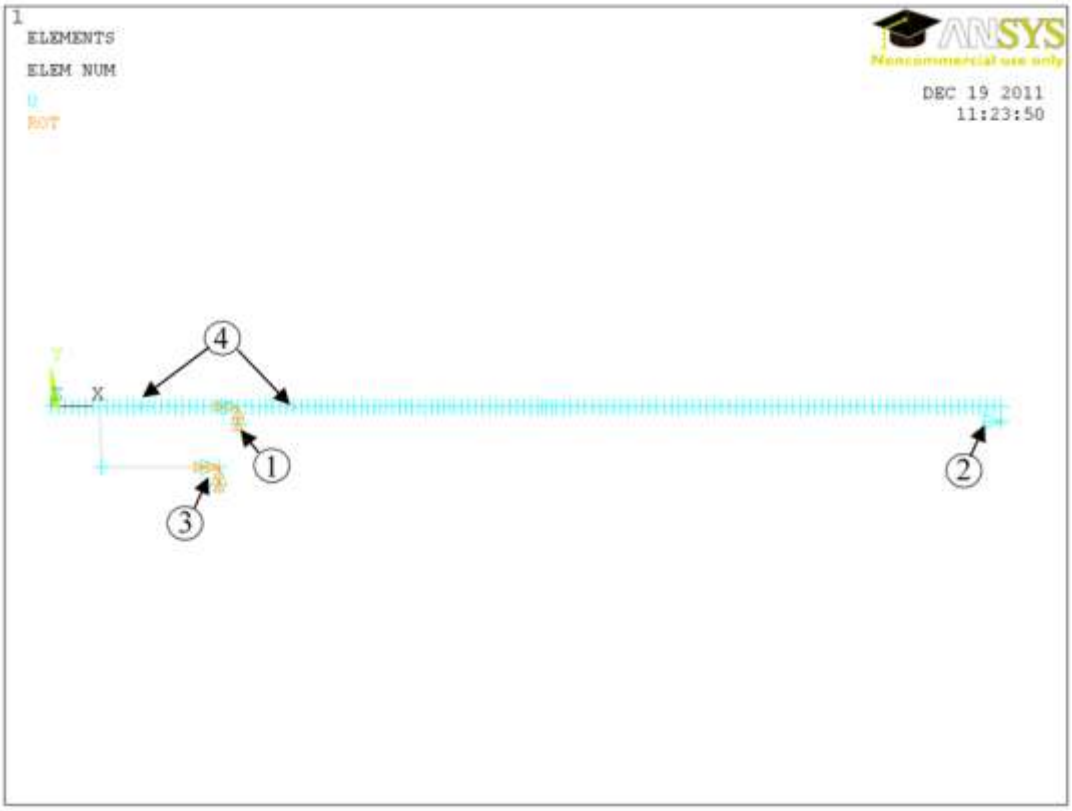

(b)

Figure 5-1. *TVA location on the long gun barrel.* ***a)*** *Solid model.* ***b)****Finite element model* ***1)*** *Revolute joint between the turret and the barrel.* ***2)*** *TVA mass-spring element.* ***3)*** *Revolute joint between the turret and elevation motor.* ***4)*** *Point masses representing front and rear components of gun barrel.*

5.1 IDENTIFICATION OF DESIGN PARAMETERS FOR TVA

In order to decrease the displacement amplitudes of the long barrel under random vibration excitation coming from the base, a TVA will be attached to the free end of

the gun barrel. The parameters that defined the dynamics of the TVA are its mass, stiffness and damping properties. In order to determine the properties several factors must be taken in to consideration:

- Dynamic properties of the main system (gun barrel).
- Type of input excitation data.
- Effective Mass of the main system in the mode of interest.
- Space available for installation.
- Operation environment.

From Chapter 4, it is found that for the long gun barrel tip displacement response due to base excitation coming from the road, the mode that dominates the overall response level is the first mode and it occurs at 6.071 Hz. Although it may seem like the tuning frequency of the TVA should be matched to this dominant first modal frequency of the barrel at first but the frequency content of the excitation should also be taken into account when deciding on the tuning frequency.

Although in chapter 4 it is seen from the response PSD graphs that response is mainly due to first resonance mode of the barrel itself which means that input excitation data has no dominative effect around first mode of the barrel. Still data taken from field test while the tank is on move at constant speed should be investigated in detail. Although overall data is plotted in Figure 4-22 at Section 4.4.1 to determine any possible dominant modes contributing from that, the data is replotted in more detail in ***Figure 5-2.*** This time a narrower frequency range is chosen that is around the first mode of the barrel, between of 0-25.

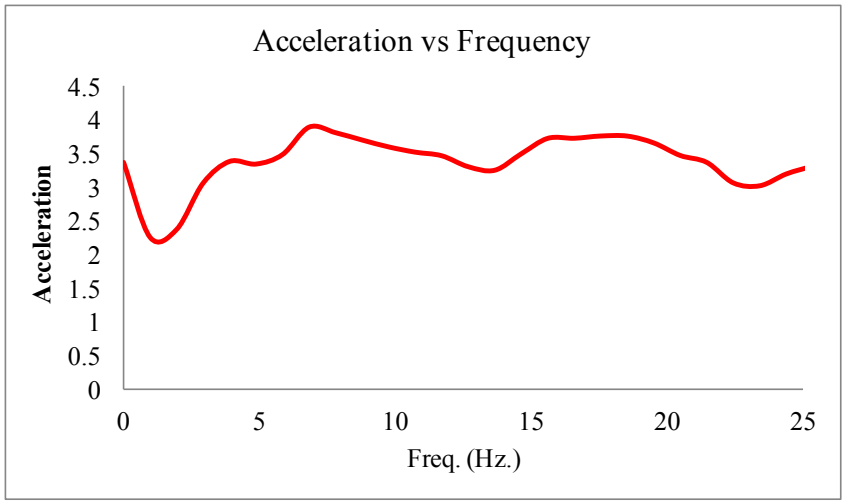

Figure 5-2. *Input PSD data 0-25 Hz.*

Looking at ***Figure 5-2***, one can see that data is close to white noise around 0-25 Hz as it is mentioned earlier. Considering the dynamic properties of the gun barrel and type of excitation it is clear to say that the peak seen in response PSD plot is mainly due to dynamic properties of gun barrel; hence our design focus is to control the first resonant mode of gun barrel at elevation plane (y direction) only so that maximum free end displacement can be minimized.

Another important result coming from the above discussion is that, tuning the TVA's first resonant frequency to that of longer gun barrel without damping can not change the response amplitude of the system at all. Since excitation levels are very similar around the frequency of interest, damping becomes the most important parameter to absorb the vibration energy of the system. It is verified later in this chapter that as much damping as possible is needed to lower the effect of first mode since vibration energy is transferred mostly with the damping property of the TVA.

Next, mass of the TVA is taken in to consideration. It is theoretically true that the least is the best assuming that you have very high damping, but it is impossible to reach that case in reality. Controlling the vibration with no additional mass would

be the best solution if it was possible since it does not increase the total weight or volume of the main system but in practice it is not possible and feasible. For systems that behave similar to a SDOF around a particular mode and excited at narrow frequency bands close to the modal frequency of interest, increasing the mass of TVA increases the energy absorbed inside TVA [17]. For the case of our system which is not a SDOF system, mass ratio is not used instead, several analyses are run with different TVA masses. It is seen from the analyses with different TVA masses that changing TVA mass has no important effect on response of the system. Playing with the TVA mass determines how far away the new peaks are formed from the original resonant peak. In the first part of analyses TVA is assumed to be an undamped TVA. At the end of the section effect of damping is studied and required damping for minimum barrel end deflection is found. The change of new resonance frequencies of the modified barrel with respect to the TVA mass is plotted in ***Figure 5-3***. For systems excited at a single or in a narrow frequency band wihch dominates the system behavior this property of mass ratio is very important. For our case since input excitation data is almost similar to white noise there is no beneficial point on moving the peaks. In order to see the effect of TVA mass on overall system and also on TVA itself several analyses are run.

In ***Figure 5-4*** relative TVA displacements with respect to barrel end vs. TVA mass is plotted. Modal displacements are found for barrel end TVA for each case and relative displacement of TVA with respect to barrel end is found as seen in ***Figure 5-5.*** It is found that increasing TVA mass decreases the displacement of TVA which is very important from the design point of view. Although the final TVA design is not done with respect to modal displacements of TVA and barrel end, it is important to see the behavior of TVA with changing TVA mass. Displacement of TVA under random base vibration is studied for final decision of required design parameters of the TVA.

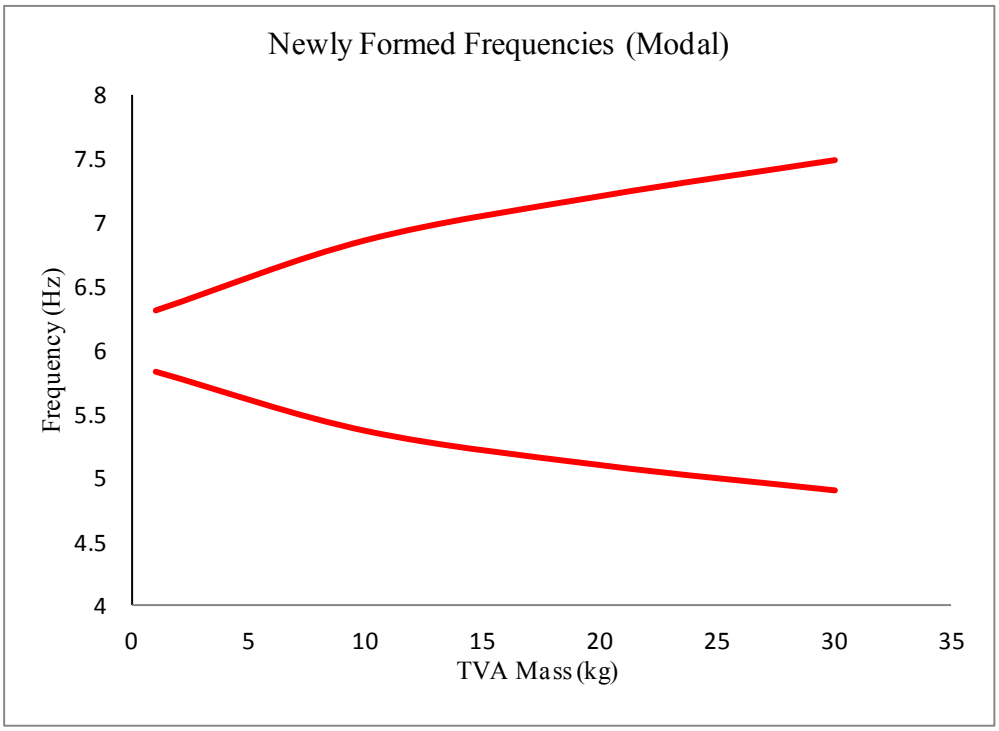

Figure 5-3. *Newly formed resonance frequencies vs. TVA Mass.*

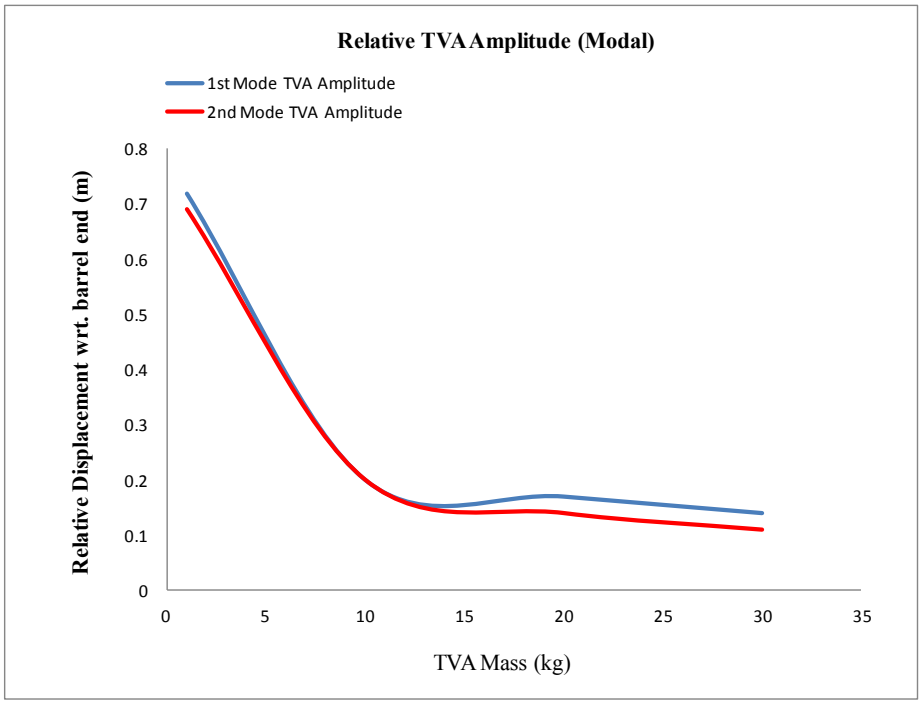

Figure 5-4. *Relative TVA displacements with respect to barrel end vs. TVA mass under modal analysis.*

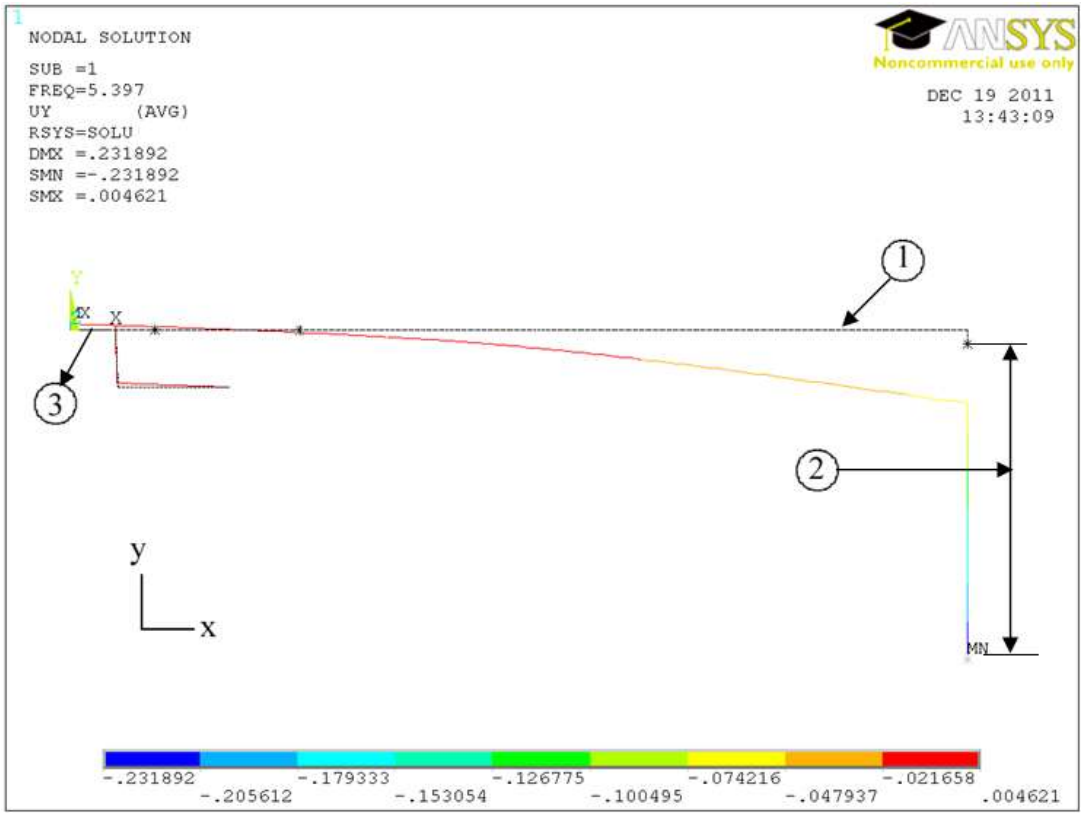

Figure 5-5. *Relative barrel end and TVA displacements for modal analysis.* ***1)*** *Undeflected reference position of the barrel.* ***2)*** *Maximum relative displacement of TVA in -y axis.* ***3)*** *Maximum displacement of barrel at positive y axis.*

In ***Figure 5-6*** the flowchart followed for determining TVA parameters is seen. As seen in ***Figure 5-6*** before determining optimum mass, harmonic analysis is done and effect of TVA mass on harmonic response of the system is investigated. In harmonic analysis a unit displacement input is applied at the trunnion node. Unmodified and modified barrels' barrel end harmonic responses for unit base displacement input are plotted in ***Figure 5-7***. Similar to relative modal TVA displacements relative TVA responses to such harmonic input is plotted in ***Figure 5-8*** for different TVA masses. Although these TVA masses are arbitrarily chosen, in literature it is found that 20 kg TVA is applied to gun barrel [1], 1 kg TVA mass

is studied to see the effect of very small TVA. TVA mass of 30 kg is applied to see the effect of large TVA mass on barrel end behavior.

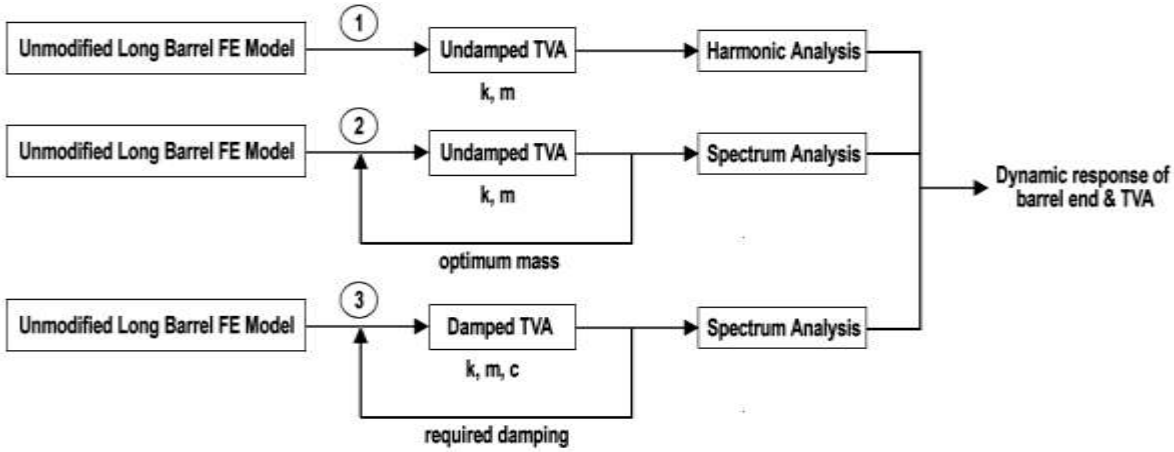

Figure 5-6.*Flowchart followed in determining TVA parameters.*

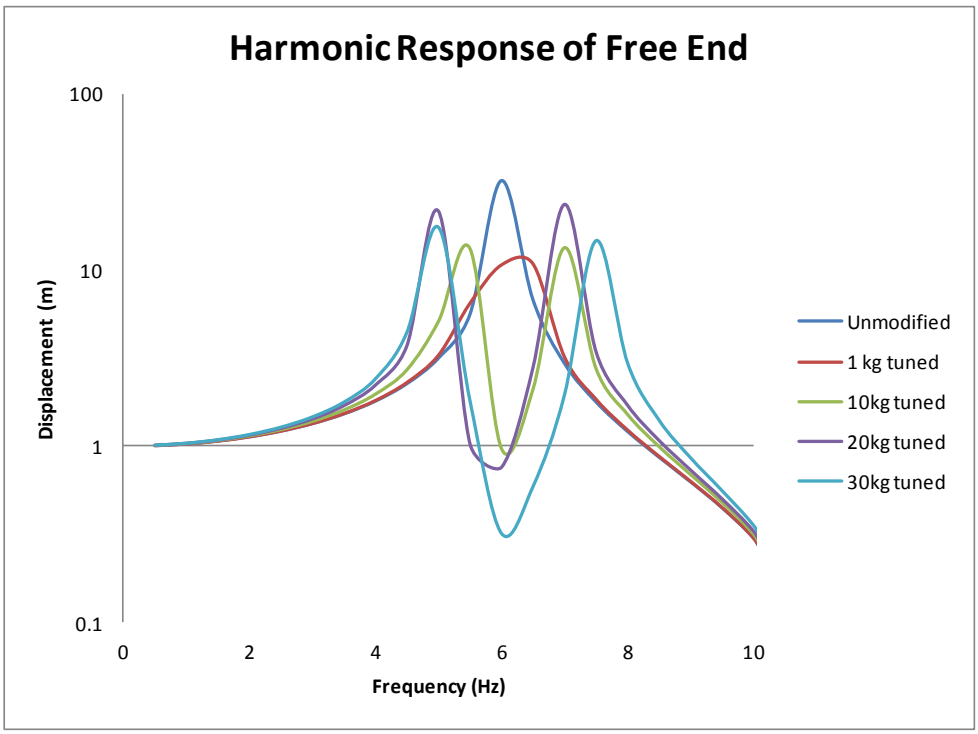

Figure 5-7. *Harmonic response of barrel end for unit base displacement for different undamped TVA masses.*

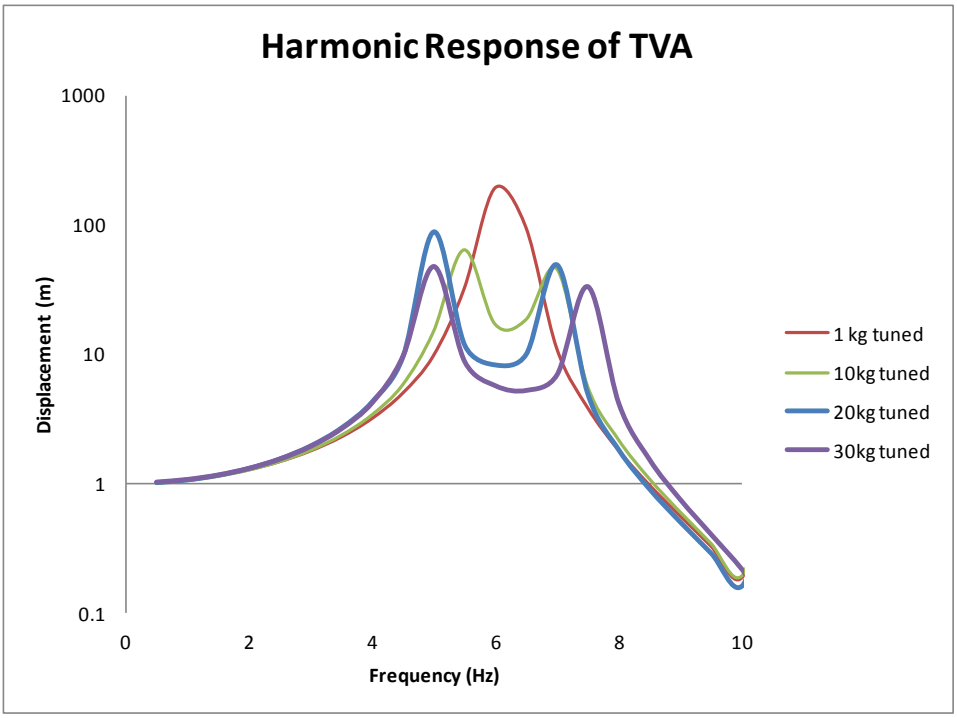

Figure 5-8. *Harmonic response of TVA for unit base displacement for different undamped TVA masses.*

By doing harmonic analysis effect of random base vibration is neglected and TVA tuning is done according to dynamic characteristics of the barrel only. As expected tuning frequencies of all TVA masses are very close to each other and it is the first resonant frequency of the barrel found from the modal analysis. In tuning the TVA the aim is to minimize the maximum response of the barrel end. Since frequency range of interest is broad, two peaks formed due to addition of TVA is tried to have equal amplitudes.

Due to possible effect of unsymmetrical behavior around the first resonance peak for TVA masses slightly different tuning frequencies are chosen. In ***Table 5-1*** tuning frequencies for different TVA masses are listed. Also percent difference from the 1st resonant frequency obtained from modal analysis is given. As mentioned above the aim is to obtain equal response amplitudes for new resonant peaks. Due to type of excitation both peaks are excited hence needed to be

minimized. Using this initial guess obtained from harmonic analysis results, modified system behavior under random field data will be studied. Fine tuning of mass and frequency will be done accordingly.

For determining optimum mass of TVA, spectrum analysis is done under field data which is collected during field tests. First tuning frequency is chosen according to harmonic analysis results given in ***Table 5-1.***

Table 5-1. *TVA Mass and Tuning Frequency with respect to harmonic analysis.*

TVA Mass	Tuning Frequency	% difference from unmodified system
1	6.16	1.5%
10	6.16	1.5%
20	5.75	5%
30	6.14	1.5%

For different TVA masses, responses of barrel end and TVA is investigated. In ***Figure 5-9*** unmodified long gun barrel free end response PSD is plotted. It is obtained from spectrum analysis that RMS amplitude of barrel end displacement of unmodified long gun barrel is 19.044 mm. In ***Figure 5-10*** and ***5-11*** response PSDs of barrel end and TVA are given for TVA tuned with respect to harmonic analysis i.e. with respect to resonant frequencies found in ***Table 5.1.*** Tuning the TVA with respect to harmonic analysis's results neglects the effect of input vibration data. In ***Table 5-2*** resultant RMS displacement amplitudes for barrel end and TVA are summarized.

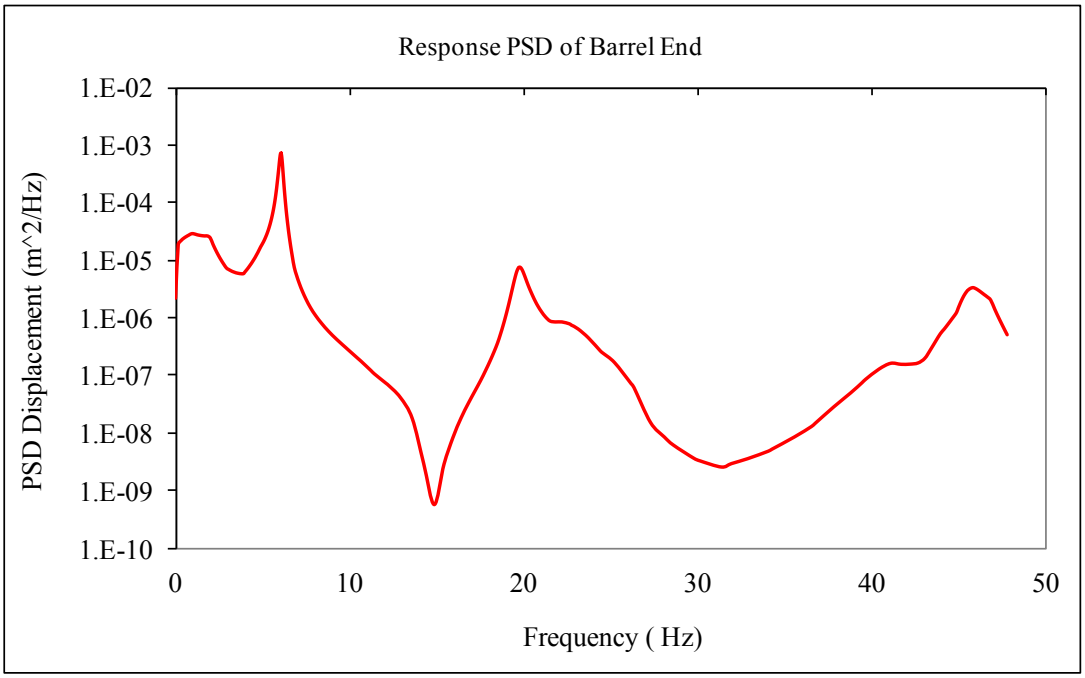

Figure 5-9. *Unmodified System Response PSD for experimentally obtained field data.*

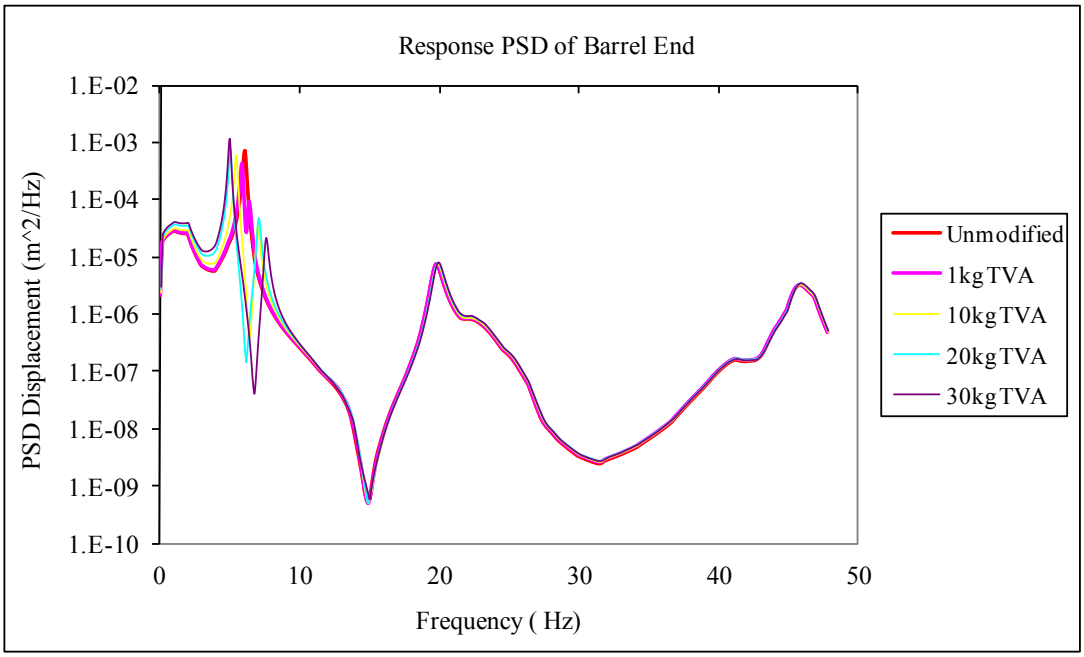

(a)

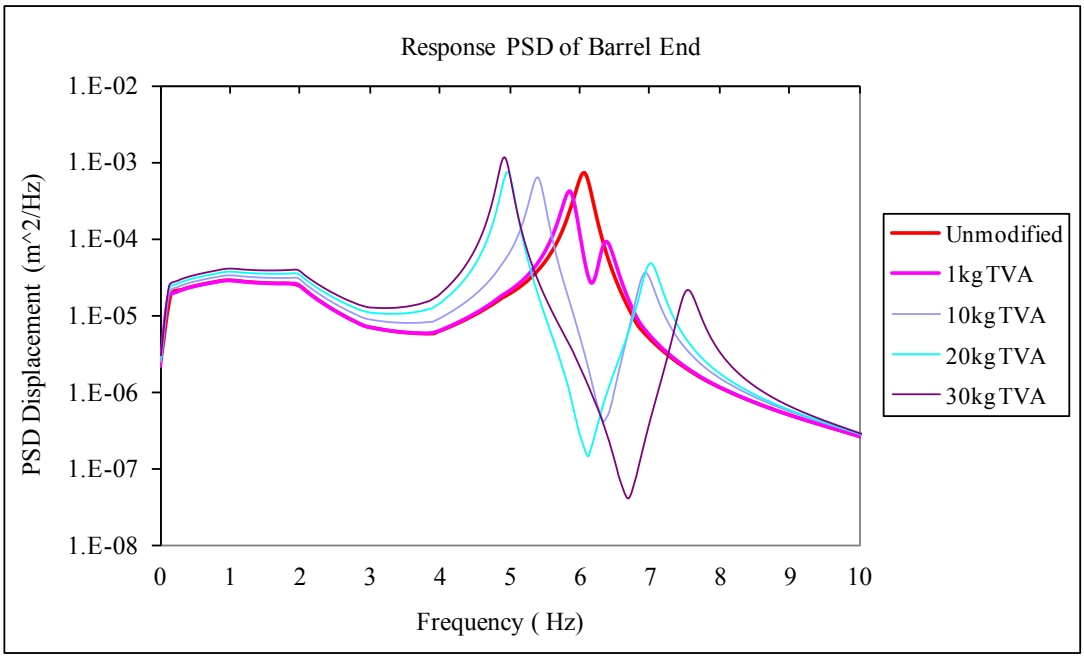

(b)

Figure 5-10. *Response PSD of the long barrel's free end with TVA for changing TVA mass when TVAs are tuned wrt harmonic analysis results* ***(a)*** *0-50 Hz.* ***(b)*** *0-10 Hz.*

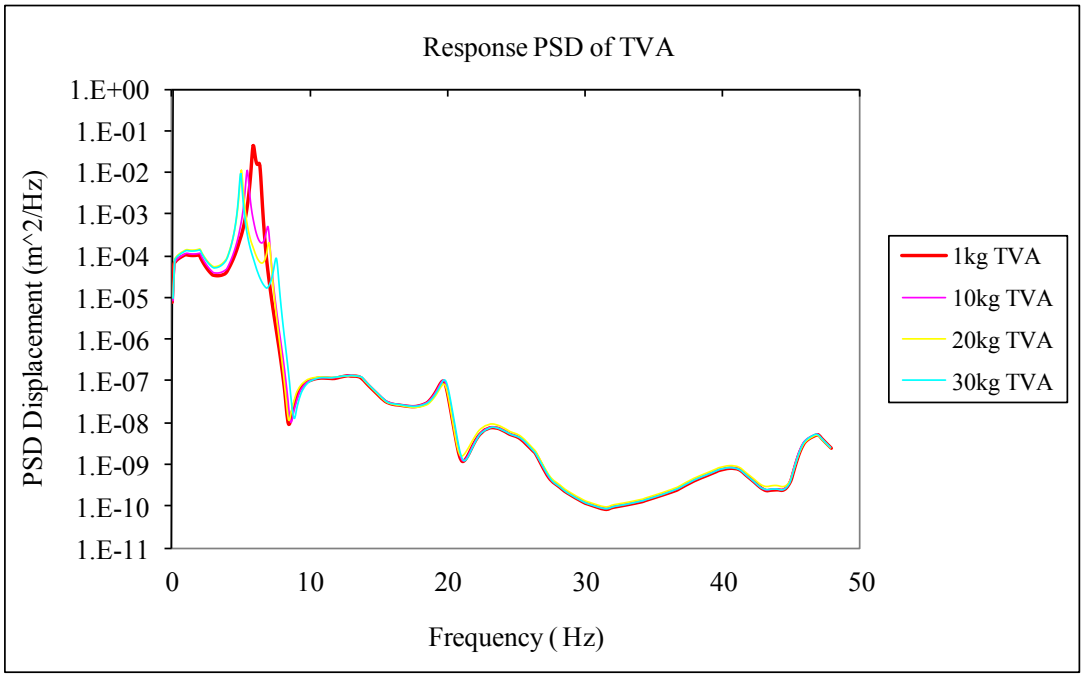

(a)

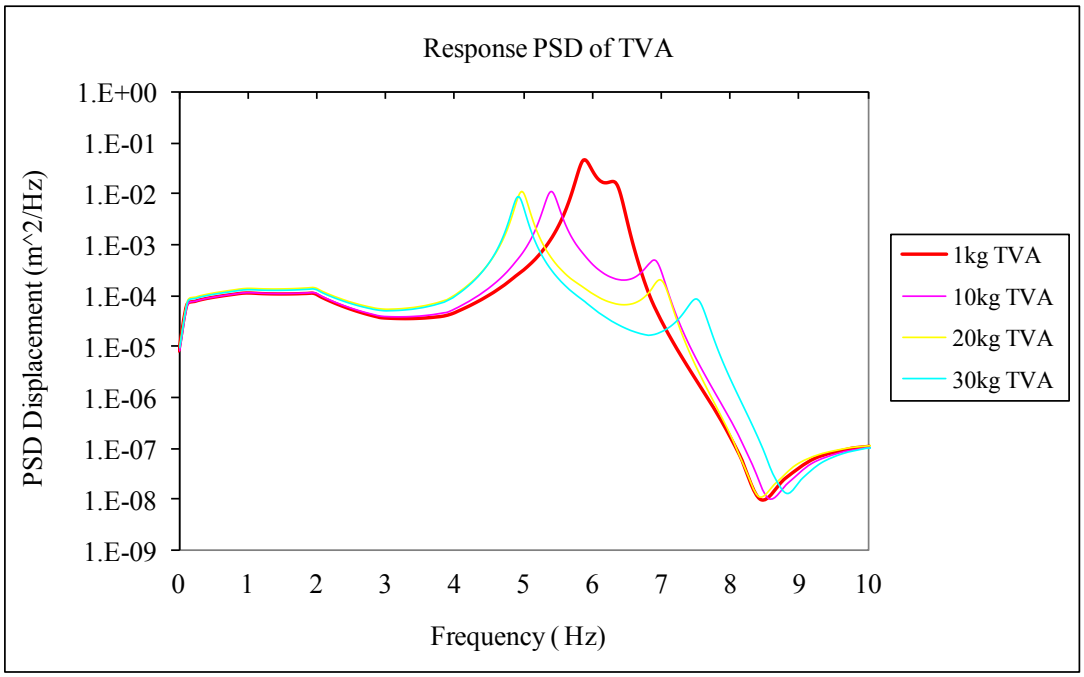

(b)

Figure 5-11. *Response PSD of the TVA for changing TVA mass when TVA is tuned wrt harmonic analysis results* ***(a)*** *for 0-50 Hz,* ***(b)*** *for 0-10 Hz.*

Table 5-2. *RMS displacement amplitudes of barrel end and TVA for different masses when TVA is tuned according to harmonic analysis.*

TVA Mass (kg)	RMS displacement amplitude of Barrel End (mm)	RMS displacement amplitude of TVA (mm)
1	16.5	136.4
10	17.69	64.2
20	18.5	61.5
30	21.47	54.45

RMS amplitudes given in ***Table 5-2*** are automatically calculated by ANSYS using the data found from the spectrum analysis; the value is the square root of the arithmetic mean of the squares of the original values.

The values given in ***Table 5-2*** are plotted in ***Figure 5-12*** to see the dependency of RMS amplitudes of TVA and barrel end displacements to TVA mass.

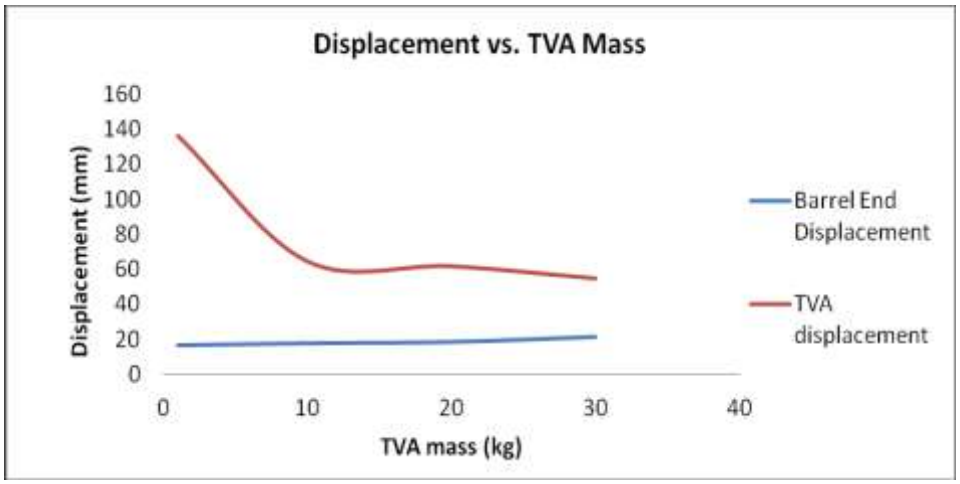

Figure 5-12. *RMS displacement amplitudes vs. TVA mass when TVA is tuned wrt harmonic analysis results.*

In ***Figures 5-10*** and ***5-11*** the tuning is done with respect to harmonic analysis results in which the tuning frequencies are found from geometry only. In fact this

approach neglects the effect of input random excitation. As a result with the additional effect of input excitation from the base TVA becomes mistuned. It is seen from ***Figure 5-10 and 5-11*** that the newly formed resonant peaks' amplitudes are not same. In order to tune the TVA for minimum barrel end response amplitudes the peaks are tried to be equalized. This is done by iteration and response PSDs of TVA and barrel end are seen in ***Figures 5-13*** and ***5-14.*** In these figures TVA is tuned by taking account of barrel geometry and imput vibration data.

Referring back to ***Figure 5-2*** it is seen that around 4 Hz, the The PSD of the base input acceleration for the long gun barrel has positive incline which results a peak in the input displacement PSD. Also a peak around 1-2 Hz which is seen in ***Figure 5-9*** of unmodified barrel displacement response PSD affects the system behavior for increasing mass. It is seen in ***Figure 5-10*** that when TVA mass is larger the left side newly formed peaks amplitude is amplified more. For the final determination of mass of the TVA, each TVA with different mass is retuned with respect to input PSD data. Experimentally obtained field data is applied from the trunnion. Barrel end response PSD plots are investigated and by iteration the peaks are tried to be equalized. This is done by changing the tuning frequency of the TVA. In ***Figure 5-13*** and ***5-14*** response PSDs of barrel end and TVA are seen.

RMS amplitudes given in ***Table 5-3*** are automatically calculated by ANSYS using the data found from the spectrum analysis, the value is the square root of the arithmetic mean of the squares of the original values.

RMS amplitudes of barrel end and TVA are tabulated. Comparing the amplitudes of ***Table 5-3*** with the ones at ***Table 5-2***, It is found that when the TVA is tuned with respect to both geometry and the input PSD data displacement amplitudes are less as expected.

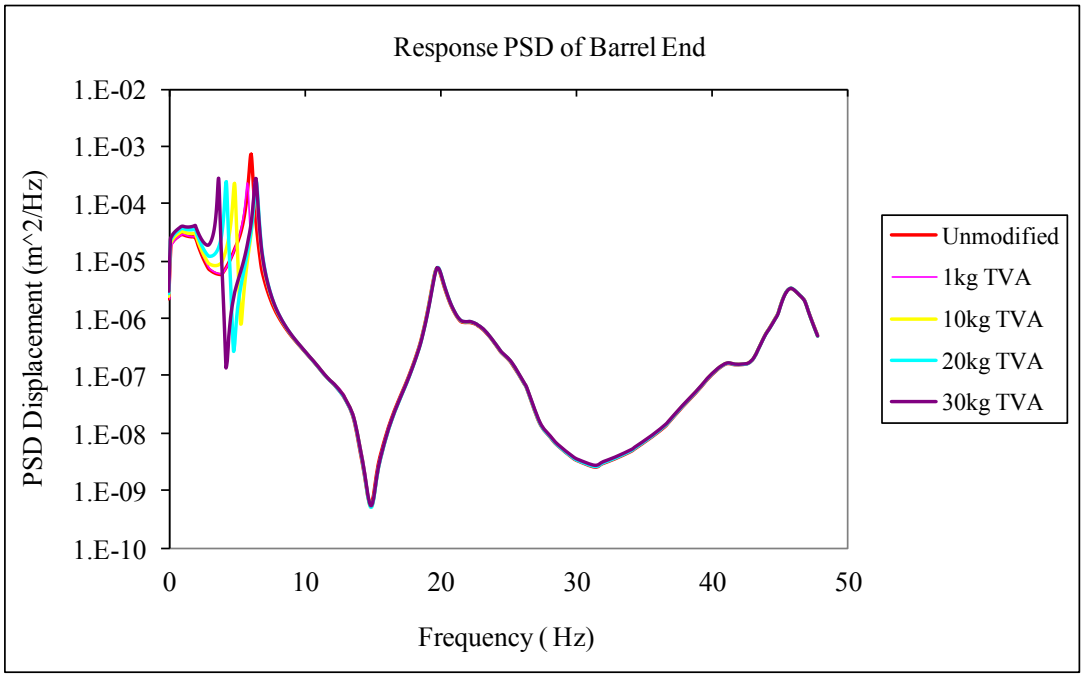

(a)

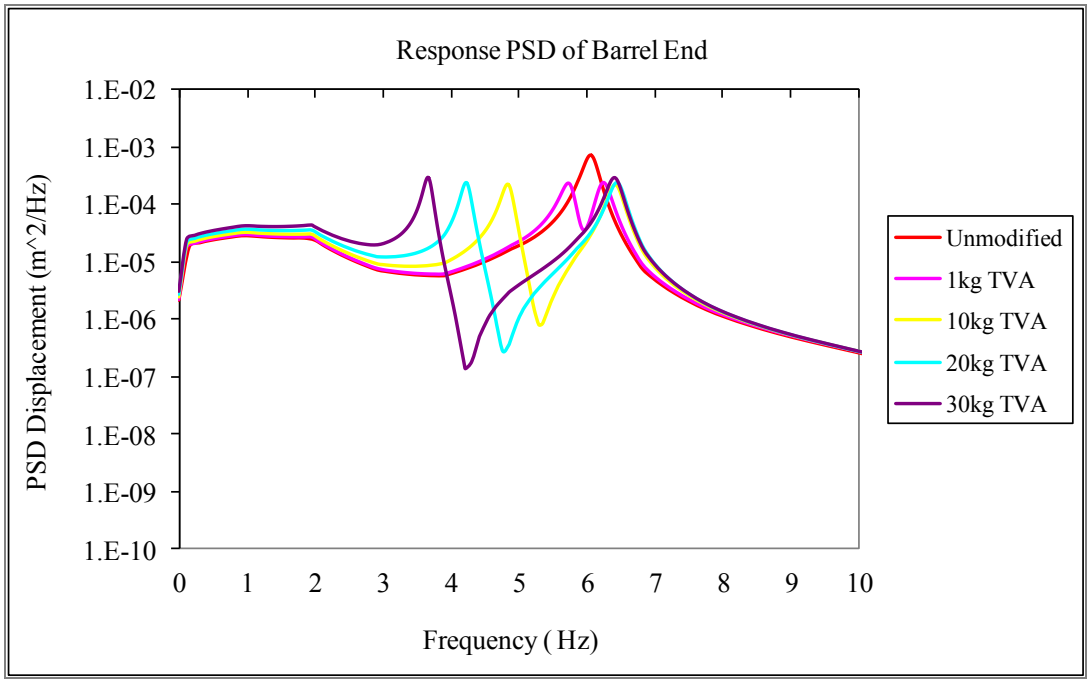

(b)

Figure 5-13. *Response PSD of barrel end for changing TVA mass when TVA is tuned with respect to geometry and the input PSD data.* ***(a)*** *for 0-50 Hz,* ***(b)*** *for 0-10 Hz.*

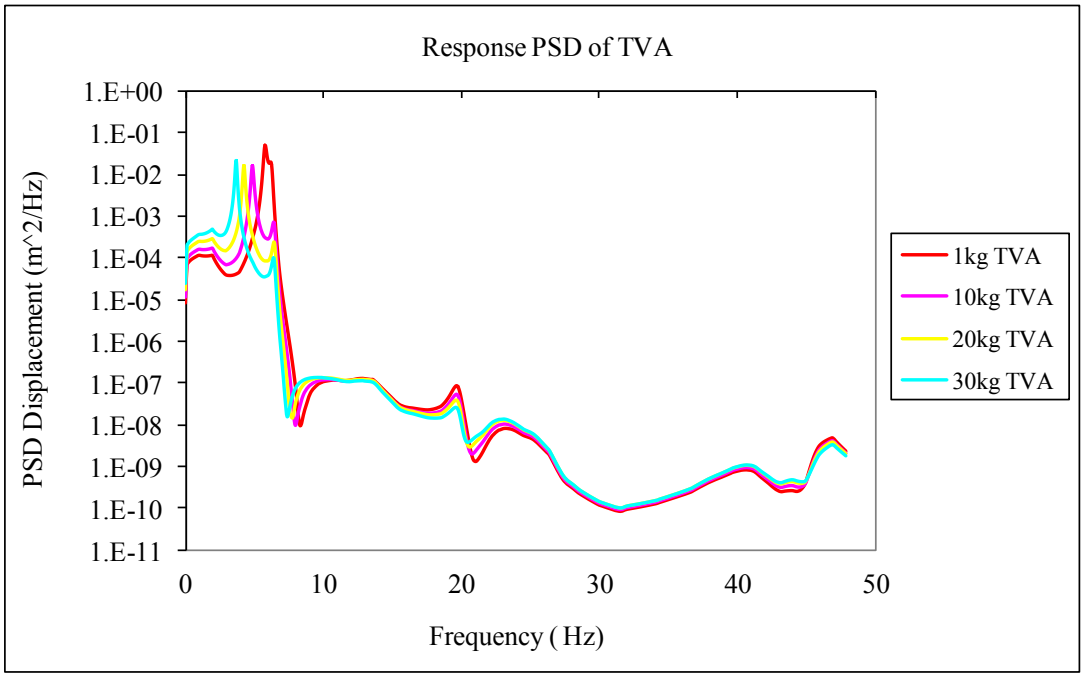

(a)

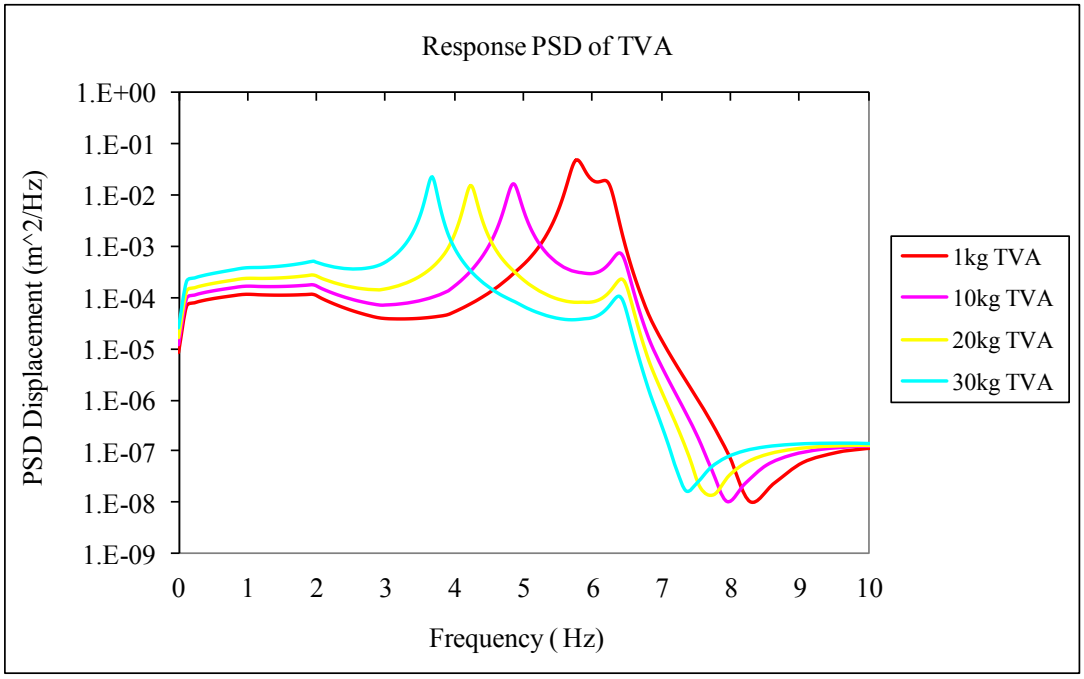

(b)

Figure 5-14. *Response PSD of TVA for changing TVA mass when TVA is tuned with respect to geometry and the input PSD data.* ***(a)*** *for 0-50 Hz,* ***(b)*** *for 0-10 Hz.*

Table 5-3. *RMS displacement amplitudes of barrel end and TVA for different masses when TVA is tuned with respect to geometry and the input PSD data.*

TVA Mass	RMS displacement amplitude of Barrel End (mm)	RMS displacement amplitude of TVA (mm)
1	15.94	145.4
10	15.74	74.9
20	16.23	69.67
30	17.28	78.69

The values given in Table 5-3 are plotted in ***Figure 5-15*** to see the dependency of RMS amplitudes of TVA and barrel end displacements to TVA mass.

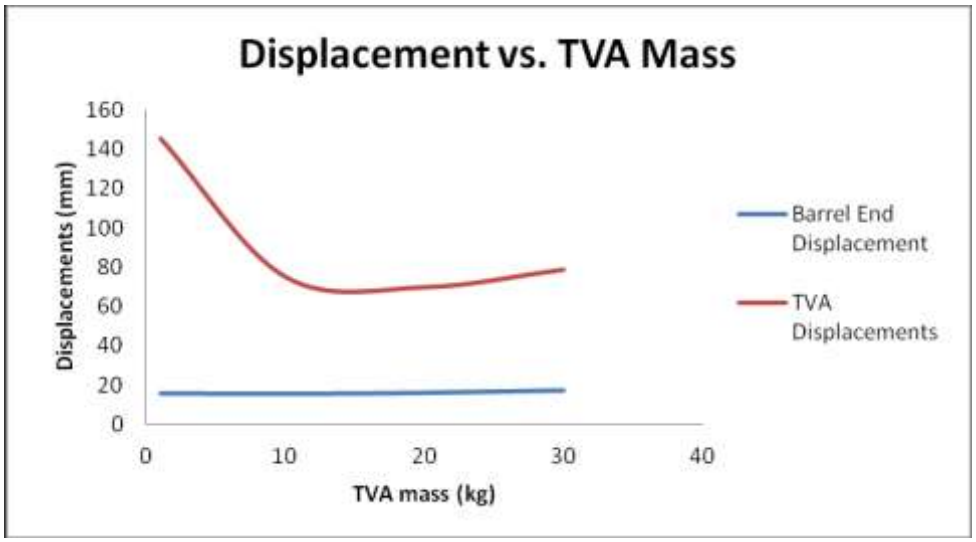

Figure 5-15. *Displacement amplitudes vs. TVA mass when TVA is tuned wrt overall optimum PSD analysis results.*

To see the effect of TVA mass on RMS amplitude of Barrel end displacement, ***Figure 5-16*** is plotted. It is seen from ***Figure 5-16*** that there should be an optimum mass for minimum RMS amplitude of Barrel end displacement between 1 and 10 kg of TVA masses. In ***Figure 5-17*** and ***Figure 5-18*** RMS amplitude of Barrel end and

TVA responses for changing TVA mass are investigated for TVA masses between 1 to 10 kg.

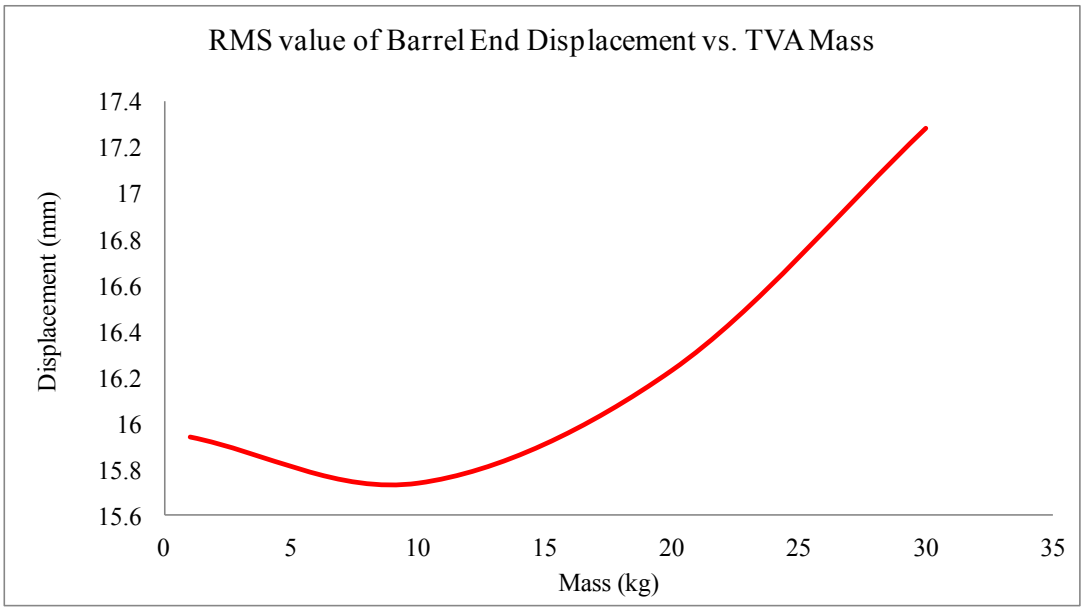

Figure 5-16. *Displacement amplitude of free barrel end vs. TVA mass when TVA is tuned with respect to geometry and the input PSD data.*

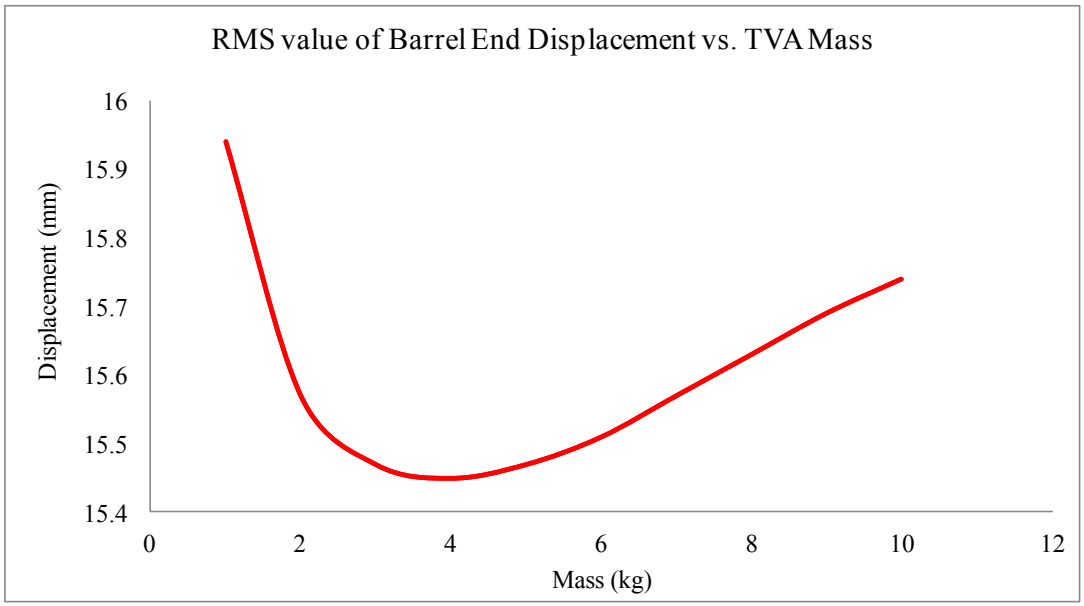

Figure 5-17. *Barrel end displacement vs. TVA mass 0-10 kg when TVA is tuned with respect to geometry and the input PSD data.*

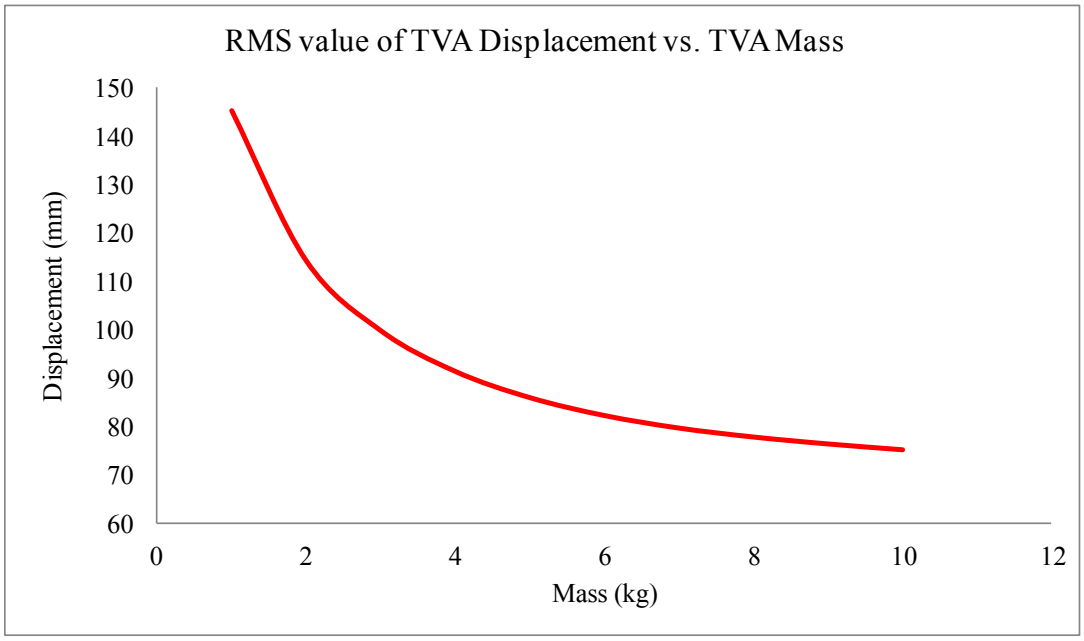

Figure 5-18. *TVA displacement vs. TVA mass 0-10 kg.*

From ***Figure 5-17*** and ***Table 5-4*** optimum mass of the TVA is found to be 4 kg. It is chosen with respect to minimum RMS value of barrel end displacement when barrel is subjected to random vibration from the base. Since gun barrel weights more than 1 tone addition of 4 kg TVA is almost negligible. For 4 kg of TVA mass barrel end displacement RMS amplitude is minimum and TVA displacement RMS amplitude is applicable. It is also seen in ***Table 5-4*** that for 1 kg of TVA, vibration displacement of TVA is as high as 145 mm. In practice displacement of TVA is also important in case of compact design. From ***Table 5-4*** it is also conluded that increasing the mass of TVA decreases the TVA vibration amplitude. Comparing the TVA masses of 20 kg and 30 kg with 10 kg it is seen that TVA displacements do not change at all. This is due to fact that after 10 kg tuning frequency becomes further away and TVA is not excited at all.

It is also found during the analyses that if one continues to increase the TVA mass which is at the end of the gun tube; it is found that barrel ends RMS displacement amplitudes are larger than the unmodified barrel.

Table 5-4. *Barrel end and TVA displacement RMS amplitudes for changing TVA mass of 0-10 kg when TVA is tuned with respect to geometry and the input PSD data.*

TVA Mass	RMS displacement amplitude of Barrel End (mm)	RMS displacement amplitude of TVA (mm)
1	15.94	145.4
2	15.57	114.19
3	15.47	99.66
4	15.45	91.19
5	15.47	85.74
6	15.51	82.02
7	15.57	79.41
8	15.63	77.55
9	15.69	76.11
10	15.74	74.9

Up to this point of the thesis study, it is found that when TVA mass is optimized to 4kg and assembled to gun barrel without any damping, it can change the system behavior. If we compare the results with the shorter gun barrel it is found in ***Table 5-5*** that it is not enough for undamped TVA to decrease the vibration amplitudes at the end of the gun barrel to the level of shorter gun barrels alone.

Table 5-5. *Comparison of Gun Barrels End Deflections RMS amplitude*

	Short Gun Barrel	Long Gun Barrel (Unmodified)	Long Gun Barrel (Modified with Undamped TVA)
Barrel End Displacement (RMS amplitude)	7.385 mm	19.044 mm	15.45 mm

Looking results given in ***Table 5-5*** is seen that without damping long barrel deflections can not be decreased to the level of short gun barrel deflections. This result is also predicted from the type of excitation; since excitation frequency is broadband tuning the TVA without damping has no strong effect since newly formed resonant peaks are also excited. In order to see the effect of damping TVA model is changed and spectrum analyses with field data are rerun.

In this thesis study ANSYS finite element software is used for all analyses. In order to apply damping in modal and spectrum analyses, one must define material dependent damping. This is due to fact that solver Block Lanczos is not able to solve problems where damping is defined directly through real constants or special elements like COMBIN 14 [19]. TVA is designed as a beam and tip mass, beam element resembles the elastic and damping properties via material properties and geometry. Point mass at the tip is for the TVA mass. Effect of damping on system is investigated for 4 kg and 20 kg masses. 4 kg is for the optimum case and results are used in next chapter for conceptual design. 20 kg TVA application is also studied to see the effect of TVA mass in addition to damping. At the end, results for both cases are compared and final design parameters are selected to be used in conceptual design.

5.1.1 APPLICATION OF DAMPING TO 4 KG TVA MASS

In ***Figures 5-16***, ***5-17*** and ***Table 5-4*** optimum TVA is found to be 4kg for minimum barrel end deflection RMS amplitude. Hence 4 kg TVA mass is chosen to be the first case to investigate the effect of damping.

For 4 kg being the mass of TVA, spectrum analysis is done for the modified system with different damping ratios. Tuning frequency is already found hence effect of damping is taken in to account. For spectrum analysis damping ratio of the TVA is modeled via special beam element which represents the elastic behavior and also

has damping properties. In ANSYS one can not assign damping to ready to use spring-damper elements. Hence beam element is designed to fulfill the elastic properties of spring i.e. the stiffness and the damping ratio. Response PSD plots of barrel end and TVA is plotted in ***Figure 5-19*** and ***5-20*** respectively. It is seen from ***Figure 5-19*** that increasing the damping ratio of the TVA resonant peak amplitude of the barrel end response PSD decreases. In ***Table 5-6*** it is seen that for damping ratio of 1.5 barrel end deflection RMS amplitude is less than half of the undamped TVAs case. The effect of increased damping is similar for TVA deflection RMS amplitudes too. Increasing the damping ratio up to critically damped case decreases TVA deflection amplitudes.

In ***Figure 5-21*** and ***5-22*** barrel end and TVA displacements vs damping ratio of TVA is plotted using ***Table 5-6***. It is seen that increasing damping decreases the displacement for barrel end and TVA.

Table 5-6. *Gun Barrels End Deflections when TVA is tuned to 4 kg with different damping ratios.*

Damping Ratio	Barrel End Disp. (mm)	Tva Disp. (mm)
0	15.45	91.19
0.02	14.03	70.67
0.05	13.02	54.73
0.1	12.2	40.72
0.2	11.36	28.38
0.5	10.23	19.54
1	9.42	16.48
1.5	6.62	17.93

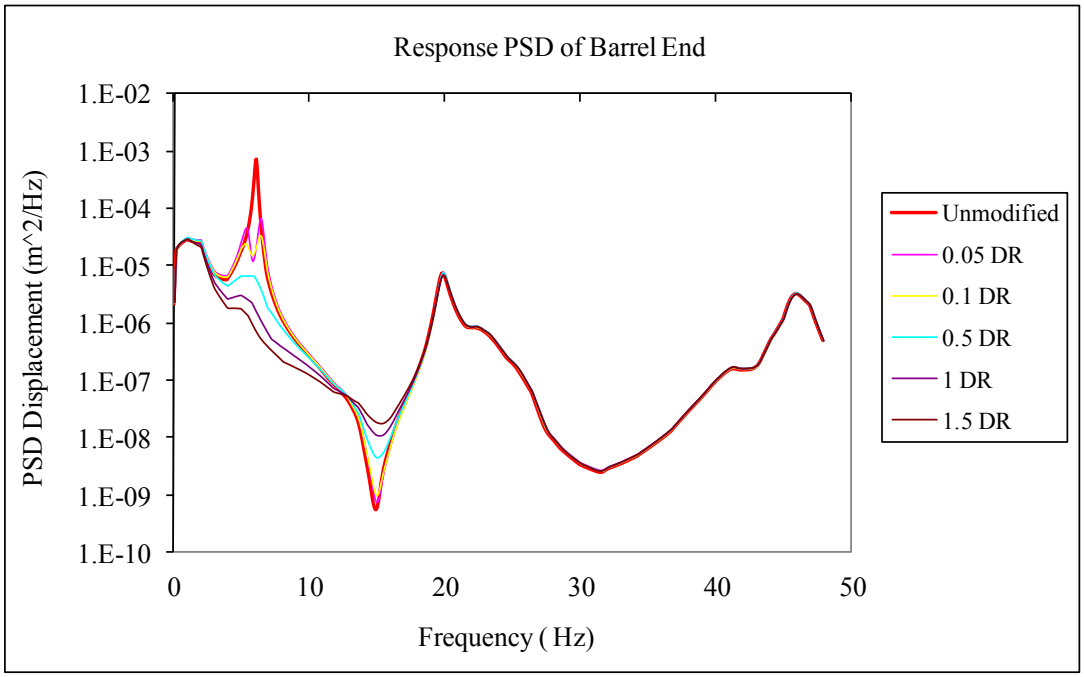

(a)

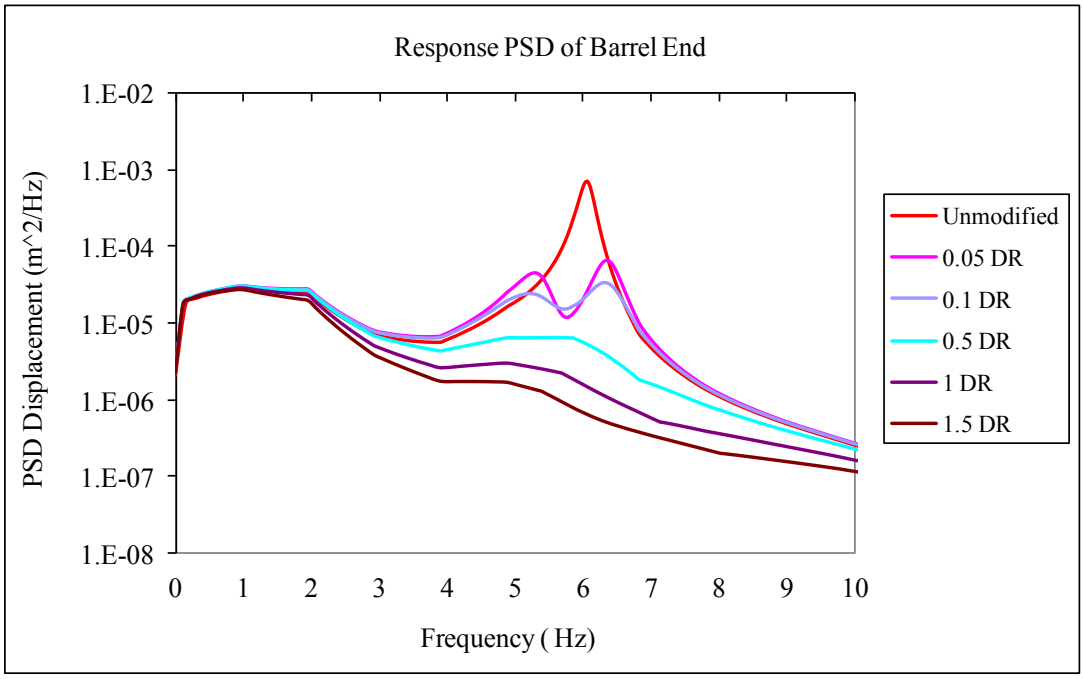

(b)

Figure 5-19. *Response PSD plot of Barrel End when TVA is tuned to 4 kg with different damping ratios.* ***(a)*** *for 0-50 Hz,* ***(b)*** *for 0-10 Hz.*

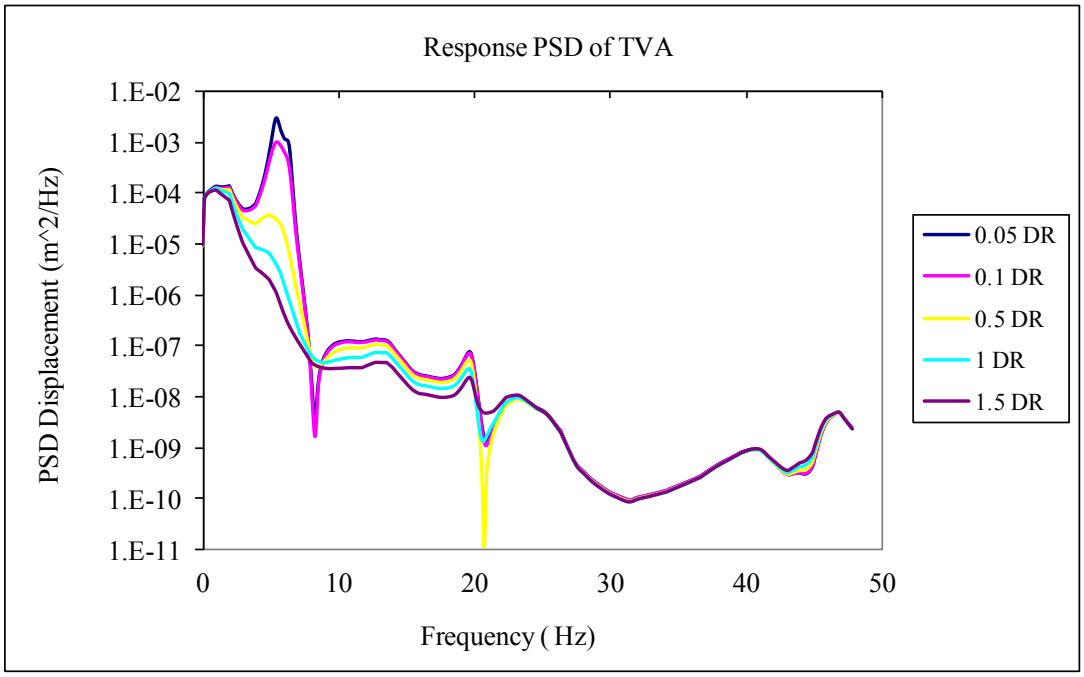

(a)

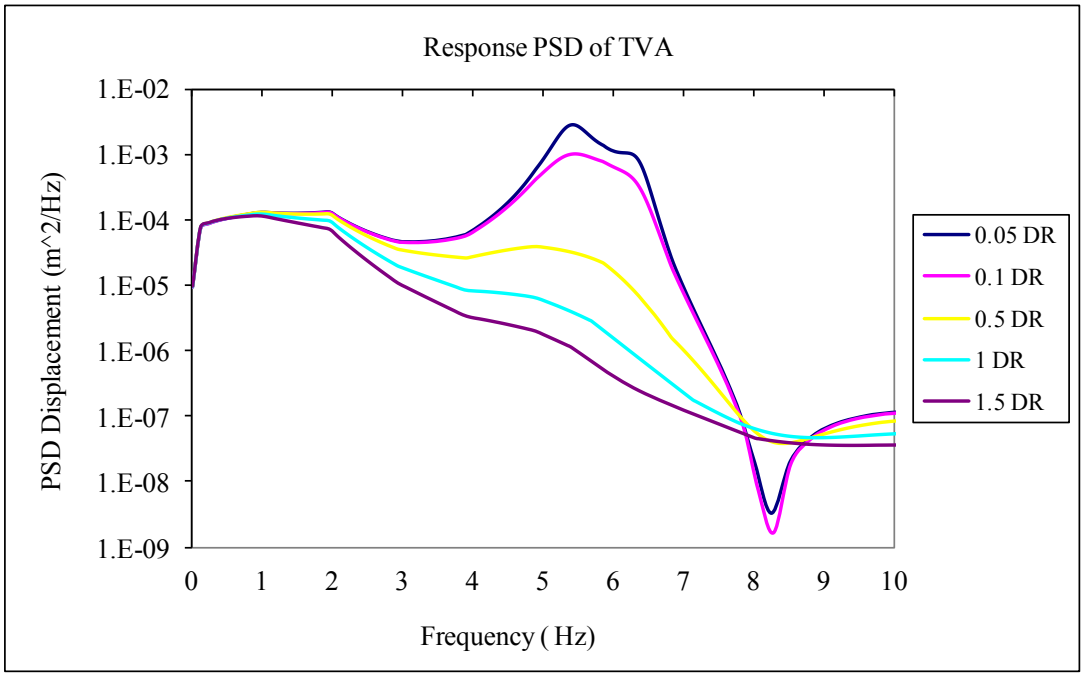

(b)

Figure 5-20. *Response PSD plot of TVA when TVA is tuned to 4 kg with different damping ratios.* ***(a)*** *for 0-50 Hz,* ***(b)*** *for 0-10 Hz.*

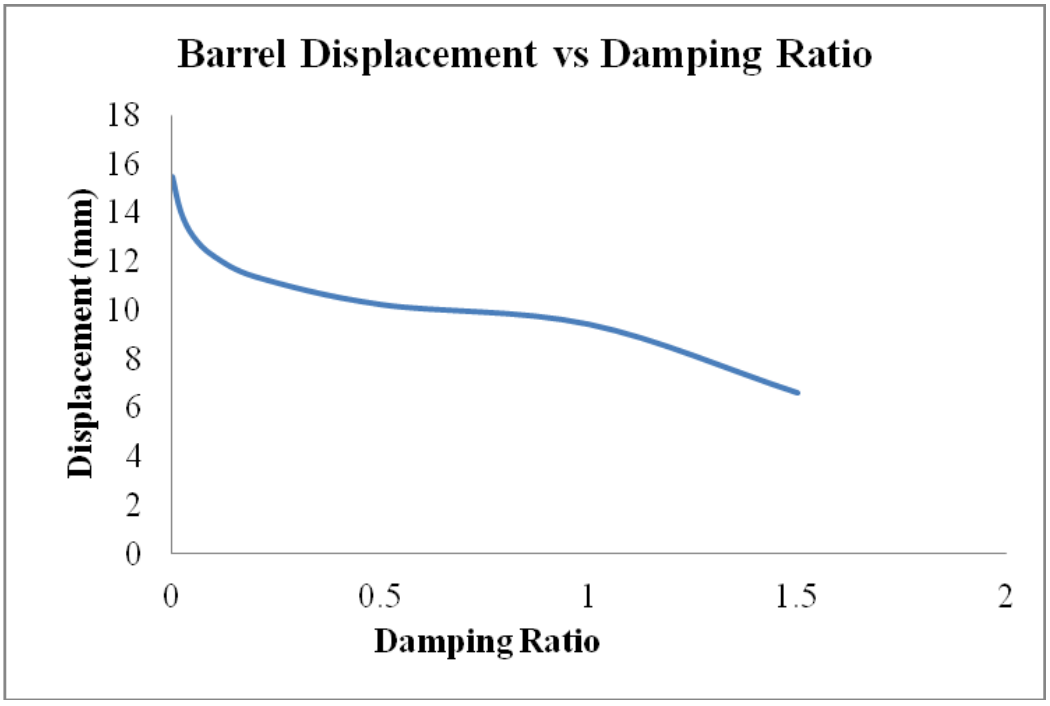

Figure 5-21. *Barrel End Displacement vs. Damping Ratio when TVA is tuned to 4 kg with different damping ratios.*

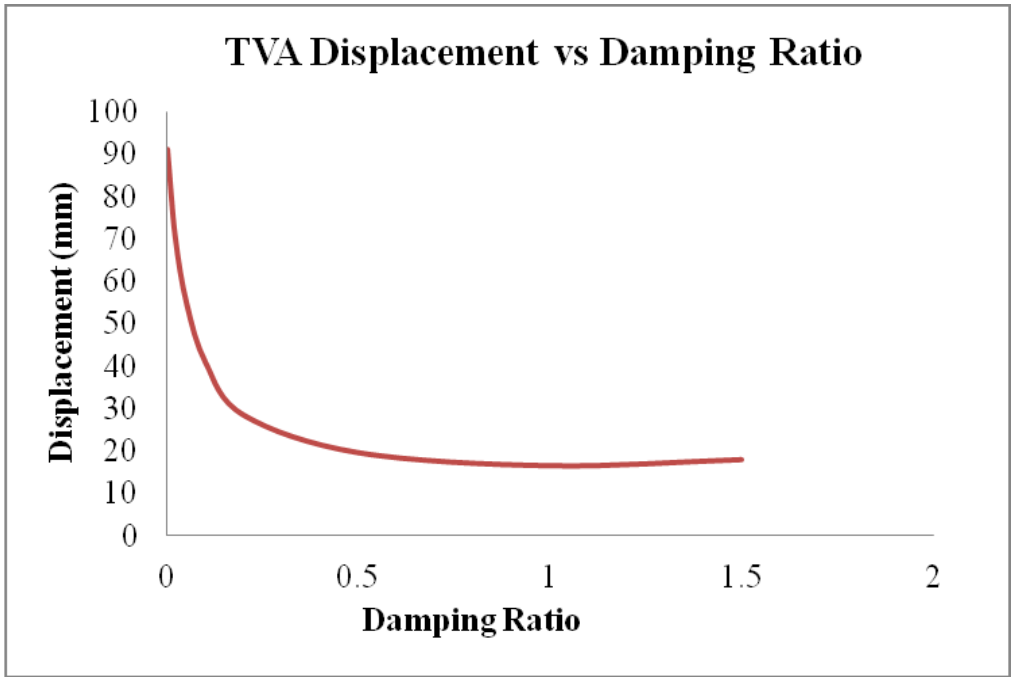

Figure 5-22. *TVA Displacement vs. Damping Ratio when TVA is tuned to 4 kg with different damping ratios.*

5.1.2 APPLICATION OF DAMPING TO 20 KG TVA MASS

For the second case, 20 kg TVA mass is studied and results are compared with case studied in Section 5.1.1. Increasing damping ratio of TVA decreases the barrel end deflection. Change in barrel end displacement and TVA displacement with respect to damping ratio is plotted in ***Figure 5-22*** and ***Figure 5-23***. Using these figures effect of damping on barrel end displacement and TVA displacement is seen. It is found that for minimum barrel end displacement damping as much as possible is required since increasing damping ratio decreases the barrel end deflection. It is also concluded that the effect of damping on overall system is found to be similar to previous Section 5.1.1.

Displacement amplitudes of barrel end for 20 kg TVA is summarized in ***Table 5-7***. When barrel end displacements found from application of 20 kg TVA is compared with 4 kg TVA, another important result is seen. Looking in ***Table 5-6*** and ***5-7*** i.e. when 4 kg and 20 kg TVAs are compared it is seen that for same damping ratio 4 kg TVA mass results are always better. For instance for critical damping barrel with 4 kg TVA deflects 9.42 mm whereas barrel with 20 kg TVA deflects 10.06 mm. When compared to short gun barrel, optimum mass reaches the same barrel end deflection with less damping. Final comparison of damped TVAs with the short gun barrel is done in ***Table 5-8***.

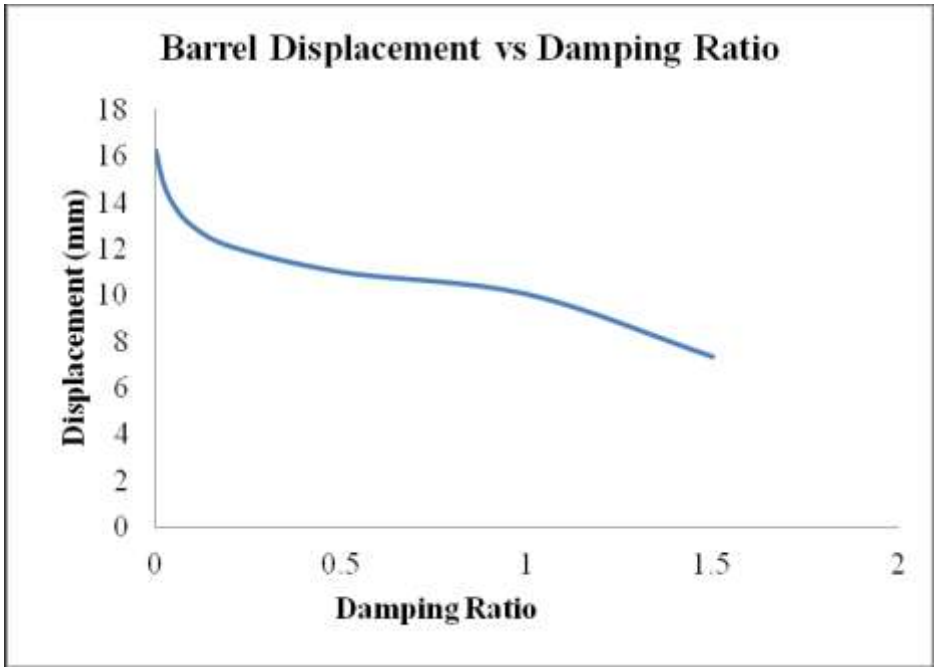

Figure 5-23. *Barrel End Displacement vs. Damping Ratio when TVA is tuned to 20 kg with different damping ratios.*

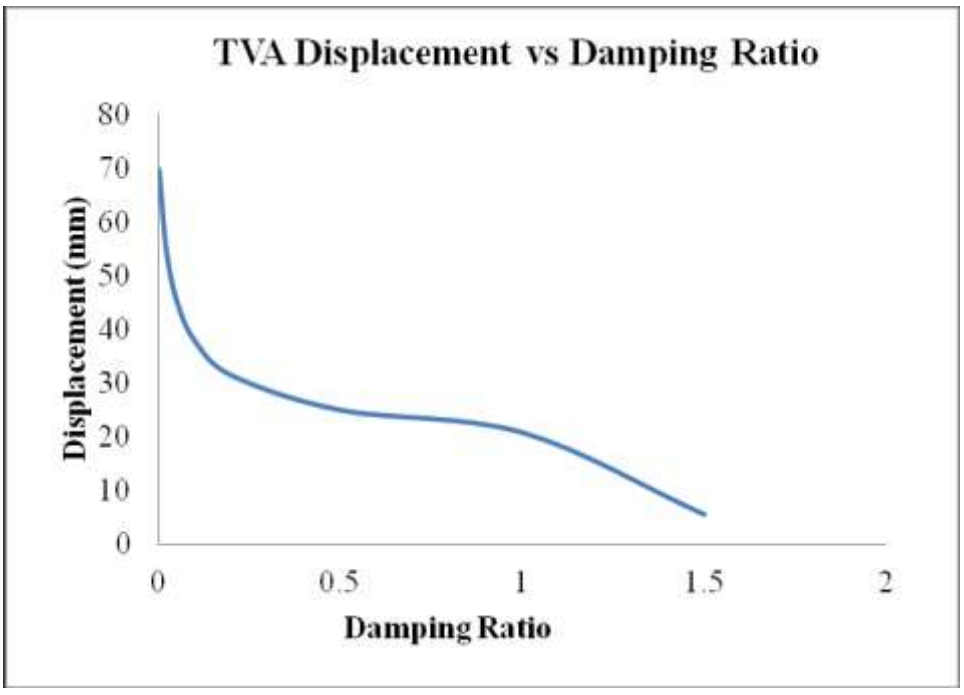

Figure 5-24. *TVA Displacement vs. Damping Ratio when TVA is tuned to 20 kg with different damping ratios.*

Optimum tuning is done for different masses and it is found that for optimum tuning and using larger masses tuning frequency must be shifted from the dominant first resonance peak of the gun barrel. This in fact results in less vibration energy storage in TVA. It is also observed that masses larger than 50 kg when applied without damping; system behavior becomes worse. After finding optimum mass of the TVA, damping properties are investigated. It is found from analyses done with different damping ratios that increasing damping decreases the barrel end displacement as a result damping in physical limits should be applied as much as possible since vibration energy mostly stored in damping elements other than mass and elastic elements. Looking at ***Table 5-6*** and ***5-8,*** it is seen that when a damping ratio of 1.5 is applied to 4kg TVA it is seen that displacement amplitude at the barrel end becomes lower than the short gun barrel. Application of damping is limited with physical properties of available materials, and some geometric constraints. Application of damped TVA availability and is studied in next section of Chapter 5.

Table 5-7. *Maximum displacement vs. damping ratio for 20 kg TVA.*

Damping Ratio	Barrel End Disp.	Tva Disp (mm)
0	16.23	69.67
0.02	14.86	54.55
0.05	13.85	44.88
0.1	12.97	37.62
0.2	12.12	31.4
0.5	11.01	24.96
1	10.06	20.79
1.5	7.37	5.57

In conclusion for optimum TVA, mass is found to be 4kg. For lower masses both TVA amplitudes and barrel end deflections are increasing, this due to fact that input

data is not constant but includes peak around 4 Hz which is slightly lower than the first resonance frequency of the barrel.

Table 5-8. *Gun Barrels End Deflections summary*

	Barrel End Displacement
Short Gun Barrel	7.385 mm
Long Gun Barrel (Unmodified)	19.044 mm
Long Gun Barrel (Modified-Undamped)	15.45 mm
Long Gun Barrel (Modified-Damped)	15.45-6.62 mm

5.2 CONCEPTUAL DESIGN SOLUTIONS FOR TVA

In the final part of the thesis study conceptual design of TVA is done. Two possible alternatives are studied, required properties of weight, stiffness and damping are tried to be achieved.

First conceptual design alternative is resonant type beam design in which a cantilever beam with tip mass is utilized as the TVA with the first resonance of the beam is the tuning frequency of TVA. For this design alternative, elastic property comes from the thin beam structure and the mass property comes from the concentrated tip mass placed at the free end of the cantilever beam design. Second conceptual design alternative consists of dash-pots and spring elements connected in parallel with rigid block acting as the mass element. For alternative conceptual designs detailed designs have been established which involves deciding on the materials and geometrical dimensions. During the design process in addition to the tuning frequency of the TVAs designed the strength characteristics of the designs

under random vibration and impact during shot are also used as performance targets.

5.2.1 FIRST DESIGN ALTERNATIVE, RESONANT BEAM TYPE TVA

First conceptual design alternative for the TVA is composed of a simple cantilevered beam with a tip mass at the end. This type of TVA is similar to alternative design which is discussed at literature survey in Section 2.4.3.5 namely bone type of TVA.

In this conceptual design TVA is tuned by playing with the beam geometry (length and cross-section) for stiffness and/or the tip mass to be placed at the free end of the beam for effective TVA mass. Once the tuning frequency is identified, geometrical dimensions and materials are to be used can be decided. In its final design configuration the resonant beam type TVA should also be subjected to static and dynamic structural analyses to see whether it can withstand large impact loads during fire.

Location of TVA on the barrel is already chosen as the free end of the gun barrel where displacements are maximum when the barrel is subjected to base excitation.

For almost every main battle tank there is a mechanical interface for assembling the muzzle reference system (MRS) at the free end of the barrel. This mechanical interface can be used to connect the TVA. Since a physical version of the tank barrel is not currently available for this thesis study, modeling of the interface is done with data taken from the manufacturer. The detailed barrel tip model including MRS interface is seen in ***Figure 5-25***.

***Figure 5-25**. Barrel free end with MRS mechanical interface.*

For thin beam part of the TVA steel is used. Ultimate tensile strength of steel is about 1 GPa and yield strength of steel is about 750 MPa. For annealed steel yield strength can go up to 1.5 GPa. For the resonant beam both shear and tensile stresses are considered. For shear stregth calculations values are taken to be half of the tensile strength values. Impact load during shot is applied both parallel and perpendicular to barrel axis. It is estimated that due to geometry of extended beam critical stresses are found as shear stresses at the region of the end of the fixed support.

Impact loading is the load at the end of the barrel which occurs due to firing event. During fire large accelerations are formed at the end of the barrel. Since TVA is placed at the end of the barrel the design must withstand such accelerations. For critical electro-optic systems such as MRSs, design is said to be withstand 1000g dynamic accelerations this criteria is accepted internationally. Since the loading is dynamic a conversion for static structural analysis is done using formulas given in [20]. In the table dynamic accelerations can be converted to static accelerations with respect to time of impact loading. Since the time of shot is not known clearly and estimated time values (around 0.5 msec) give lower results than expected the scale factor for dynamic to static conversion is taken to be 1. As a result 1000g static

acceleration is applied parallel and perpendicular to barrel axis as shown in ***Figure 5-26***.

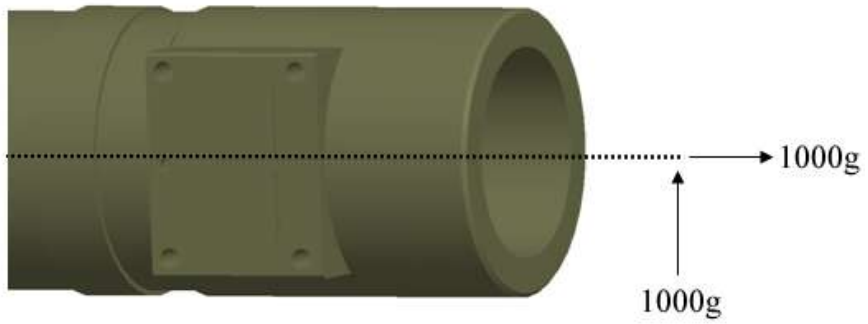

Figure 5-26. *Static accelerations and their directions applied at the free end of the barrel.*

For the concentrated tip mass part of the TVA which is located at the free end it is found from both analytical and finite element analyses that any eccentricity between the neutral axis of the beam and the mass causes amplified stresses parallel to barrel axis. For tension stresses it is known that maximum stress occurs at the surface farthest from the neutral surface/axis. Hence for increased eccentricity in well known stress formula given below c term is increases and maximum stress is also increases hence eccentricity should be minimized.

$$\sigma_{\max} = \frac{M \times c}{I} \qquad \text{(Eq.5.1)}$$

Another important design criteria to consider is the ease of assembling the beam and the concentrated tip mass is designed so that for better tuning they can be easily assembled and disassembled for cases where manufacturing is not perfect and needs to be modified for fine tuning.

Damping will be added to the TVA at the end of the analyses in order to decrease displacements of the tip mass. Damping is applied as surface layer treatments using appropriate materials.

It is already found in previous section 5.1 that optimum TVA is 4 kg and first resonant frequency is tuned to 5.67 Hz. In order to decide on geometry and mass properties analytical cantilever beam formulas are used. Some geometric constraints are defined prior to design stage; it is constrained that the beam length must not exceed 500 mm. It is important to note that designed TVA must withstand impact load due to firing event as mentioned earlier.

For the design of resonant beam type TVA first required geometric properties for optimum tuning is decided using well-known beam formulas. For a cantilever beam given in ***Figure 5-27 (a)*** and ***(b)*** analytical relationships are given by below equations [25].

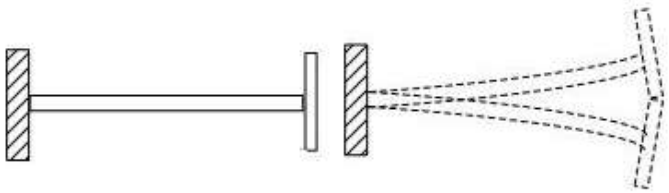

(a) ***(b)***

Figure 5-27. *Cantilevered beam* ***(a)*** *stationary,* ***(b)*** *vibrating.*

Equation of motion of the system is given in equation 5-2 [25], it is seen that the system is assumed to be SDOF system, hence equivalent mass and stiffness is obtained.

$$m\ddot{y}(t) + ky(t) = 0 \qquad \text{(Eq.5.2)}$$

For cantilevered beam transverse stiffness is given in Eq 5-3 [25]. For resonant beam type TVA first resonant frequency occurs at transverse direction which is seen in ***Figure 5-27*** (b).

$$k = \frac{3EI}{l^3} \qquad \text{(Eq.5.3)}$$

Using the stiffness one can find the undamped first resonant frequency of the system using Eq 5-4 [25].

$$\omega = \sqrt{\frac{k}{m}} \qquad \text{(Eq.5.4)}$$

here m is not the concentrated mass but the equivalent mass. If the beam element has mass equivalent mass is calculated using equations 5-7and 5-8 below. Substituting Eq 5-3 into 5-4 first resonance frequency formula can be re-written as Eq 5-5.

$$\omega = \sqrt{\frac{3EI}{ml^3}} \qquad \text{(Eq.5.5)}$$

In the above equation 5-5 E is the modulus of elasticity of beam element and depends on material properties. I is the moment of inertia and for a rectangular cross section beam I is found as,

$$I = \frac{wt^3}{12} \qquad \text{(Eq.5.6)}$$

where w is the width and t is the thickness of the beam. For evenly distributed mass of beam element and equivalent mass of overall system is taken as,

$$m_b = \frac{33}{140} \times m_{beam} \quad \text{(Eq.5.7)}$$

$$m_{eq} = \frac{33}{140} \times m_{beam} + m_{end} \quad \text{(Eq.5.8)}$$

Using analytical equations above resonant beam type TVA geometry is constructed and tuned to 5.67 Hz. For the beam element steel is used and for tip mass tungsten is used since its density is higher. Equivalent mass is tuned to optimum value of 4 kg. Initial design parameters found analytically is given in ***Table 5-9.***

Table 5-9 *Initial Geometric Properties of TVA found analytically.*

L	0.45 m
W	0.15 m
T	0.004 m
Mass of the beam	2.1 kg
Mass at the tip	3.7 kg
Material	Steel, density 7850 kg/m^3, E=200 GPa Tungsten, density 19300 kg/ m^3, E=400 GPa

For the initial design parameters of TVA maximum stresses are calculated analytically using below formulations [27] Both bending and tension stresses are calculated and summed for total stress calculations. For the tensional stress any eccentricity from neutral axis of the beam is neglected.

It is already defined that 1000g static acceleration is applied on TVA in parallel and perpendicular to barrel axis, for a simplified TVA sketch location of TVA and applied accelerations are seen in ***Figure 5-28***.

.

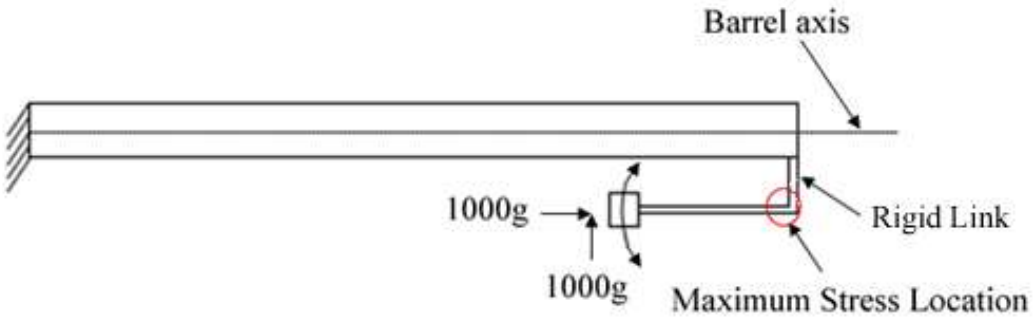

Figure 5-28. *TVA assembled to gun barrel.*

Forces and moments acting on both directions are found as eq 5-9 and 5-10.

$$F = a \times m_{eq} \quad \text{(Eq.5.9)}$$

$$M = F \times L \quad \text{(Eq.5.10)}$$

For tensile stress it is force per cross-section area,

$$\sigma_{tensile} = \frac{F}{A_{cross-section}} \quad \text{(Eq.5.11)}$$

Bending moment stress is found by equation 5-12 below:

$$\sigma_{shear} = \frac{Mc}{I} \quad \text{(Eq.5.12)}$$

$$\sigma_{total} = c_{tensile} + \sigma_{bending} \quad \text{(Eq.5.13)}$$

Note that for tensile stress effect of moment is neglected by inserting the mass symmetric to neutral axis of the beam. The mass used in calculations is the optimum TVA mass that is moving mass of the TVA. It is found as 4 kg which

reveals best results for minimum barrel end deflection RMS value when the tank is subjected to random base vibration. For the rigidly connected part of the TVA the mass is not crucial since the barrel weights more than 1 tone and TVA total mass is decided not to exceed 20 kg.

Using above analytical formulas maximum stresses for initial design is found to be 47 Gpa. The design is found to be not appropriate from strength point of view. For annealed steels yield strength is around 1.5 GPa which is 30 times lower than the found stress on TVA.

Before verifying the analytic results with numerical solution, several geometries are tried to see whether stresses can be decreased to an appropriate level around 1.5 GPa. ***In Table 5-10*** stresses for different TVA geometries are summarized:

Table 5-10. *TVA properties and maximum Von-Mises Stress Values found analytically*

Alternative Number	Beam Thickness (m)	Beam Length (m)	Mass at the tip (kg)	Maximum Stres (GPa)
1	0.004	0.39	6	63
2	0.004	0.35	9	82
3	0.006	0.39	21	94
4	0.006	0.6	6	44

Playing with beam thickness for increasing the strength of the TVA is seen to not work. This is due to required tuning frequency. For all cases investigated in Table 5-11 TVA is tuned to 5.67 Hz, beam width is also taken constant as 0.15 m. To tune the TVA to 5.67 Hz. while increasing the beam thickness for increased strength one must increase the length of the beam or add more mass at the tip. As a result it is

seen that maximum stresses are always larger than yield strength of steel which is 1.5 GPa.

An additional damping layer is assumed to be not useful for lowering the stresses down to 1.5 GPa. Since damping materials have lower strength values than steel. Although it is found that stresses are much greater than the yield strength of available materials a numerical analysis and solid model of TVA is done using Pro/E and ANSYS softwares. For the ease of analyses solid model built in Pro/E converted to step file and transferred to ANSYS Workbench for static structural analysis. Meshed solid model transfere from Pro/E to ANSYS Workbench is seen in ***Figure 5-29***.

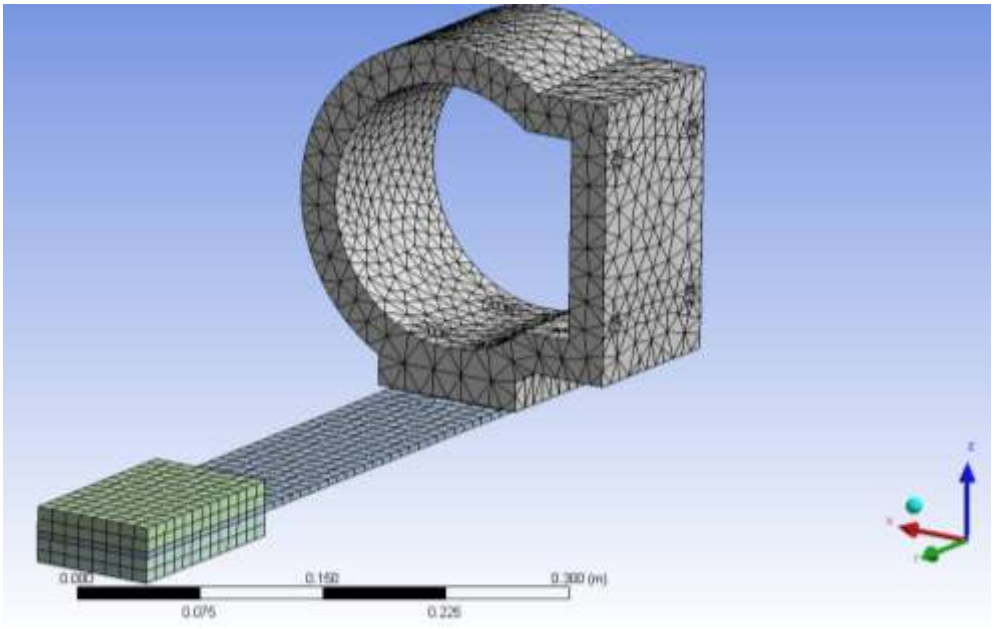

Figure 5-29. *Meshed resonant beam type TVA finite element model.*

Geometry of the numerical model is constructed with respect to Table 5-11 case 2, beam thickness is taken to be 4mm, beam length is taken to be about 300 mm and mass at the tip is around 10 kg. Although numerical model must be modified for

fine tuning changes are minor. For manufacturing purposes finite element model should be taken in to account since it consists of more detailed geometry.

Firstly the tuning frequency which is the first resonant frequency of TVA is checked with modal analysis. For both modal and static structural analyses boundary conditions of resonant beam type TVA is taken to be same; TVA is fixed to gun barrel with four M12 screws. As it is mentioned in the beginning of the section these screw locations are decided upon mechanical interface information taken from the manufacturer. Another boundary condition is added to the system since TVA is tightly inserted to barrel. A cylindrical joint is formed between inner surface of TVA and outer surface of gun barrel. The boundary conditions are seen in ***Figure 5-30 (a)*** and ***(b).***

Modal analysis results verify that TVA is tuned around 5.67 Hz first mode shape of the TVA is seen in ***Figure 5-31***. Minor differences are done for correctly tuning the TVA in numerical solution. The length of the beam, mass at the tip are changed but differences are almost negligible.

Static structural analysis is also done numerically using ANSYS software. As in the case of analytic solution accelerations are applied in parallel and perpendicular to barrel axis on TVA with magnitudes of 1000g. Results revealed that stresses are much higher than the yield strength of beam material, steel. Maximum stress location is formed at the fixed end of the beam as expected. In ***Figure 5-32*** maximum equivalent (Von-Mises) stresses are seen.

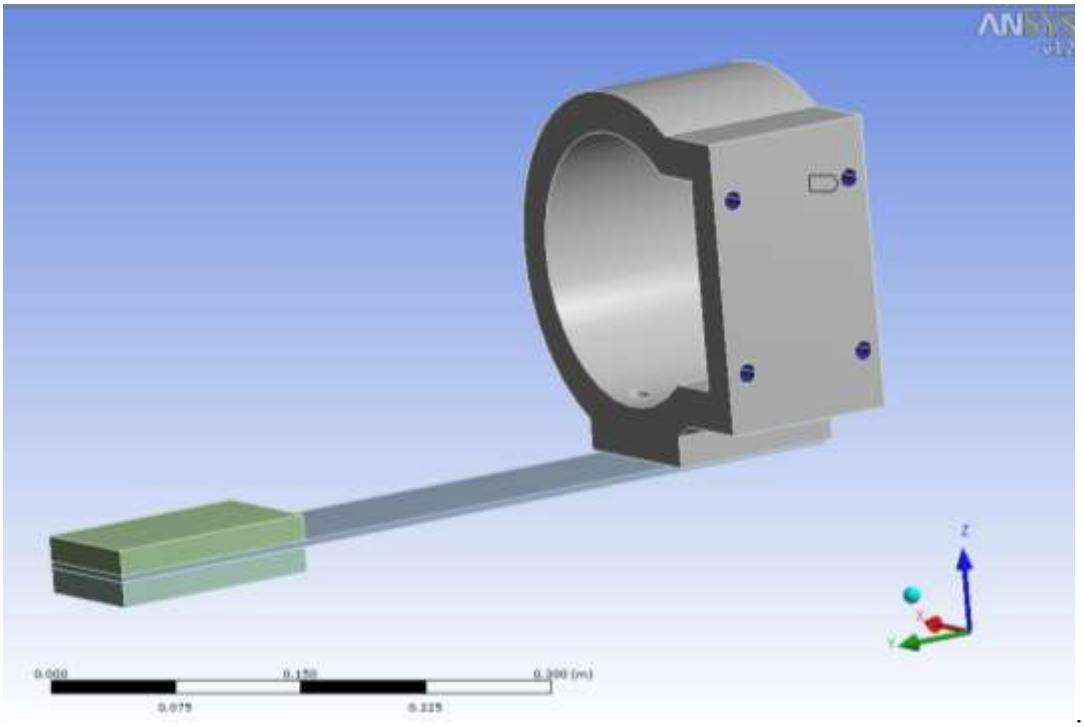

(a)

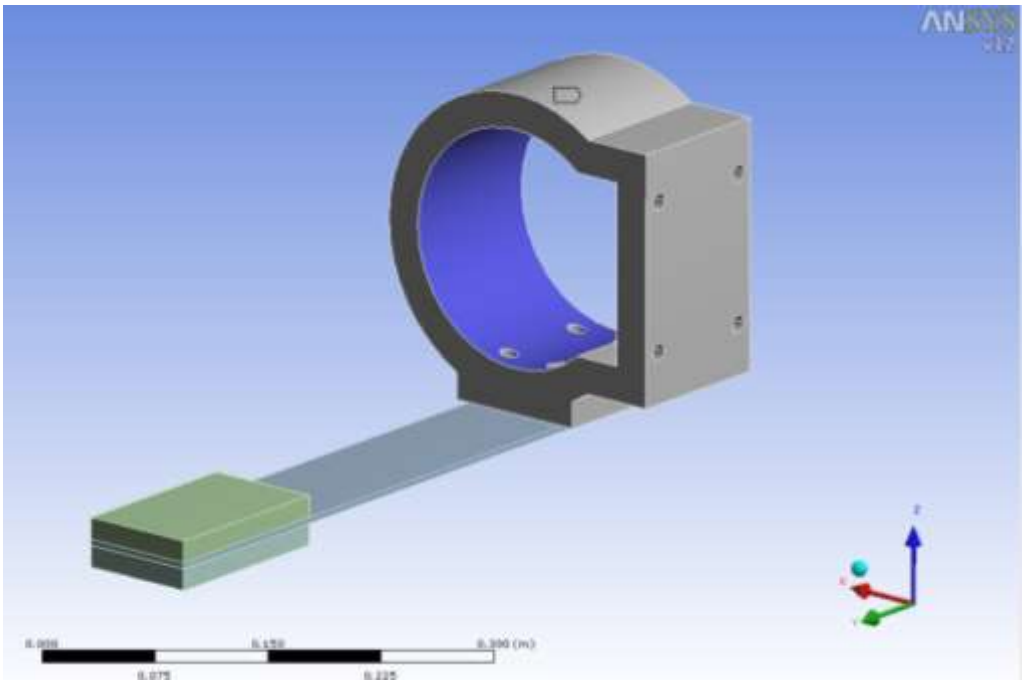

(b)

Figure 5-30. *Boundary conditions for TVA. (a) 4 fixed screw locations. (b) cylindrical joint formed between barrel outer surface and TVA inner surface.*

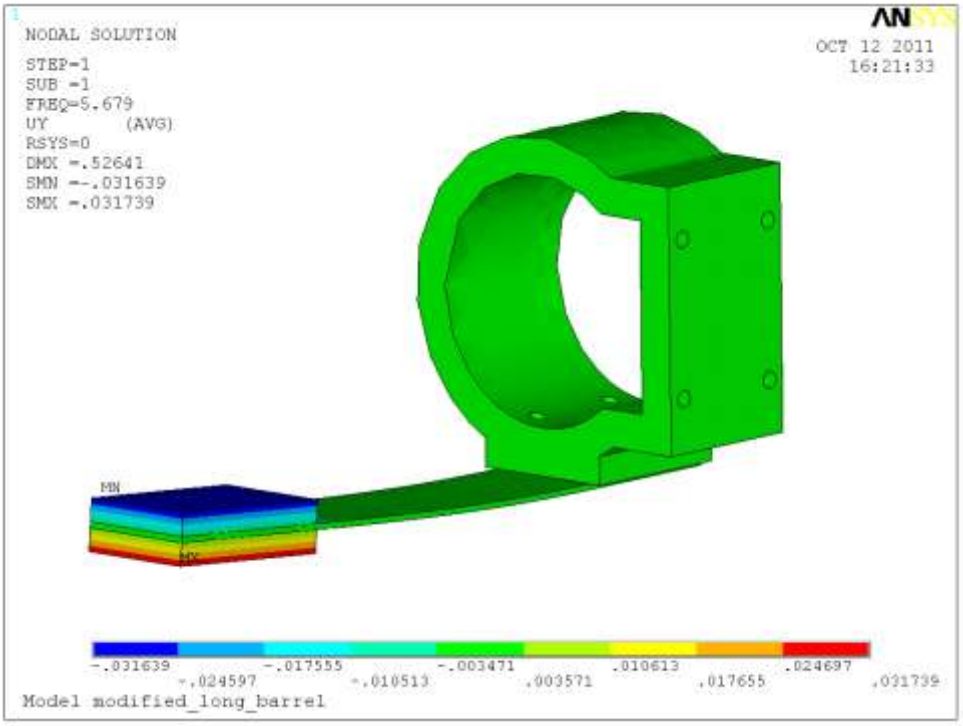

Figure 5-31. *First mode shape of resonant beam type TVA.*

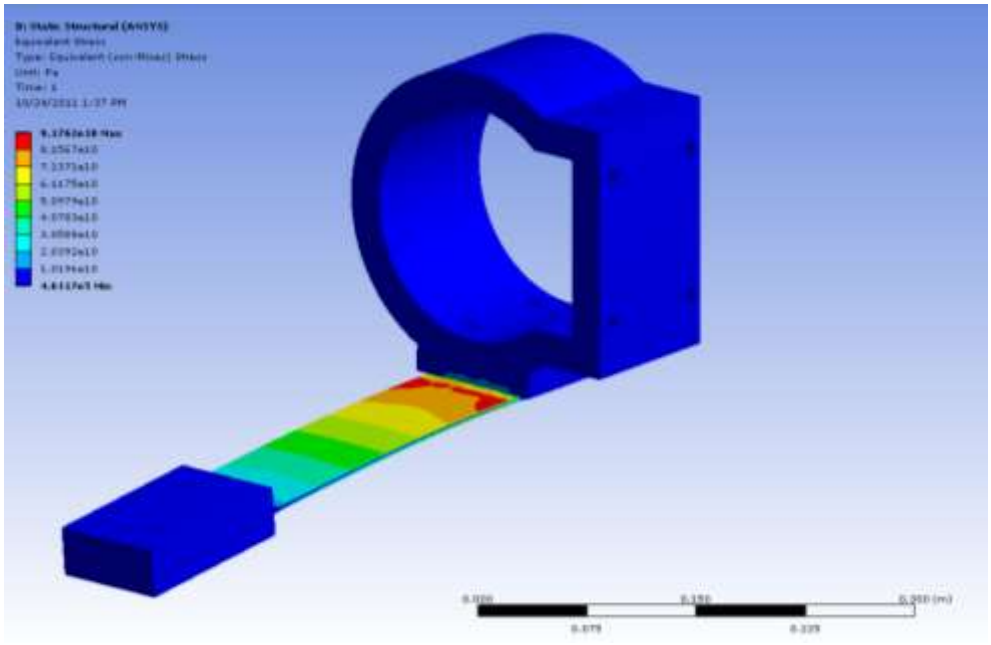

Figure 5-32. *Maximum Von-Mises stress locations of TVA.*

Results of numerical solution is around 95 GPa which is larger than analytical calculation result (82 Gpa). The difference is as high as 15%. This error is due to simplifications and assumptions of analytical calculations and also due to minor changes done in numerical model in tip mass and beam properties while tuning the TVA. For both methods it is found that resonant beam type TVA is not an appropriate solution for controlling gun barrel vibrations. Stresses are always larger than the yield strength of used materials. This is mainly due to high strength requirements and low tuning frequency.

5.2.2 SECOND DESIGN ALTERNATIVE, SPRING DAMPER TYPE TVA

It is already found that in order to modify the longer gun barrel successfully so that the vibration amplitudes at the free end of the barrel is as low as possible required TVA parameters are 4 kg mass and as much as damping. It is also found that tuning frequency is 5.67 Hz which is slightly lower than the first resonance frequency of the longer gun barrel; it is due to type of random base excitation. Designed TVA must also withstand high accelerations that occur during shot.

The mass of the TVA also determines vibration amplitudes of TVA itself, hence for physical design it must be taken into account. The elastic and damper elements must withstand such vibration amplitudes. In the design 4 kg mass is obtained via simple rectangular prism made of stainless steel. The mass is not too big related to volume available at the free end of the barrel. In order to lower the space required one may choose higher density materials such as tungsten. For the ease of manufacturing and availability in steel is chosen.

Next, elastic and damper elements are designed and connected to the mass. Firstly theoretical design by using catalogues and already found formulas is done. Next 3D model of such alternative is drawn and analyzed whether it fulfills the requirements.

For the elastic and damping elements the force at the end of the barrel is calculated. Summation of these forces is also applied to TVA and results in TVA mass acceleration. The design is done using ready to sale products found from catalogues. The design process of each member is not independent from each other. Instead overall design is done by considering every element of the TVA simultaneously.

For the TVA mass of 4 kg undamped optimum tuning is done at stiffness of 5070 N/m. Max TVA displacement is found to be around 92 mm in ***Table 5-6.*** Increasing damping decreases the TVA displacement and for critically damped TVA displacement is as low as 17 mm. Hence it is important to know how much damping can be obtained with available damping products. Damper cataloges are surveyed and several alternatives are found in market. Some kind of rubbers and hydraulic dampers are found. Rubber's damping properties are not as high as it is required and hydraulic dampers are found too big to apply to the barrel end. Best alternative found is dash-pots. From catalogues airpot dashpot is found with required properties [28]. In ***Figure 5-33*** a photo of dashpot is seen. In ***Figure 5-34*** a typical application example taken from the catalogue is seen.

Figure 5-33. *Dashpot used in TVA design* [28].

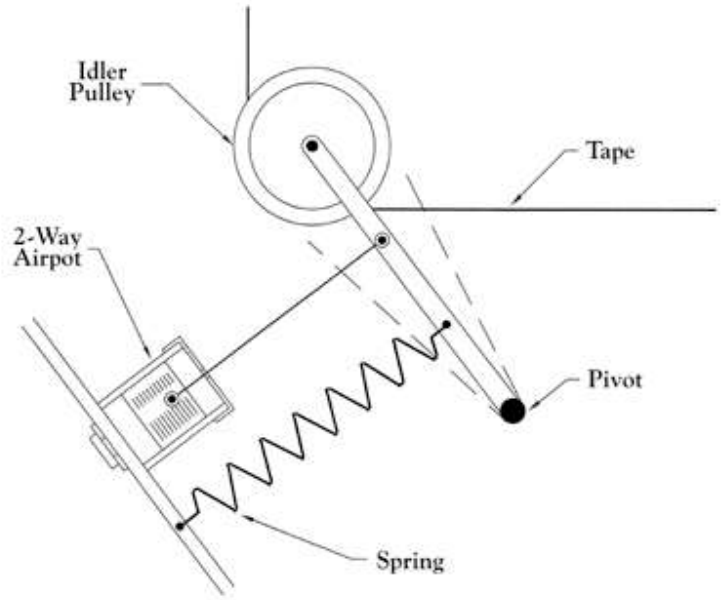

Figure 5-34. *Dashpot in parallel with spring is used to dampen vibration activity* [28].

In order to see the displacement of TVA which depends on damping also, dashpot damping characterics must be known. It is said on the catalogue that damping coefficient range is between 0-7 N/mm/s. Refering back to damping ratio which is C/C_{cr} we need critical damping coefficient of TVA. Knowing the mass and stiffness critical damping coefficient of the TVA is found from well known Formula given in 5-14.

$$C_c = 2 \times \sqrt{k \times m} \qquad \text{(Eq.5.14)}$$

which is found to be 0.284 Ns/mm. Hence damper allows both underdamped and highly overdamped TVA. Hence TVA is designed to be critically damped.

Returning back to elastic member design stage for critically damped TVA the displacement is 17 mm.

$$F = k \times x \quad \text{(Eq.5.15)}$$

From the well-known Hooke's law force equation for springs given in Eq 5-9, force is found as 86 N. Hence elastic elements must withstand such forces when the tank is on move.

The damper is chosen respectively. The stroke length is 1 inch which is less than TVA displacement and the damper consists of impact resistant case EPDM. Damping direction is both in compression and extension.

The stock dashpot is 80 mm long when it is retracted position. It is maximum allowable length is 105 mm. Next it is important to look at force on TVA damping elements, which is velocity times damping coefficient. For the velocity of TVA when it is critically damped is found from spectrum analysis.

RMS velocity amplitude of TVA is found to be 0.9 m/s. Force on damping elements is found to be 255.6 N. Which is larger than the maximum force that dashpot can work (130 N). Hence 4 dashpots in parallel are used so that forcing on each damper is about 65 N with a safety factor about 2. It is also important to note that for critically damped TVA damping coefficient is found to be 0.284 Ns/mm whereas chosen dashpot's damping coefficient range is 0-7 N/mm/s. This dashpot is chosen in order to fulfill force requirements as well as damping properties. Using same catalogues different type of dashpots with smaller damping coefficient range can be chosen but this time in order to reach forcing requirements number of dashpots must be increased [28].

Next appropriate spring is chosen. 2 compression springs are used in parallel similar to 4 dashpots in parallel. The reason of using 2 springs in parallel instead of 1 is symmetry of TVA. Hence spring rate is 2560 N/m and maximum allowable force that spring must withstand is found by Hooke's law as 44 N. Free length of

extension spring is 80 mm same as the dashpot with a minimum allowable length of 105 mm.

From catalogues available spring from stocks is found the properties of compression spring is given in ***Table 5-11***.

Table 5-11. *Details of spring chosen for spring damper system, [24]*

Wire Diam. [mm]	2.5
Ext. Diam. [mm]	30
Free Len. [mm]	82.6
Spring Rate [daN/mm]	0.258
Material	Stainless Steel
Allowable Length	29.95
Nr of Coils	9.4
Weight [g]	31.47
Hole [mm]	30.9

Detailed design of TVA is done using Pro/E software. The model is assembled to barrel. Then as in the alternative 1 it is subjected to static structural analysis under 1000 g acceleration applied along the axis of the barrel and upwards direction. Solid model of the TVA assembled to barrel is seen in ***Figure 5-35*** and ***Figure 5-36***.

2 springs and 4 dashpots are assembled in parallel as seen in ***Figure 5-36***. TVA mass which is tuned to 4 kg is attached to damper and elastic members. Mechanic stops are preventing over motion of TVA mass during shot.

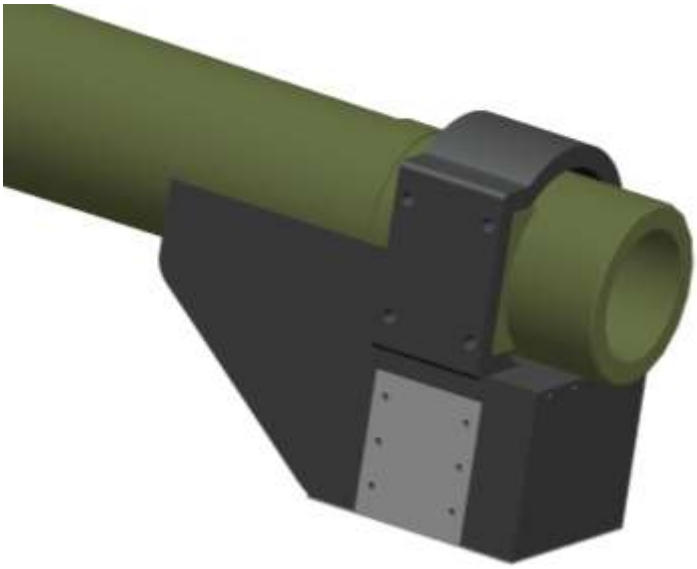

Figure 5-35. *Solid TVA design assembled to the gun Barrel with casing.*

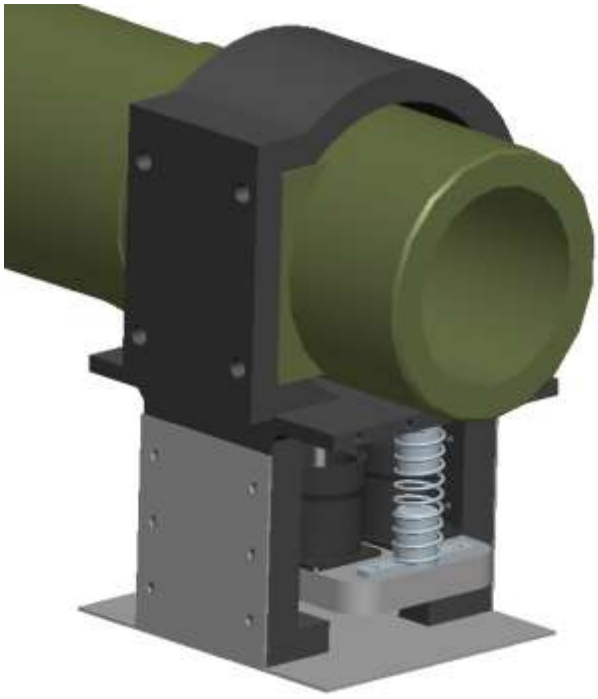

Figure 5-36*. Solid TVA design assembled to the gun Barrel without casing.*

The sliding 4 kg TVA mass has two arms on both sides which act like linear bearing and the dark grey fixed part has hallow parts on both sides which act like rails for sliding arms of TVA mass the sliding part is colored with red in ***Figure 5-38***.

TVA solid model transformed to ANSYS Workbench, supports are applied to the fixed part of TVA as in the first alternative. 4 holes are fixed to the barrel and a cylindrical joint is assigned where TVA inner surface is in contact with the gun barrel. Boundary conditions applied to TVA is seen in ***Figure 5-39***.

Meshing of TVA is done finely element size is assigned to be 3 mm, the meshed TVA can be seen in ***Figure 5-40***. And maximum stress is found to be 1 GPa, around the location of screw holes see ***Figure 5-41*** and ***5-42***. Compared to first alternative it is seen that this type of TVA is much feasible to apply. Since there is no extension from the fixed support stress levels are reduced.

For 1 GPa equivalent stress, material used in manufacturing the TVA is chosen to be water or oil hardened steel whose yield strength is 1310 Mpa and 1450 Mpa respectively. [26]

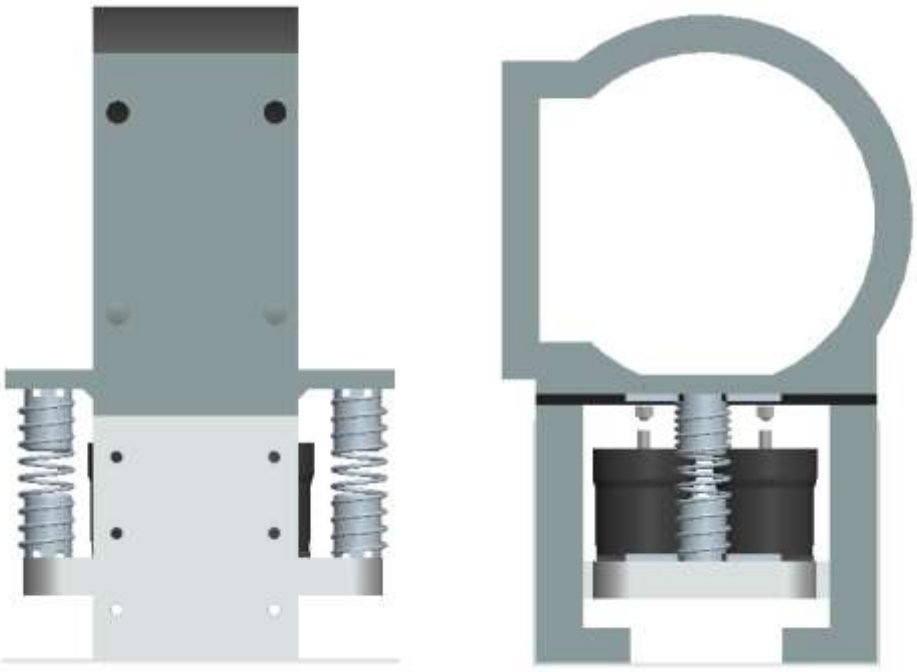

Figure 5-37. *Solid TVA design.*

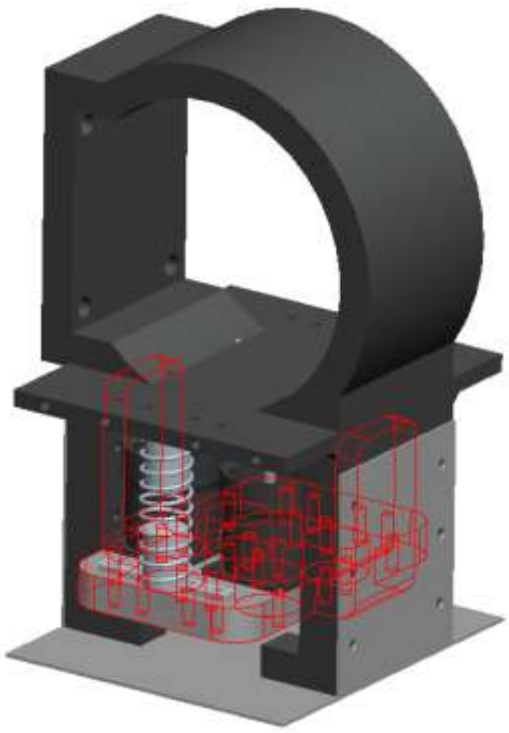

Figure 5-38. *TVA mass slides inside the fixed part on two sides also behaves like mechanical stops.*

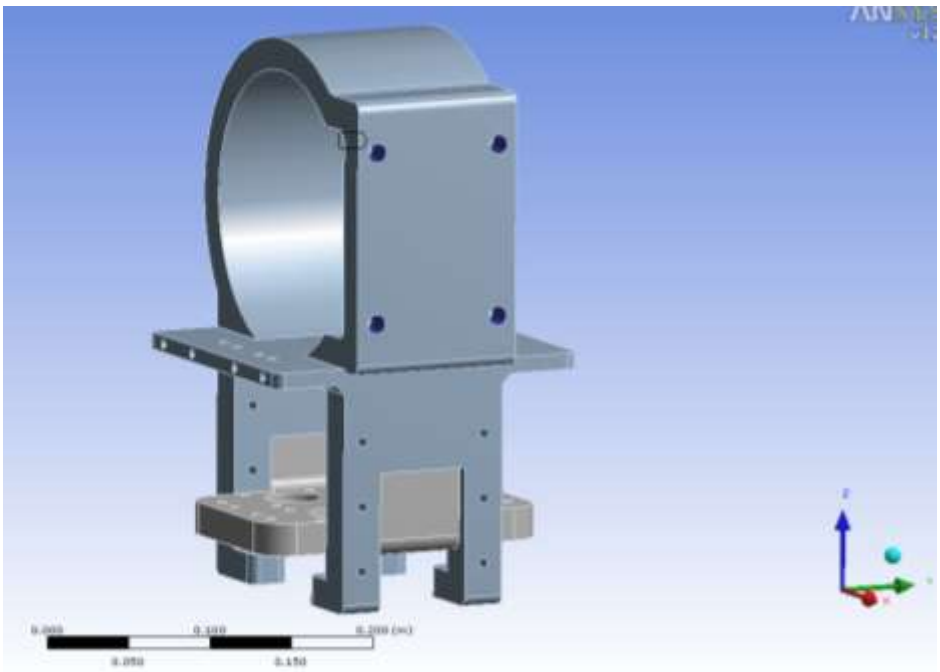

(a)

Figure 5-39. *Boundary conditions applied to second TVA.* ***(a)*** *4 thread locations.* ***(b)*** *cylindrical joint between barrel tube and TVA.*

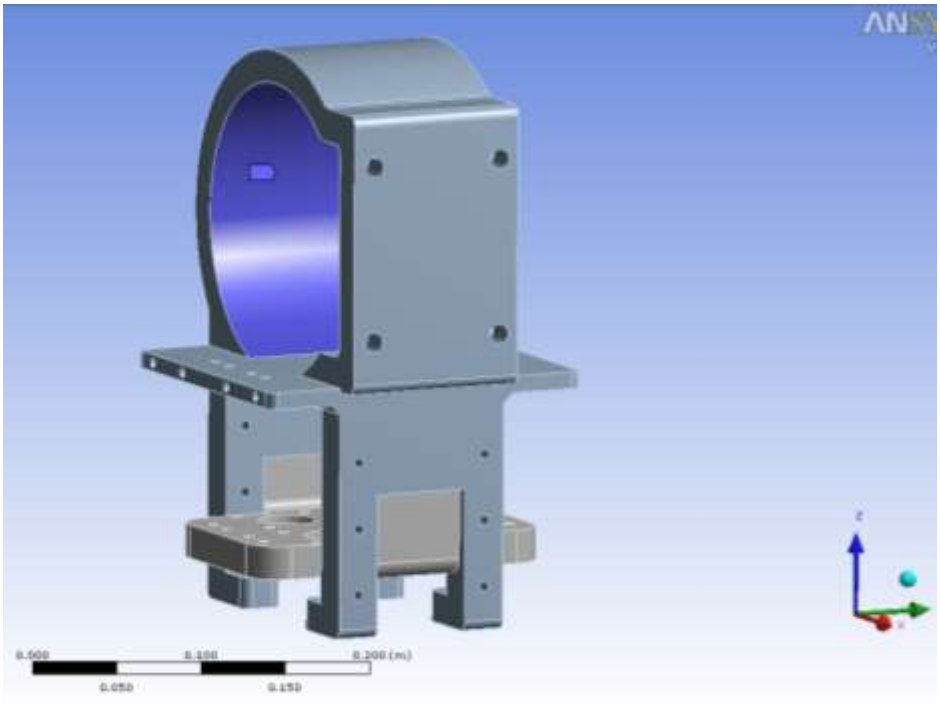

(b)

Figure 5-39. contd' *Boundary conditions applied to second TVA.* ***(a)*** *4 thread locations.* ***(b)*** *cylindrical joint between barrel tube and TVA.*

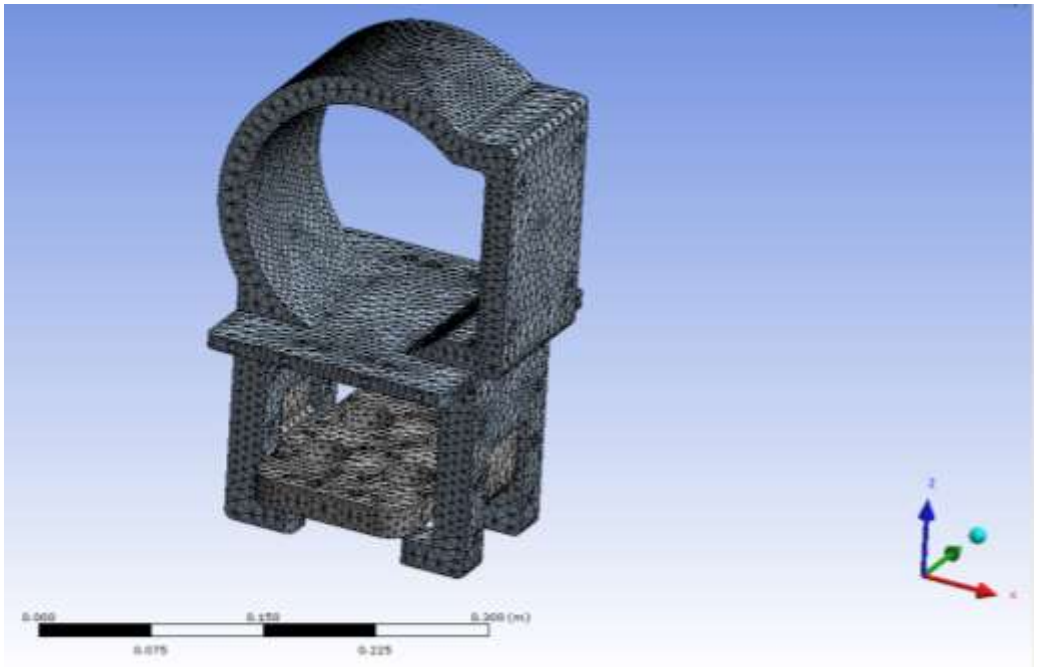

Figure 5-40. *Meshing of second type of TVA.*

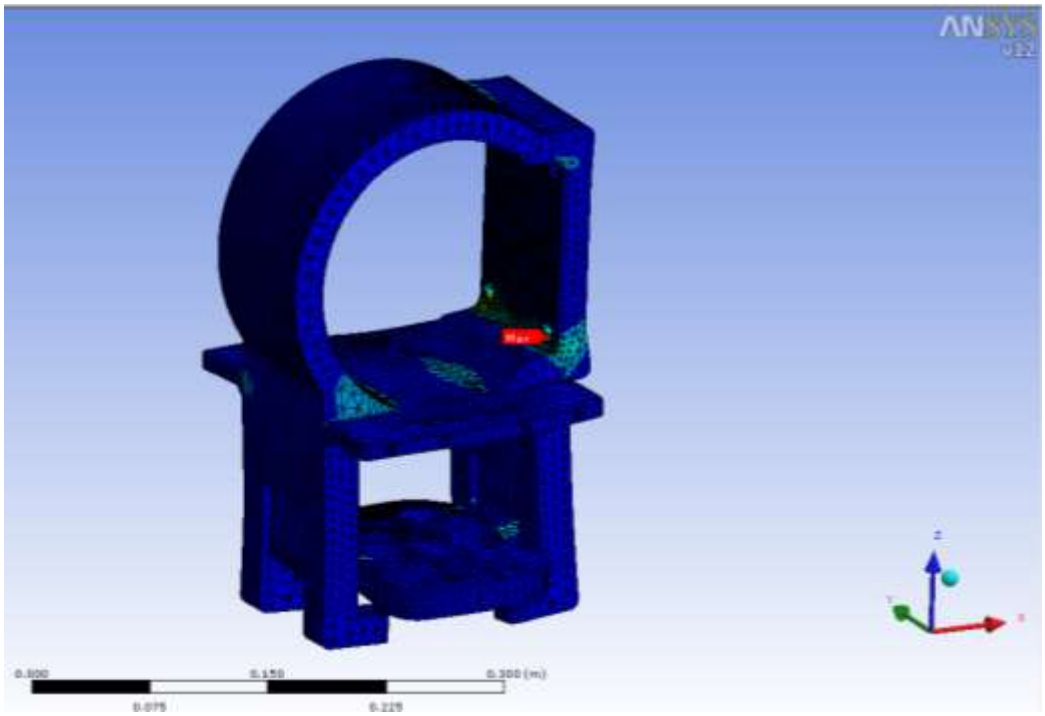

Figure 5-41. *Maximum stress occurred in screw holes in a narrow region.*

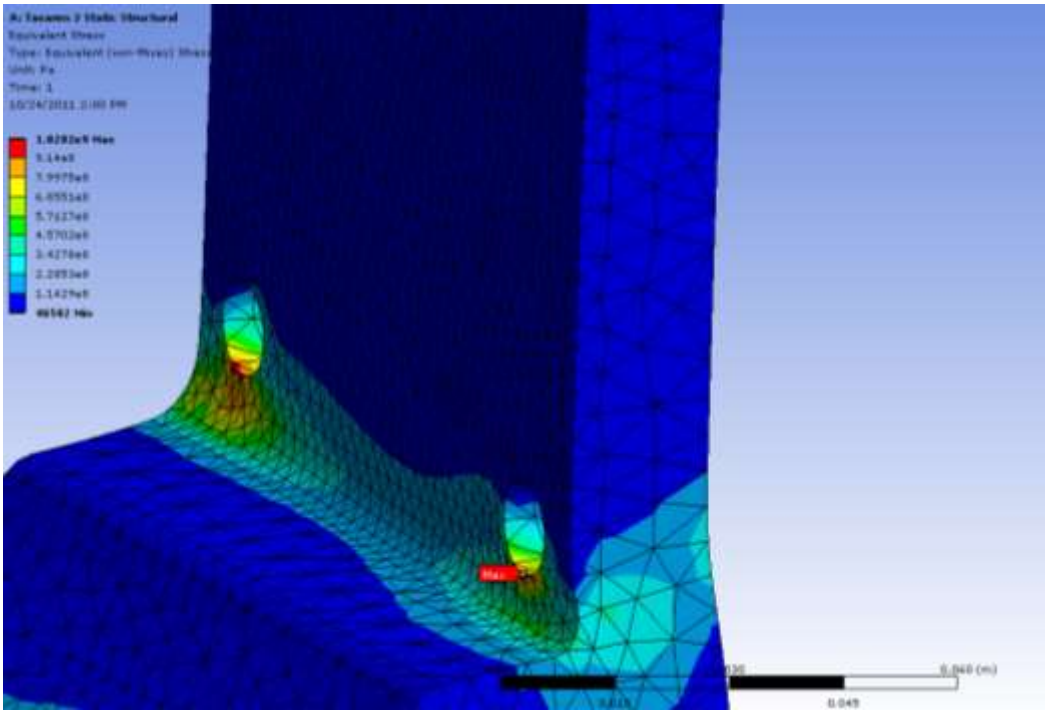

Figure 5-42. *Maximum stress locations scaled view.*

In conclusion, second alternative TVA design is found to be more feasible for gun barrel applications where large accelerations are induced to TVA. The stress levels are tolerable where hardened steel materials are available. ***Table 5-12*** reveals the results of barrel end displacement RMS values. In ***Figure 5-43*** dynamic responses of barrel ends are seen. It is seen that first mode resonant frequency of long gun barrel is almost eliminated by proper TVA application.

Table 5-12. *Gun Barrels End Deflections summary*

	Barrel End Displacement
Short Gun Barrel	7.385 mm
Long Gun Barrel (Unmodified)	19.044 mm
Long Gun Barrel (Modified)	9.42 mm
Percent Improvement	51%

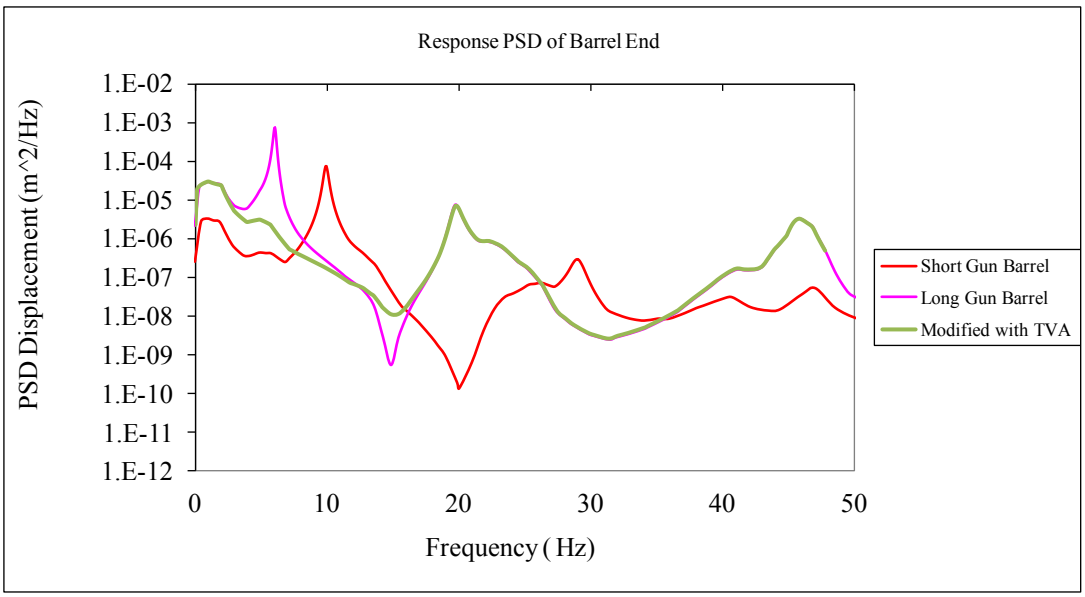

Figure 5-43. *Maximum stress locations scaled view.*

CHAPTER 6

CONCLUSION

Long gun barrels are being adopted to newly designed or modernized main battle tanks in order to attain increased kinetic energy during impact and also higher range of shot. In this thesis dynamic characteristics of both short and long gun barrels are investigated and compared. In order to reduce the vibration amplitude of long gun barrel to the level of short gun barrel a conceptual TVA is designed.

In design of controlling vibrations at the free end of the barrel where vibration activity is maximum, a passive vibration control approach, namely tuned vibration absorber is used. In order to use the vibration absorber effectively the absorber must be tuned accurately. Tuning is done with respect to barrel geometry and also input excitation. In this thesis study, tuning of TVA is done with respect to verified model of shorter gun barrel and experimentally obtained input PSD data.

Tuning is done by playing with the TVA mass, stiffness and damping properties. In this thesis work by considering the type of excitation and also mechanical/dynamical properties of barrel the vibration absorber is tuned to first resonance frequency of the long gun barrel.

The type of excitation is random vibration type of excitation which is applied at the base i.e. the trunnion axis of the gun barrel. The field data is obtained in field tests while the tank is moving at constant speed.

The data is applied to newly constructed and verified short gun barrel finite element model and also long gun barrel finite element model. Using 3D solid model and direct measurements short and long gun barrels finite element models are constructed. Dynamic behavior of short gun barrel which is known to be successful on tests while the tank is on move is investigated in order to determine the required vibration amplitude or maximum displacement at the free end of the long gun barrel for a successful shot. Modeling of the short gun barrel is verified with experimental modal test done on already manufactured and available short barrel. Long gun barrel which is not manufactured yet is modeled with respect to 3D solid model taken from the manufacturer by using the same approach followed in modeling verified short barrel finite element model.

On both barrels static structural, modal, spectrum and harmonic analysis are done, results are compared. It is found that while the tank is on move maximum displacement at the free end of the unmodified long gun barrel is more than twice of the short gun barrel. As a result first shot hit probability and accuracy of the long barrel is less than the short barrel.

TVA parameters are determined to reduce the vibration level of long gun barrel free end to the short barrel's free end. It is found that mass of the TVA has not much effect on tuning due to type of broadband excitation. 4 kg of TVA with overall stiffness of 5000 N/m is designed for minimum barrel end displacement RMS amplitudes. It is also seen from the results that damping as much as possible positively affects the barrel end deflections. For damping ratios about 1.5, long gun barrel response decreases to short gun barrel.

Following the determination of optimum parameters conceptual design of TVA is studied. Some already manufactured parts are found and listed. 2 alternative types of TVAs are designed conceptually. First alternative bases on resonant beam type

TVA. Due to fact that large amount of impulsive load occurs on fire, not only the dynamic characteristics of TVA are studied but also strength of TVA is studied on conceptual design part. TVA mass is chosen to be 4 kg and TVA geometry is optimized so that tuning frequency is close to optimized frequency of 5.67 Hz and barrel end deflection RMS amplitudes are minimum.. It is observed that resonant beam type of TVA is not applicable for barrel end applications where large impact loads occur. Since tuning frequency of TVA is very low, making the TVA with very low stiffness and high strength is not possible.

Second conceptual TVA design alternative consists of parallel springs and dashpots. Both springs and dashpots are found from ready to buy catalogues. In the second alternative design, TVA consists of 2 parallel springs and 4 parallel dashpots. It is seen that changing the geometry and restricting the motion of the sliding TVA mass, required strength properties are reached for the second alternative.

With the application of TVA long gun barrel accuracy is increased to that of short gun barrel which means a higher range of shot, increased kinetic energy during impact without any loss of accuracy due to increased barrel length.

As a future work when the long barrel is available, TVA should be manufactured and assembled to barrel. The design should be finalized by considering possible effects of temperature change due to firing event/environmental conditions and fatigue failure. Use of linear bearings for vertical motion of mass should also be considered in the final design of TVA. Modified long barrel should be tested in field and according to the results of experimental study TVA should be optimized.

REFERENCES

[1] Eric Kathe, Lessons learned on the application of vibration absorbers for enhanced cannon stabilization. Shock And Vibration 8 (2001), pp.131-139. ISSN 1070-9622.

[2] Department of Defense Handbook, Fire Control Systems - General, MIL HDBK-799(AR), April 1996

[3] Peter L. McCall, Measurements of gun tube motion and muzzle pointing error of main battle tanks. Shock And Vibration 8 (2001), pp.157-166. ISSN 1070-9622.

[4] Eric L. Kathe, Matlab modeling of non-uniform beams using the finite element method for dynamic design and analysis. Technical Report US ARMY Armament Research Development and Engineering Center, April 1996.

[5] Department of Defense Test Method Standard. MIL-STD-810F Environmental Engineering Considerations and Laboratory Tests. Method 514.5, pp 11, May 2003.

[6] Mark Bundy, James Newill, Vince Marcopoli, Michael Ng. and Charles Wells. A methodology for characterizing gun barrel flexure due to vehicle motion. Shock And Vibration 8 (2001), pp.223-228. ISSN 1070-9622.

[7] Nadeem Ahmed, R. D. Brown, Amer Hameed. Finite Element Modelling and Simulation of Gun Dynamics using 'ANSYS'. Cranfield University, UK, 2008.

[8] Andrew Littlefield, Eric Kathe. Adaptive Gun Barrel Vibration Absorber. Technical Report US ARMY Armament Research

Development and Engineering Center, March 2002.

[9] De Silva Clarence W. (Ed.) Vibration Damping, Control and Design. Taylor and Francis, 2007.

[10] John C. Dixon The Shock Absorber Handbook (2nd Edition), Wiley, 2007.

[11] Eric L. Kathe. Gun Barrel Vibration Absorber. U.S. Patent No. 6,167,794 B1, 1998.

[12] J. H. Bonsel, R. H. B. Fey, and H. Nijmeijer. Application of a Dynamic Vibration Absorber to a Piecewise Linear Beam System. Nonlinear Dynamics issue 37. pp. 227–243, 2004.

[13] Alessandro Fasana, Ermanno Giorcelli. A vibration absorber for motorcycle handles. Meccanica, issue 45, pp. 79–88, 2010.

[14] M. Najafi, M.R. Ashory, E. Jamshidi. Optimal design of beam vibration absorbers under point harmonic excitation. Society of Experimental Mechanics, 2009.

[15] Simon Hill, Scott Snyder and Ben Cazzolato. An Adaptive Vibration Absorber. Innovation in Acoustics and Vibration Annual Conference of the Australian Acoustical Society, November 2002.

[16] Hugo Bachmann, Benedikt Weber. Tuned Vibration Absorbers for Damping of Lively Structures. Structural Engineering, Issue 1, 1995.

[17] De Silva Clarence W. . Vibration Fundamentals and Practice. CRC Press LLC, 1999.

[18] David J. Purdy. Comparison of balance and out of balance main battle tank armaments. Shock And Vibration 8 (2001), pp.167-1. ISSN 1070-9622.

[19] ANSYS Mechanical APDL Structural Analysis Guide. Release 13.0, November 2010.

[20] Rao, Mechanical Vibrations, 4th Edition pp. 325, 2003.

[21] Suspension Mount - Spring Type (Metric) http://www.globalspec.com/SpecSearch/PartSpecs?partId={98C66F09-55D7-492D-9C8F-2B5B2C4F59B0}&vid=285853&comp=956, (Accessed 12 September 2011)

[22] Spring Mounts Foam Type – To 1250 N http://www.vibrationmounts.com/RFQ/VM05007.htm (Accessed 4 September 2011)

[23] Gas Springs Push Type GS-15, ACE Gas Springs And Hydraulic Dampers, Ace Control Inc. Hydraulic Damper Catalogues. Catalog No 200-0030, Issue: 04/03, 2011.

[24] Advanced search for extension springs with english hooks. http://www.vanel.com/english-extension-adv-search.php?lang=english&sessionid=14412212024e5fb6e8cf85c25852299856852326716 41#results (Accessed 5 September 2011)

[25] Forced Vibrations of a Cantilever Beam with a Lumped Mass at Free End http://iitg.vlab.co.in/?sub=62&brch=175&sim=272&cnt=1 (Accessed 6 September 2011)

[26] Overview of materials for Oil-Hardening Steel http://matweb.com/search/DataSheet.aspx?MatGUID=adde50ccbf7a43af9749c342f9f2337f Accessed 6 September 2011)

[27] F.P. Bear, E.R. Johnston, J.T. Dewolf, D.F. Mazurek, Mechanics of Materials, 4th edition in SI Units McGraw Hill, 2006.

[28] Airpot Dashpot specifications http://www.airpot.com/htm/dashpot.html (Accessed 10 December 2011)

[29] How to Determine the Modal Parameters of Simple Structure http://www.bksv.com/doc/bo0428.pdf (Accessed 10 December 2011)